Faculdade de Engenharia da Universidade do Porto

Using Renewable-Based Microgrid Capabilities for Power System Restoration

João Pedro Pereira Carvalho

Dissertação realizada no âmbito do
Mestrado Integrado em Engenharia Eletrotécnica e de Computadores
Major Energia

Orientador: Prof. Doutor João Paulo da Silva Catalão
Coorientador: Prof. Doutor Miadreza Shafie-khah

Julho de 2018

Resumo

O sistema elétrico de energia apresenta-se em constante mudança. Em cada ano que passa, cada vez mais recursos energéticos distribuídos são integrados nas redes de energia elétrica, como é o caso das unidades de produção, e dispositivos de armazenamento de energia. Tal significa que novos desafios irão surgir relacionados com a operação de todo o sistema elétrico.

A tendência crescente é que as redes de baixa tensão se transformem em micro-redes e que toda a rede de distribuição se torne "inteligente", de forma a acomodar os recursos distribuídos e as suas características sem existir a violação de qualquer restrição operacional. Os consumos elétricos têm vindo a aumentar ao longo dos anos e prevê-se que este aumento continue no futuro pelo que, ao integrar sistemas elétricos inteligentes nas redes de distribuição, consegue-se que os investimentos realizados sejam mais sustentáveis e não tão elevados quando comparados com o reforço da rede.

Uma vez que o sistema elétrico de energia tem aumentado em termos de dimensão e complexidade, a probabilidade de ocorrência de *blackouts* também tem seguido essa tendência. A forma convencional de realizar o restauro do sistema considerando um *blackout* total no sistema elétrico, passa por explorar uma estratégia denominada *top-down*, em que o processo começa com as grandes centrais e unidades de produção que através do processo de *black-start*, começam a energizar a rede de transmissão seguindo depois o sentido descendente em direção ao consumidor. Esta estratégia pode demorar várias horas ou até mesmo dias.

Uma outra alternativa passa por realizar o restauro do sistema utilizando uma perspetiva *bottom-up* em que se começa o processo de restauro pelas grandes centrais na rede de transmissão, como também pelas várias micro-redes espalhadas pela rede de distribuição, ao nível da baixa tensão. Esta alternativa é possível precisamente porque as micro-redes têm os recursos energéticos necessários para funcionar em modo isolado, sem qualquer dependência da rede de média tensão.

No presente trabalho, um sistema multiagente descentralizado é proposto como forma de lidar com o processo de restauro de uma micro-rede. Neste esquema proposto, cada um dos agentes que compõem este sistema está associado a um consumidor ou unidade de produção distribuída e estes irão comunicar entre eles, transmitindo a sua informação local de forma a

chegar a uma decisão comum. Os agentes resolvem um problema designado "*0/1 Knapsack*" de forma a determinar a melhor sequência de conexão das cargas durante o processo de restauro da micro-rede. O sistema proposto é testado segundo dois casos de estudo distintos: o primeiro considerando um *blackout* total e o segundo um *blackout* parcial, sendo que neste último são considerados os programas de emergência de *demand response*. O modelo proposto é desenvolvido em ambiente MATLAB/Simulink e validado através da realização e análise das simulações dinâmicas correspondentes.

Palavras-Chave – *Black-start*; *Demand response*; Recursos Distribuídos; Micro-rede; Sistema multiagente; Restauro.

Abstract

The electrical power system is changing and evolving rapidly. Every year more distributed energy resources (DER), such as distributed generation units and storage devices, are employed in the network. This means that new challenges will arise which are related to the operation of the grid.

The tendency is that the low voltage grids start to transform themselves in microgrids and that the entire medium voltage (MV) grid becomes "smarter" in order to accommodate the abovementioned DER without any operational constraint violation. The electrical consumptions have increased throughout the years and it is expected to continue to increase in the next ones, so the "smartness" of the electrical power system is the option that enables the sustainable growth and integration of the increasing consumptions, and does not involve the expensive procedure associated with the complete grid reinforcement.

Since the electrical power system has been increased in both dimension and complexity, it is more subject to the occurrence of blackouts, total or partial, that may compromise the service level promised to the consumers. The conventional way of doing the restoration procedure, considering a total blackout is to use a top-down approach in which the power plants and generation units at the highest voltage level are black-started, the transport network is built, and only then the distribution network is restored enabling the supply of the consumers' needs. This takes several hours to several days.

An effective way to decrease the total restoration time is to start the restoration procedure by using a bottom-up approach in which the restoration procedure, besides starting in the power plants in the highest voltage level, it also starts from the existing microgrids in the low voltage level. This is possible since these microgrids are able to work in island mode, completely independently from the MV grid.

In this work, a decentralized multi-agent system (MAS) for dealing with the microgrid restoration procedure is proposed. In this proposed method, each agent is associated to a consumer or microsource (MS) and these will communicate between each other in order to reach a common decision.

The agents solve a 0/1 Knapsack problem to determine the best load connection sequence during the microgrid restoration procedure. The proposed MAS is tested in two different case studies: a total blackout and a partial blackout, in which the emergency demand response programs are considered. The proposed model is developed in the MATLAB/Simulink environment and is validated by performing the corresponding dynamic simulations.

Keywords – Black-start; Demand response; Distributed resources; Microgrid; Multi-agent system; Restoration.

Acknowledgements

I would like to thank my MSc. Supervisor, Prof. Dr. João Paulo da Silva Catalão, for giving me the opportunity to work with a much-diversified team in an area that is of utmost interest for me, and also for the availability throughout the entire development of this work.

I would also like to thank my MSc. Co-Supervisor Dr. Miadreza Shafie-khah, for all the valuable insights during the entire development of this dissertation, and for pointing me in the right direction in the beginning of the work.

To Dr. Gerardo Osório and Dr. Ebrahim Rokrok, I would like to give my sincere acknowledgement for all the help, all the availability during the development of this work and also for all the help in the technical field, which meant a lot to me. Thank you.

I could not leave *Faculdade de Engenharia da Universidade do Porto* without a proper thank you for these five wonderful years of studies. It was amazing to grow intellectually and personally in a way that I never thought possible.

Finally, to my parents, my grandparents and my amazing aunt for all the support in all the decisions and help during these five years full of challenges. Without all of you, I would not get to where I am today.

"Quality means doing it right when no one is looking."

Henry Ford

Contents

Figures list

Tables list

Abbreviations and Symbols

List of Abbreviations

AFC	Alkaline Fuel Cells
AGC	Automatic generation control
BPS	Bulk power system
BSU	Black-start unit
CAMC	Central autonomous microgrid controller
CPP	Critical peak pricing
DB	Demand bidding
DER	Distribution energy resource
DLC	Direct load control
DMFC	Direct Methanol Fuel Cells
DMS	Distribution management system
EMS	Energy management system
ESD	Energy storage system
EV	Electric vehicle
GAST	Gas turbine
I/C	Interruptible/curtailable services
LC	Load controller
LV	Low voltage
MAS	Multi-agent system
MCFC	Molten carbonate fuel cells
MC	Microsource controller
MG	Microgrid
MGCC	Microgrid central controller
MMG	Multi-microgrid
MMO	Multi-master operation
MPPT	Maximum power point tracking

MV	Medium voltage
MS	Microsource
NOCT	Normal operating cell temperature
PAFC	Phosphoric Acid Fuel Cell
PEMFC	Proton exchange membrane fuel cell
PMSG	Permanent magnet synchronous generator
PV	Photovoltaic
PWM	Pulse width modulation
RMS	Root mean square
RTP	Real time pricing
SMO	Single master operation
SOFC	Solid oxide fuel cell
SOC	State of charge
SPA	Standing phase angle
SSMT	Single-shaft microturbine
TOU	Time of use
VSI	Voltage source inverter
WECS	Wind energy conversion system

List of symbols

Photovoltaic system model:

I	PV cell current (A)
I_{ph}	PV light generated current (A)
I_0	PV cell reverse saturation current (A)
I_{sa}	PV Array current (A)
V	Voltage (V)
V_{oc}	Open circuit voltage (V)
V_{sa}	PV array voltage (V)
R_s	Series resistor (Ω)
R_{sh}	Shunt resistor (Ω)
N_s	Number of series PV modules
N_p	Number of parallel modules
q	Electronic charge (1.602*10^-19 C)
A	Ideality factor of solar cell
k	Boltzmann's constant)1.3807*10^-23 J/K)
T	Cell temperature (K)
$NOCT$	Normal operating cell temperature (K)

Wind generator model:

P_m	Mechanical power (W)
ρ	Air density (kg/m^3)
C_P	Performance coefficient of the wind turbine
A	Area swept by the blades (m^2)
V	Wind velocity (m/s)
λ	Tip speed ratio (rad)
β	Pitch angle (deg.)

Microturbine model:

T_1, T_2	Fuel system time constants (s)
T_3	Load limit time constant (s)
D_{tur}	Damping of turbine
L_{max}	Load limit parameter
V_{max}	Maximum valve position
V_{min}	Minimum valve position
K_T	Temperature control loop gain
K_i	Integral gain of PI controller
$\bar{P}_{ref}$	Active power reference (p.u.)
$\bar{P}_{dem}$	Demanded active power (p.u.)
K_P	Proportional gain of PI controller
$\bar{P}_{in}$	Active power applied to the turbine (p.u.)

Solid Oxide Fuel Cell model:

p_{H_2}, p_{H_2O}, p_{O_2}	Partial pressure of hydrogen, water and oxygen, respectively (atm)
k_{H_2}, k_{H_2O}, k_{O_2}	Valve molar constant for hydrogen, water and oxygen, respectively (kmol/(s atm))
τ_{H_2}, τ_{H_2O}, τ_{O_2}	Response time for hydrogen flow, water flow and oxygen flow, respectively (s)
${q_{H_2}}^{in}$, ${q_{H_2}}^{ou}$	Input and output hydrogen flow, respectively (kmol/s)
K_r	Constant for modelling purposes ($N_0/(4 \cdot F)$ (kmol/(s.A)))
I	Current (A)
${q_{O_2}}^{in}$	Input oxygen flow (kmol/s)
U_f	Fuel utilization
${q_{H_2}}^{r}$	Reacting hydrogen flow (kmol/s)
U_{opt}	Optimal fuel utilization
E_0	Ideal standard potential (V)
N_0	Number of cells in the fuel cell stack, in series
E	Electrical potential (V)

R	Universal gas constant (8314J/kmol.K)
T	Absolute temperature (1273K)
F	Faraday's constant (96487C/mol)
r	Ohmic loss (Ω)
r_{H_O}	Ratio of hydrogen to oxygen
U_{max}	Maximum fuel utilization
U_{min}	Minimum fuel utilization
T_e	Electrical response time (s)
T_f	Fuel processor response time (s)

Inverter models:

E_d, E_q	Electrical potential in d and q axis, respectively (V)
V_d, V_q	Voltage in d and q axis, respectively (V)
i_d, i_q	Current in the d and q axis, respectively (A)
R	Output filter resistance (Ω)
L	Output filter inductor (H)
$i_{d\,ref}$, $i_{q\,ref}$	Reference current for d and q axis, respectively (A)
$k_{p,id}$, $k_{p,iq}$	Proportional coefficient of d and q axis current component, respectively
$k_{i,id}$, $k_{i,iq}$	Integral coefficient of d and q axis current component, respectively
k_P, k_Q	Active and reactive power droop coefficients
ω	Angular frequency (rad/s)
V	Voltage (V)
T	Transformation matrix
v_a, v_b, v_c	Three phase voltage (V)
v_α, v_β, v_0	Voltage in axis α, β and 0, respectively (V)
i_a, i_b, i_c	Current in phase a, b and c, respectively (A)

Multi-agent system variables:

$f(x)$	Total value
v_i, v_{ij}	Value of item *i*, priority of load *j* of consumer *i*
x_i, x_{ij}	Inclusion of item *i*, Connection status of load *j* of consumer *i*
w_i, w_{ij}	Weigh of item *i*, active power of load *j* of consumer *i*
W	Sum of weights/SSMT's reserve

Chapter 1

Introduction

This chapter has the purpose of making a brief introduction about the topics and problems discussed in this dissertation. It gives a framework to the problem and also the motivation behind it. Besides, it is also presented the dissertation structure as well as the notation used.

1.1 - Framework

Nowadays electric energy is the source of all the economic activities and it became part of the life of every person. So, when the electric energy fails due to a specific reason, it can be problematic according to several reasons. Some examples are the loss of energy supply in hospitals, universities and commercial buildings, which can cause panic during the power outage endangering people present in these facilities.

In past years, several blackouts worldwide have occurred. On 14th August 2003, a blackout occurred in North America, that was caused by the contact between three transmission circuits and trees, more specifically in the northeast Ohio. This event caused a chain of reactions that led to the collapse of the power system in the Great Lakes, the northeast of the United States and also some parts of the eastern Canada grid. This event lasted approximately two weeks until it was resolved [1]. Another example is the power outages that occurred on the 30th and 31st July 2012, in India. On the 30th of July, a power line in the state of Uttar Pradesh was tripped which, after a cascade of several other events that resulted from this action, caused a blackout that affected around 370 million people and also 35.67GW of load was shed. Due to another failure in the power system, on the next day another blackout occurred, which affected the northern, eastern and northeastern power grids. In total 50GW of load was shed [2]. It is possible to see the impact that blackouts can have in society through these examples.

The limited operational margins of the power systems have increased the risk of power outages, blackouts and the collapse of the systems, over time. In this matter, power system

restoration (PSR) appears as one of the most important problems to be approached. In the conventional procedure, the restoration process starts at the transmission system by starting the power plants and generation units that are able to provide the black-start capability in the shortest time possible, such as hydroelectric generating units, gas and fuel turbine units, and also the incoming power from the interconnected systems in the vicinities [3]. This way, it is possible to energize the transmission system and from there supply the consumers near the power plants first. This means that the consumers at the distribution system will wait a longer time to be supplied.

Over the years, it has been a restructuring of the power systems regarding the integration of renewable and non-renewable energy sources in the distribution systems establishing a new concept: the Microgrid (MG). This changes the paradigm completely because the power flow becomes bi-directional and this type of grid can also work in islanded mode if necessary [4]. This new characteristic, when properly used, can be very helpful in terms of PSR. Besides, it will allow distribution system consumers to be supplied faster than using the conventional way.

However, by introducing the microgrid concept new challenges will arise regarding the power system restoration. The most relevant ones are related to the fact that microgrids include non-controllable energy resources such as micro-wind turbines and photovoltaic systems, for example. These resources will vary their production according to the wind speed and irradiance in every instant, respectively. This means that there will be a high degree of uncertainty and variability in the power production of these units, which can affect the power system's restoration procedure [5].

In conclusion, the combination of the DER with the flexibility of the consumptions associated to microgrids can improve significantly the restoration process. Moreover, it is important not to forget that microgrids need to be coordinated in the most efficient way to ensure that all the benefits can still be preserved [6].

1.2 - Motivation

As can be stated, blackouts are very infrequent events, however when these situations occur they can lead to very harmful consequences. As a result, since the electrical power system is being modified over the years by the inclusion of dispersed generation units, new possibilities in the power system restoration field of studies have appeared. These studies usually focus on:

- Minimizing the overall restoration time [7];
- Minimizing the restoration cost [8];
- The maximization of the amount of restored load during the grid restoration process [9].

The first studies made in this subject are based on the conventional power system restoration, which does not consider DER [10], [11]. However, by introducing the microgrid concept, these three objectives can be accomplished and improved, when compared to the conventional power system restoration solutions [4], [9].

Microgrids have the feature of working in island mode, which is very helpful in the power system restoration problem since these can work as black-start sources during the initial stages of the restoration process, when under certain conditions. The main benefit is that the consumers located at the distribution system can be supplied much faster [12].

In order to enable this capability on microgrids, first it is necessary to study ways to improve the restoration procedure of the microgrid itself. By ensuring a fast and secure restoration procedure of microgrids, the more suited these will be to be able to help the remaining of the power system in its restoration procedure.

In conclusion, this project was developed to contribute specifically to this last area of studies, where an algorithm based on a multi-agent system is proposed to ensure the restoration of a modelled microgrid in the shortest time possible by using the microgrid's available capabilities, regarding the controllable and non-controllable generation units but also exploring the control possibilities of its loads.

1.3 - Methodology

The work presented in this dissertation is related to the microgrid restoration procedure, more specifically it uses a multi-agent system in which every microsource and load are associated with one specific agent.

The agents then communicate between each other in order to determine the loads to be connected according to the free reserve of the microturbine and the load priority thus, establishing a coordinated control structure that enables the microgrid restoration procedure.

The agents will solve a 0/1 Knapsack problem using a dynamic programming algorithm in order to reach a feasible solution. The objective is to enable the microgrid restoration procedure in the fastest time possible, minimizing the impact on any restriction of the microgrid itself, such as the voltages and frequency values for example.

The work is developed entirely in MATLAB/Simulink environment. The dynamic simulations are obtained using Simulink and the dynamic programming algorithm to solve the 0/1 Knapsack problem is developed in MATLAB.

1.4 - Dissertation Structure

This dissertation is divided in 7 chapters. In chapter 2 the state of the art of both conventional power system restoration and the microgrid restoration is presented based on a literature review. Both of these concepts are then compared. In chapter 3 the dynamic modelling of the microgrid is presented, including all the dynamic models of the microsources, loads, storage device, inverter control, feeders and MV grid equivalent. The mathematical equations and working principles of every element are also presented. Chapter 4 presents the benchmark microgrid model validation through the simulations of the microgrid in island mode, in single master operation and multi-master operation. These simulations are useful to check the model functionality, including the operation of every distributed energy resource. These two operation scenarios are also compared, and some conclusions are presented. In chapter 5 it is shown that the restoration procedure of the modelled microgrid is possible, and the general assumptions of this procedure are also presented. In chapter 6, the proposed multi-agent system model associated with the 0/1 Knapsack problem is presented and validated by performing a dynamic simulation of the microgrid restoration procedure. Also, in this chapter the emergency demand response program (EDRP) is considered in the simulations by using the proposed multi-agent system in a partial blackout case study, in which it is necessary to shed loads in order to stabilize the microgrid after a fault in a pre-defined feeder. In chapter 7 the conclusions, suggestions for future work and also the main contributions of this dissertation are presented. Finally, the final sections include the reference section and the appendix section.

1.5 - Notation

This dissertation uses the same notation that is used in the scientific literature, harmonizing the common aspects when possible and it is written accordingly to the English standards. The tables and figures are ordered according to the chapter where they are inserted, restarting its numbering from the beginning of each chapter and being identified by X.X. The references that support the chapters that compose this dissertation are identified by [XX], while the mathematical equations are numbered by (X.X), being identified by the chapter that they are inserted in, and the order within that same chapter. The acronyms follow the technical information and name abbreviation accordingly to the English standards, well accepted in the scientific community.

Chapter 2

State of the art

This chapter presents the conventional power system restoration, including all the steps to be followed in order to ensure the restoration in the fastest and most secure way possible but also the problems that this process needs to overcome in order to succeed. The microgrid is then presented as well as its capabilities and the new resources available for its operation and control. Finally, several novel approaches regarding power system restoration and microgrids are presented and described.

2.1 - Conventional Power System Restoration

When a blackout occurs, it is necessary to define a strategy that the system operator can follow in order to reestablish the normal operation conditions in the shortest time possible. This strategy should follow two objectives of the restoration process per se. These objectives include the reconstruction of a stable power system, in the first place, and finally the restoration of all the unsupplied consumers. In order to accomplish these objectives, it is necessary that several steps are taken by the system operator. These steps include [10]:

- Prevent not only human injury but also equipment damage. This is achieved avoiding the steady state overloads and over-voltages;
- Ensure the balance between power production and loads, the balance in reactive loads and the stabilization of the voltages;
- Observe the restart time limits of the generators and emergency backup generators, thus minimizing the total time of restoration;
- Give priority to critical loads, such as hospitals;
- Ensure the system flexibility thus resolving problematic situations that may occur during the restoration process.

This process is properly structured as shown in Figure 2.1, adapted from [10].

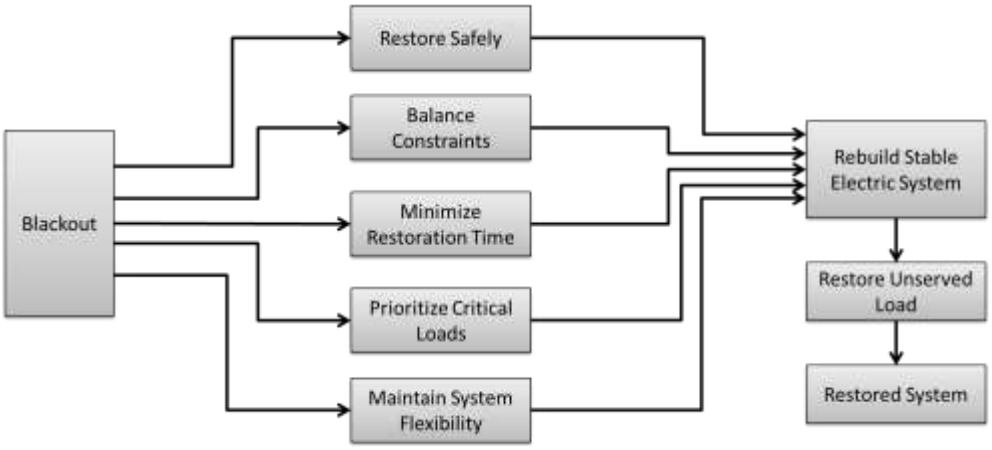

Figure 2.1 - Description of the restoration objectives.

2.1.1 - Sequence of Actions

After the occurrence of a power outage there are two conditions that need to be assessed before starting the actual restoration process.

In the first place, it is necessary to verify the operating conditions of the system to know the exact extension of the problem. It is clear that according to the type of problem, there will be different actions to be taken. Secondly, after the verification phase it is necessary to limit the power outage and also ensure that it is stabilized, in order to avoid its progression into another areas of the power system [10].

After the previous initial assessment, the restoration process will begin. The power system restoration procedure is divided into three major steps, being the cranking power supply to the non-black-start units, building the skeleton of the bulk power system, and finally minimizing the unserved load [13]. From here, a proper sequence of actions in order to restore the power system can be identified, being presented as follows [14]:

1. **Beginning of the Restoration**

In this phase, several restoration options must be considered based on the restoration plan. This process should not take much time so that the restoration process does not delay excessively [10].

2. **Black-Start Units (BSU)**

The objective of this step is to provide an initial cranking source to re-energize tripped generators, or non-black-start generators, which were chosen in the previous phase. The preferred technique is to use the “top-down” approach, which consists in restarting the tripped generators from the Bulk Power System (BPS). This is the preferred approach since it enables a more stable integration of the restarted generation units.

If this is not possible, the other option consists in using an isolated black-start generator in a “bottom-up” approach, which is characterized by the creation of sub-systems with black-start capabilities that are later connected together in order to form a larger stable system [10].

Accordingly to [15], these black-start units include:

- Hydroelectric generation units, since these possess a fast response to the necessary demand which makes them very useful when available;
- Diesel generators. These types of units require electric batteries in order to start and can do this in a fast way. They cannot pick-up significant amounts of load which means that the primary function will be providing power to start larger units;
- Aero-derivative gas turbine generation units. These units can provide a fast load pick-up process. As the previous units, they also need an electric battery in order to start;
- There is another possibility that consists in larger gas turbines, that does not possess black-start capabilities per se, but can be coupled to diesel generators which makes the power plant a black-start source, which can be very useful in the restoration process.

3. Restoration Path Preparation

After starting the black-start units, in order to ensure the supply of cranking power to larger generator units, it is necessary to prepare a proper path. This preparation includes overcoming system problems, giving priority to supplying critical loads, matching connected loads with the load pick-up capabilities of the generator, taking small steps of load increments in order to prevent over-voltages [10].

4. Create Stable Sub-System

Since the restoration paths are already prepared, it is necessary to build sub-systems, or islands, through the synchronization of some of the previously formed islands. This step is important because the power system will increase its capacity and size, becoming more resilient. In order to build a stable sub-system it is necessary to restart, stabilize and synchronize the generators through the restoration paths, and also to pick-up critical loads to the restoration process [10].

The sub-systems are built by energizing the skeleton of the islands created in order to send the cranking power from the black-start units to the remaining ones located at the same island [16].

5. Connect Sub-System to BPS

After building a stable sub-system, the next step is to connect the black-started generators and the island sub-systems to the BPS in order to achieve a larger interconnected system that possesses more inertia which means that it is more capable of responding to frequency deviations [10].

6. Connect Neighboring Sub-Systems Together

At this stage, the objective is to connect the individual island sub-systems. This stage is necessary because one or more tie paths to the BPS might not be available which, means that it is not possible to connect the islands individually to the BPS. In this case, it is necessary to connect the several islands to form a larger sub-system that should be connected to the BPS [10].

Accordingly to [16] and [17], it is necessary to ensure a proper sectionalizing strategy in order to maintain the system stable throughout the restoration procedure. This means that the following criteria must be considered: in every island a minimum of one black-start unit must exist; the islands should have monitoring equipment in order to ensure the proper stability and security required; every island must have voltage control capabilities in order to maintain the voltage values between the limits; the frequency in each island must be kept stable by balancing the load and generation; and the tie lines between sub-systems must have proper monitoring equipment in order to ensure the synchronization of the islands before connecting them together.

7. Supply Unserved Load

After creating a large and stable power system, the next step would be to restore the unserved loads as soon as possible. In order to accomplish this objective, the strategy to be followed consists in energizing the lines that connect the stable system to the load centers, and consider small load increments to avoid large frequency deviations [10].

This stage is characterized by a multi-step procedure in which the system operator is responsible for determining which loads can be restored, and which loads are able to be supplied simultaneously. Furthermore, the number of loads to be restored depends on the inertia of the system in every time-step [18].

8. Follow-Up After Ending Restoration Procedure

In this stage it is assumed that the load is finally restored and connected to the BPS, which means that it is necessary to provide proper reserves by restarting additional generators and the remaining transmission lines should be energized.

Finally, the power system is completely restored. The next step is to document the events encountered during the process, in order to enhance the future restoration processes [10].

2.1.2 - Example of a Restoration Process

Considering the actual restoration process after a wide area blackout, it is clear that it is a very complex problem. The primary objective is to re-energize a high number of elements of the power system, such as generation units, tie lines and loads, therefore several restoration steps are required. It is important to understand that at every step of this process the reliability and the stability of the grid should be assessed before taking the next one [19]. An example of a possible restoration process is shown in Figure 2.2, where it is considered the IEEE 14 bus power system that went in a complete blackout status.

In **stage A**, the power system is in a complete blackout status. No energy is being supplied and, therefore, there are no loads connected to the grid. This is the starting point of the process in which the conditions presented in Section 2.1.1 where assessed and verified.

In **stage B**, the black start units are dispatched, such as hydroelectric power plants and gas and fuel turbine units. These units start to supply some local loads thus creating two different islands.

In **stage C** the two islands are synchronized together, thus the system becomes bigger and more robust. Then, the generators start to re-energize the lines connecting other power plants that do not possess black-start capabilities, and also the grid transformers and shunt devices [19].

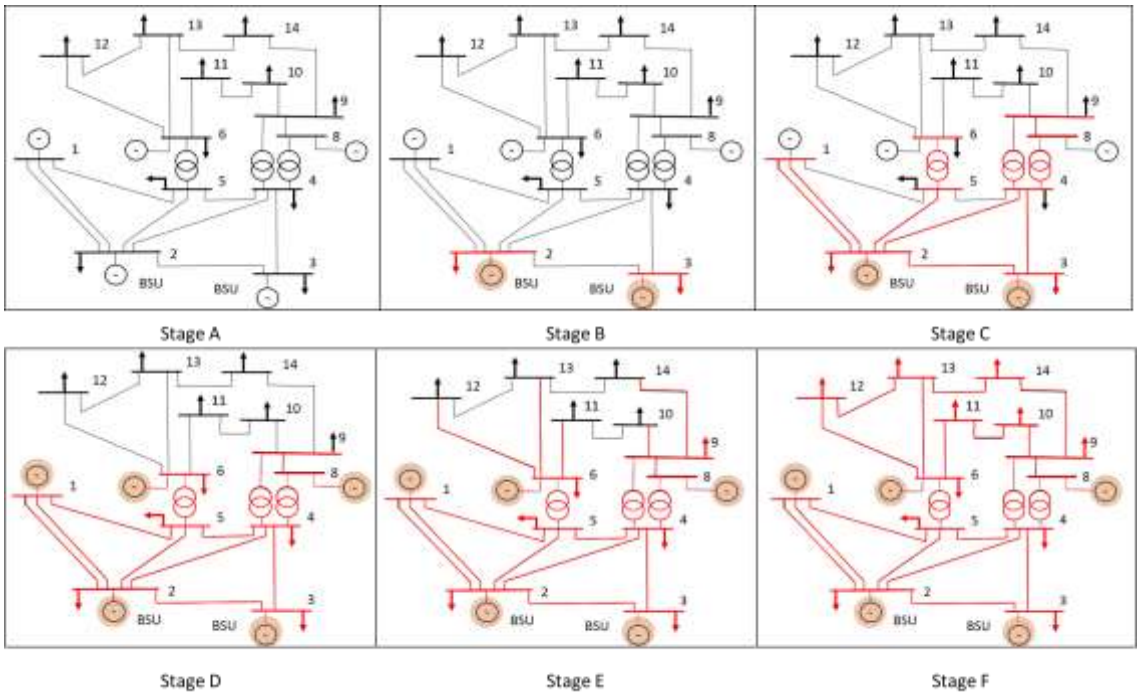

Figure 2.2 – Different phases of a restoration process in the IEEE 14 bus system.

In **stage D**, the units without black-start capabilities are started and connected to the power system. After the system stabilizes, more loads are able to be connected to the grid to balance its production and consumption. This stage of load and generation increase, consists in a slow pick-up load process to increment both production and load maintaining the system balanced. At this point, it is important to check for any limit violation regarding the power system parameters.

In **stage E**, the remaining lines are energized and some more loads are connected to the power system according to the available reserve of the generation units. Finally, in **stage F** the system is fully restored and operational

It is important to notice that the causes of a blackout are directly connected to the time that the restoration process will take. If the problem is related to the infrastructures, in general caused by natural catastrophes, since the existing transmission lines and other infrastructures may not be available, the process can take much more time than when the problem is caused by other small scale incidents [19].

It is also important to state that island formation should be avoided if it is not planned. This is due to the fact that by isolating a smaller system from the interconnected grid it is more difficult to maintain the stability and balance of the grid constraints, since there is a reduction of the system's inertia. If this situation cannot be avoided, then the island should be connected to the BPS as soon as both systems are synchronized [10].

2.1.3 - Problems Faced During the Process

During the process described in the previous section, it is likely to encounter several problems that will make the system operator shift the strategy in order to overcome these issues.

The most common issues related to power system restoration involve reactive power balance, switching transient over-voltages, self-excitation, load and generation balance, load and generation coordination, cold load pick-up, load shedding, standing phase angles and low frequency isolation schemes [11], [20], [21].

Reactive power balance is directly connected with keeping the voltage magnitudes within the predefined limits. This means that, in order to maintain this balance, it will be necessary to provide the proper excitation level to the generators, deactivate switched static capacitors as well as connect shunt reactors and make adjustments in transformer taps [11], [22].

It is clear that energizing small sections of the power system will indeed increase the total restoration time, which means that energizing large sections of the latter should be a priority. However, this means that switching transient voltages are likely to occur and to have a more significant impact in the restoration process, in terms of damaging the insulation of the installations [11].

This phenomenon can be explained by the fact that transmission lines have the particularity of having inductive characteristics, which means that a connection between these lines and a system will undoubtedly produce a transient. The arresters installed along the transmission system help to manage these types of over-voltages. These over-voltages are directly connected with the charging currents of the transmission lines which may cause the absorption of reactive power by the black-start units in the early stages of the restoration process. In this case there is the risk of self-excitation, meaning that the voltage will rise uncontrollably causing a severe stability problem [21].

In order to maintain the load and generation balance, it is common to use small incremental steps of load, thus minimizing the possibility of frequency instability. Due to this procedure, it is usual to supply the smaller loads in first place. It also important to state that the increments of load are defined by the frequency response of the prime movers, which usually consist of hydro, combustion and drum type units [11].

One important issue is the load and generation coordination [23]. This problem is related to the required time intervals required to restart certain generation units, such as steam units which can take several hours to restart depending on the current status of the plant, if it is hot or not. This time intervals affect the connection time of the loads which can increase the restoration time [11].

Another major problem related to the restoration phase consists in the cold load pick-up phenomenon. It occurs when, a few hours after the power outage, the load demand is higher than it was before the event [21]. This means that when the load is restored, the demand will lead to an excessive current in the lines and cables, which are dimensioned taking into consideration simultaneity factors, and this means that the circuit breakers will act, thus the load will become unsupplied again.

The major contributors to this phenomenon include lighting devices, motors and also loads that are controlled thermostatically [15]. In [24] a quick assessment of the system frequency dynamics during cold load pick-up events is provided, in which were used linearization and optimization methods in order to simplify the model of the governors of the system's generators.

One way to stabilize the power system, preventing frequency and voltage collapse in case of a blackout, consists in load shedding. This means that it is necessary to determine the most adequate loads to be disconnected from the grid. In [25], [26] two possible strategies regarding implementation of load shedding schemes are presented. In the first one, a load shedding methodology applied to distribution systems, which is based on a teaching learning-based optimization method is presented, while the second one proposes a different approach considering a voltage instability index. Through load shedding it is clear that more consumers will be affected, which means that this method is normally used as a last resource [26].

When transmission lines are connected between two separated systems, it is necessary to assess the difference between the standing phase angles (SPA) of each system [11]. If this difference is excessive, it can lead to a recurrent power outage and also to rotor shaft impact [27]. This last effect is caused by the induced torques in the rotor of the machines which leads to malfunction of the generators [28]. Accordingly to [11], the limits of the SPA for different power systems are 60º for 500 kV systems, 40º for 230 kV systems, and 20º for 115 kV systems.

The low frequency isolation scheme is responsible for isolating a generating unit by supplying local loads thus ensuring that the generating unit does not need to be restarted from a complete shutdown, which saves several hours of the restoration process. However, it is difficult to maintain the balance between the generation and the load since the latter is continually changing [29].

2.1.4 - Frequency and Voltage Control

In order to maintain the system stable throughout the entire restoration process described in Section 2.1.1, it is necessary to control two major components: frequency and voltage.

In terms of frequency control, when the power system is in normal conditions of operation, the frequency is controlled by the proportional control, also known as droop control, and the integral control, or automatic generation control (AGC), of every turbine speed governors. For example, when a variation of load or generation exists in any part of the system, the frequency will increase or decrease, depending of the nature of the variation. The droop control is responsible for stabilizing the resulting frequency deviation. In order to take the frequency back to its nominal value, the AGC acts in order to eliminate the frequency deviation.

However, during the black-start stage the AGC is not operating. This means that the frequency control will be managed by the speed governor of the prime mover of the BSU, working in a isochronous (with constant frequency) control mode [21]. As soon as the non-black-start units are available, the frequency control will return to be managed by the droop control and the AGC.

Regarding the voltage, this will be controlled by the automatic voltage regulator (AVR) which is responsible for regulating the generators' excitation system, by measuring the voltage deviation and adjusting the excitation applied to the rotor of the machine. It is clear that as the load is incremented throughout the restoration process, this regulation system will be of an extreme importance [21].

2.1.5 - Power System Restoration Planning

In order to improve the restoration process when a black-out occurs, it is necessary that proper plans may exist, so that the system operator has the right tools and knowledge to successfully restore the system in the shortest time possible. It is certain that every black-out

is unique, which means that the planning process needs to be flexible in order to fit the restoration process in the different situations [19].

The objective of the planning phase is to develop procedures to be followed to meet the required criteria in terms of reliability and allow the presentation of a forecast related with the status of the power system during a blackout. It basically consists in an optimization problem where it is necessary to select the BSU, the unit start-up sequence, the restoration lines to be used and the right load pick-up sequence [19], among other variables.

Several analyses need to be addressed in order to develop a restoration plan. These include the study of potential failures and its causes, and the analysis of the restoration possibilities where the options of success of the restoration process are analyzed [10]. From here, a flexible restoration plan should be developed in order to accommodate unpredicted situations during the process. In [30] a sectionalizing planning is proposed in order to ensure the power system restoration after a complete blackout. The planning strategy determines the lines that are not suitable to be restored.

From the descriptions above explained, it is possible to show that this process is a very complex one, in which the variables keep changing, for example in the restoration planning it is considered the black-start of a unit which in that period of time actually is not available, or even the use of a tie-line that is unavailable at the same time, so it is necessary to adjust the strategy often. In order to prevent these situations from stopping the restoration process, it is necessary to create feasible alternatives.

2.2 - Power System Restoration using Microgrid Capabilities

With the growing concern regarding global warming, there has been a change of paradigm in the electric power systems. The paradigm is characterized by the increase of DER that include renewable energy sources, which means that the power systems became decentralized in terms of energy production. This led to the emergence of a new concept, the microgrid, explained in the next section.

2.2.1 - Microgrid Concept

Microgrid can be defined as a low voltage distribution grid with distributed generation units of reduced installed capacity (usually around tens of kW). These units can be included in a new category: the microsources (MS). It includes microturbines, fuel cells, renewable sources of energy such as solar photovoltaic panels (PV), wind energy conversion systems (WECS), and also energy storage units such as batteries and flywheels. Since the generation is located near the consumption points, this type of grid enhances the reliability of the power system. Furthermore, the several equipment that belong to this grid (loads and generation) possess a

controller that is constantly communicating with the microgrid central controller (MGCC), located in the low voltage side of the substation, in order to ensure the correct operation of the grid in terms of grid management and control scheme [31].

This type of low voltage grid can operate in two different modes [12], [6]:

- Grid connected mode, where the microgrid is being supplied by the medium voltage (MV) grid, in case of low distributed production, or is injecting power into the MV grid, when the distributed production is higher than the microgrid's consumption;
- Emergency mode, in which the microgrid is in island mode, being disconnected from the MV grid.

Considering a microgrid working in islanded operation, the balance between the power generated by the MS and the load cannot be instantly achieved. This means that it is necessary to ensure this balance, which is usually done by using energy storage devices (ESD). Accordingly to [32], these devices can consist in batteries, super capacitors, flywheels, superconducting magnetic energy storage, pumped hydroelectric, compressed air and thermal energy storage. There has been a new approach regarding energy storage based on electric vehicles (EV), which can be seen as a more flexible device that can improve the microgrid frequency regulation capacity, when connected to the grid, by absorbing or injecting a determined active power value [33]. A typical low voltage microgrid scheme is presented in Figure 2.3.

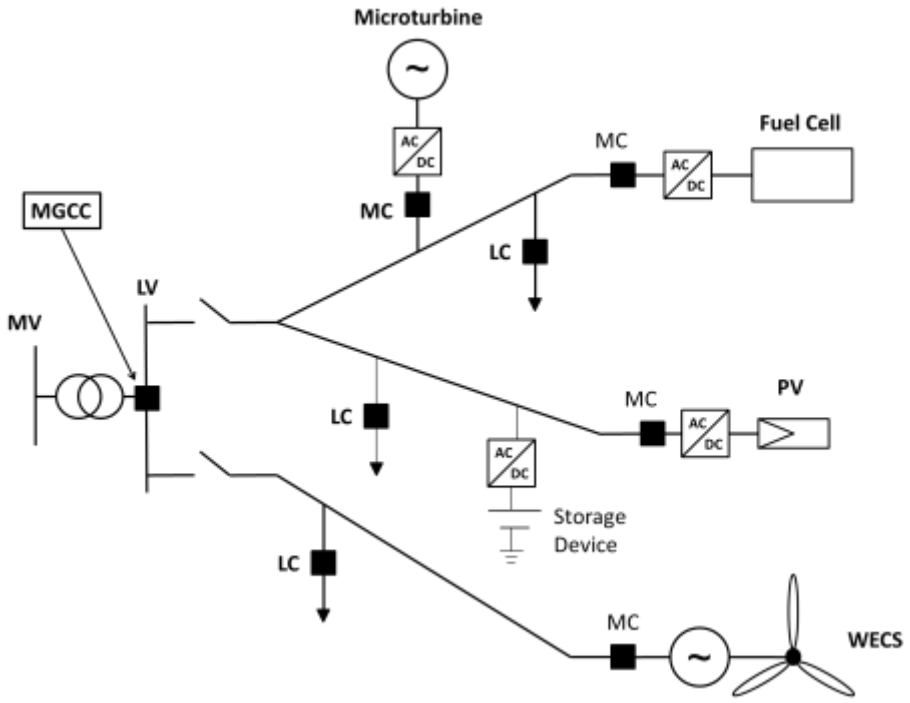

Figure 2.3 – Example of a low voltage microgrid.

Considering a large penetration of electric power from dispersed generation units, it is likely that MV grids will include several microgrids and dispersed generation units. Accordingly to [31], this means that a new environment will be created that will fall in a new category: the Multi-Microgrid (MMG). This concept is related to the possibility of controlling a large number of microgrids from a central autonomous management controller (CAMC), which will be the control level immediately below the distribution management system (DMS) and will receive measurements from the remote terminal units and the MGCC. It is established at the MV level. The hierarchical control structure is represented in Figure 2.4, adapted from [31].

Since the multi-microgrid concept is out of the scope of this dissertation, this is not presented in detail, however in [34] it is presented a complete analysis regarding the operation of MMG. The control and management architecture, the voltage control problem, the frequency control problem, the black-start capabilities and the restoration procedure guidelines are also approached.

2.2.2 - Microgrid Control and Management

The microgrid is centrally controlled by the MGCC. This device is responsible for managing the economic and technical constraints of the microgrid. It is located at the low voltage bus of the substation and also sends set-points to the load controller (LC) and microsource controller (MC) devices in order to maintain generation and load balance in the microgrid. The LC is located directly at the consumption points and enables the local load control and shedding schemes, in emergency situations. The MC allows the control of the MS by adjusting their active and reactive power injection into the microgrid [35].

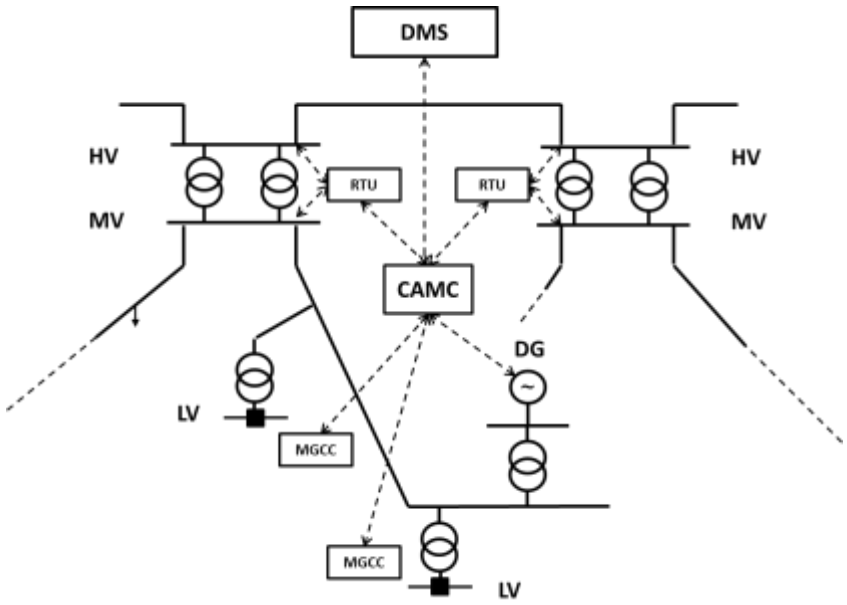

Figure 2.4 – Example of a multi-microgrid.

Microgrids are characterized by having a determined hierarchical control structure which consists in a primary level, a secondary level, and a tertiary level [36], [37]. This structure is extremely important in order to maintain a secure operation of the microgrid when it is in islanded mode.

The primary control is responsible for controlling the voltage magnitude and frequency in the connection point of the MS converters to the microgrid, through the control of the active and reactive power injection into the latter. It is also the control level that acts faster, and conventionally it is based on droop control techniques. Furthermore, it provides islanding detection, output control and power-sharing [38]. It acts in order to stabilize the voltage and frequency deviations but does not eliminate them.

The secondary control will act as the energy management system (EMS) of the microgrid and it is responsible for the improvement in power quality, voltage and frequency restoration and resynchronization of the microgrid with the MV grid. This level of control will eliminate the voltage and frequency deviations, stabilized in the first place by the primary control level [39].

The tertiary control will take in consideration the economic aspects of the operation of the microgrid and will be responsible for the power flow control between the microgrid and the MV grid, when the first is in grid connected mode. It is the control level that will take longer to act and by receiving the active and reactive power reference, it will adjust the voltage and frequency reference of the microgrid in order to control the power flow between grids [40].

In [41], an enhanced hierarchical control structure is presented, considering multiple current-loop damping schemes, as well as the modelling, the design of the controllers and the stability analysis, including small signal analysis for an islanded microgrid.

Since the microgrid concept is associated with the inclusion of several new controllable elements in the grid, the complexity of the microgrid operation problem will increase significantly. This means that new challenges related to bidirectional power flows, stability issues, low inertia and power production uncertainty will arise [42].

By including several MS, it is likely that reverse power flow situations may occur. This can be problematic since the distribution feeders were planned and designed to withstand unidirectional power flows. This can lead to overloads in the feeders which will cause the circuit breakers to act [43].

Stability issues can be related to the interaction between the control system of the MS, which means that it is necessary to perform not only small signal stability analysis but also transient stability analysis [44].

Since the working principles of these types of grids are based in inverters, which are based on power electronics, they will not provide inertia to the overall system, which makes the grids more vulnerable in terms frequency deviations, when working in emergency mode [44].

Several distributed generators included in a microgrid will be renewable based, which means that it is necessary to resort to weather forecasts. This will lead to energy production uncertainty. The load profile also has some uncertainty associated [42].

2.2.3 - Ancillary Services and Demand Response

In the conventional power systems, the ancillary services such as active power/frequency control and reactive power/voltage control are provided by the traditional power plants. Due to the high integration of distributed generators, the change in the paradigm of the power supply led to a situation where those ancillary services are considered as separate services, contrary to what happens in the conventional power systems, where those services were part of the integrated electricity supply [45].

Accordingly to [4], it is stated that the microgrids will be able to provide ancillary services as a part of the distribution system. This means that these services will be provided by the load and MS, having the advantage of making the process more efficient since these are local services, contrary to what happens in the conventional power systems where these ancillary services are provided from distant units. The most likely ancillary services to be provided are reactive power/voltage control, frequency response, regulation, supply of reserves, load following and black start.

As stated in [46], the MGCC will receive the information regarding selling and buying bids sent by the MS and load controllers, respectively, and will send this information to the market operator, and it will also acknowledge the set-points to be applied to both loads and MS sent by the market operator. Then based on this set-points, it will implement a technical study to check for any constraint that does not allow the set-points sent by the market operator.

Another interesting capability of the microgrid consists in Demand Response (DR). This capability appeared as a means to avoid loss of reliability, due to the large integration of the DER's in the distribution system, and it is related to the possibility of adjusting the demand patterns in certain consumption points as a response to several factors, such as the electricity prices and the system reliability [47]. One possible example consists in shifting the demand of certain electrical appliances at residential consumption points, to off-peak periods where the electricity prices are lower.

Accordingly to [48], [49] and [50] the demand response (DR) programs applied to residential and commercial consumers can be divided into two categories: incentive-based (or dispatchable) and price-based (or non-dispatchable) programs. The incentive-based programs allow the consumers to adjust some of their power consumptions during the peak periods or emergency periods (periods where the system's reliability may be compromised). Direct load control (DLC), interruptible/curtailable services (I/C), demand bidding (DB) and EDRP are the

most used schemes that remunerate the consumers when reducing their consumptions to determined values.

The DLC is characterized by enabling the system operator to remotely disconnect pre-defined appliances of residential and commercial consumers, for instance the heat and cooling systems, in order to avoid the loss of reliability. These consumers receive monetary incentives for that partial interruption of their consumptions. The I/C program implements a consumption curtailment that is applied in contingency situations. The interruption time, payments, penalties and capacity are specified by the contracts between the consumers and the electricity suppliers [50].

DB programs enable the consumers to participate in the electricity market by bidding determined load reductions [48], [50]. According to [51], the EDRP is very useful in situations where the power system reliability is threatened, which is the case of a total or partial blackout in a power system. This means that this program can be used during the microgrid restoration procedure, following a blackout in the latter.

Regarding the price-based programs, these enable the consumers to adjust their consumptions as a way to respond to the change of retail electricity prices over time and include three different major schemes: time-of-use (TOU), real-time pricing (RTP) and critical peak pricing (CPP). The goal of these schemes is to balance the demand curve by increasing the prices during peak periods and decreasing them in the off-peak periods [48].

The TOU scheme consists in an electricity price rate that is variable during the day and can reflect the costs of the electricity supply variation in the time periods during the day. These rates include peak and off-peak pricing and also seasonal pricing. This will make the consumers to adjust their consumptions according to the current price however, since this scheme is applied in a long-term basis in daily or seasonal cycles, in case of temporary emergency situations, the TOU scheme will not be able to encourage the consumers to adjust its demand [50].

The RTP scheme consists in a program that applies a dynamic pricing scheme, where the prices are updated in time intervals of one hour or less. In the case of CPP scheme, it considers fixed prices for several time periods just like the TOU programs but, at least in one of these time periods the prices are able to change, [50], [52]. It is important to mention that all of the previous described price-based schemes are not used in the restoration process.

2.2.4 - Islanded Operation

A microgrid will need to operate in an islanded configuration in case of maintenance of the MV transformer, fault occurrence in the MV distribution network and during the restoration procedure. Considering an islanded operation scenario of the microgrid, in which there is no connection to a synchronous generator, the microgrid needs to be able to control both voltage and frequency, in order to maintain the system stable. This control is achieved by using

inverters at the MS terminals that can be operated in V/f control (also known as VSI control) or PQ control mode [35], [4].

These control schemes are presented and described in Section 3.2. According to [12], in order to accomplish the goal of ensuring a stable islanded operation of the microgrid, two different control strategies can be identified, regarding the operation of the inverters:

- Single-Master Operation (SMO)

In this type of islanded operation, only one inverter is controlled using V/f control, thus acting as a master, and can be used as the voltage reference. The storage device inverter is the only unit that is controlled in V/f control, in this operation scheme. The remaining inverters are operated in PQ control mode. This operation scheme can be found in Figure 2.5.

- Multi-Master Operation (MMO)

When in islanded operation, MMO is an operation scheme where more than one inverter is operated in V/f control and it is presented in Figure 2.6. Generally, both storage devices and single-shaft microturbines are the units controlled under V/f control mode. There can be other inverters operated in PQ control mode. In this case, a power sharing situation will occur, in which the frequency deviation will cause different active power output variations in each one of the VSI, as follows [35]:

$$\Delta P = \sum_{i=1}^{n} \Delta P_{\mathrm{i}}, \tag{2.1}$$

where ΔP corresponds to the total active power variation and ΔP_{i} represents the active power variation of one VSI only. Besides, it is possible to calculate the frequency deviation by applying the equation below [35]:

$$\Delta\omega = k_{pi} \cdot \Delta P_{\mathrm{i}}, \tag{2.2}$$

where k_{pi} represents the proportional droop coefficient of the VSI number i.

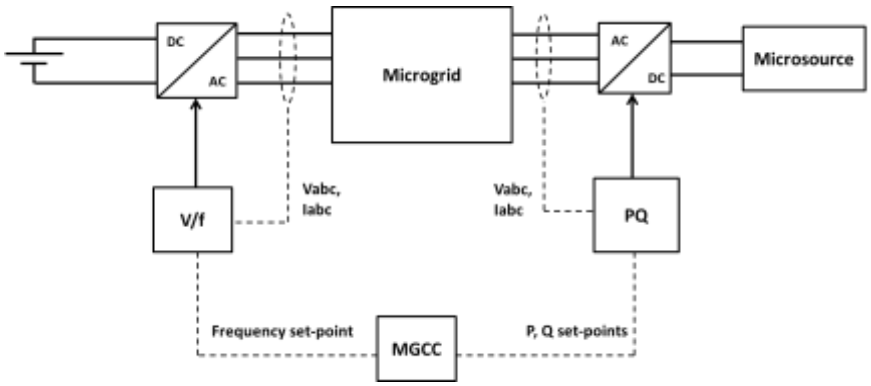

Figure 2.5 – SMO operation.

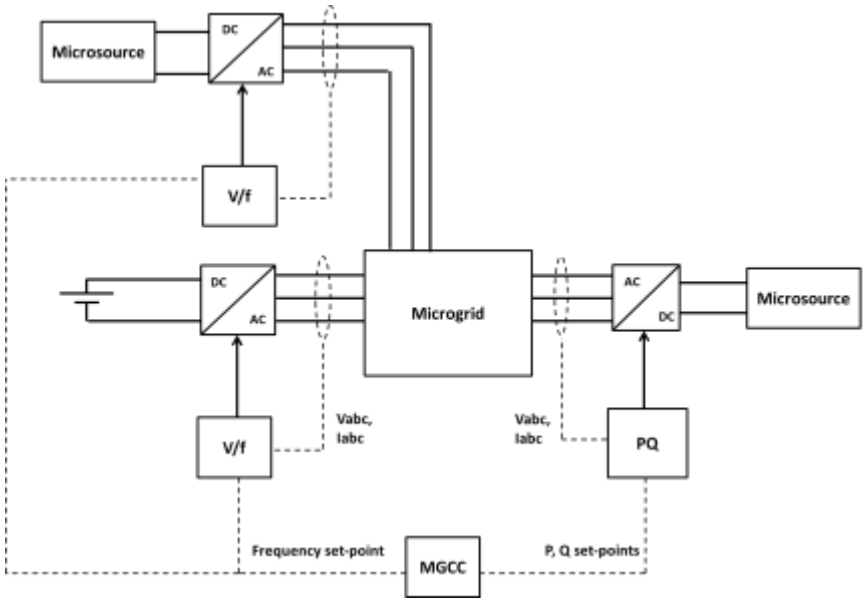

Figure 2.6 – MMO operation.

For instance, in [53] a microgrid management strategy for islanded operation is presented, based on a fuzzy approach, with the objective of maximizing the number of customers supplied, for a determined period of time. Furthermore, a unit commitment methodology for microgrids in islanded operation is formulated.

2.2.5 - Restoration procedure in microgrid

After a general blackout, it is necessary to restart the power system as soon as possible. In order to accomplish this task, the first step is to start the distributed generation units of the microgrid that have black-start capabilities.

In [54] and [12], an overall restoration procedure based on the microgrid capabilities is presented. The restoration procedure is characterized by the following steps, which are applied to the restoration of the microgrid, assuming that all the DER are disconnected and therefore, no load is being supplied:

1. **Microgrid status evaluation**

The initial stage of the restoration procedure consists in an assessment of both the upstream network and the microgrid, provided by the MGCC. The objectives of this assessment are that the MGCC will only begin the restoration procedure if there is a confirmation of the actual occurrence of a blackout by the distribution system operator, since it is possible that a blackout did not occur, but instead a switch malfunction occurred, and also to verify the status of all the components of the microgrid to look for a possible local fault or failure of one or more components [54], [33].

2. Restarting Black-Start units

In this stage, the MGCC is the controller responsible for sectionalizing the microgrid, ensuring that all the loads and MS are disconnected from the low voltage microgrid. After this assessment, the MS classified as black-start units are restarted and will supply local loads in order to maintain the balance between power production and consumption, thus stabilizing the process. This means that small islands will be created inside the microgrid [12].

According to [55], in a microgrid the dispersed generation units with black-start capabilities are the ones that possess storage devices in the DC link of the corresponding inverters, such as batteries or super-capacitors. This means that these units are able to start without any other auxiliary power source in the initial stage of the restoration process. Furthermore, the inverters of these units must be operated in V/f control mode. Hence, these units must possess a short charging time and must be able to establish, and maintain, the voltage and frequency of the microgrid [56].

3. Energizing the low voltage microgrid

After restarting the black-start units, the next step is to energize the microgrid using the central storage unit located at the low voltage bus of the substation. Since both loads and generation units are still disconnected from the low voltage grid, the frequency and voltage of the grid will be at its nominal value [54].

4. Synchronization of the islands

After energizing the low voltage microgrid, the next stage will be to synchronize the previously formed islands, formed by restarted MS and local loads, with the latter. This is accomplished through the MGCC, in coordination with the MC, by checking the frequency and voltage values. The assessment of the phase sequence is also important for the synchronization process. It is desired that, by assessing these conditions, large transient currents are avoided. [12].

5. Load and non-controllable MS reconnection

The next step will be to reconnect the controllable loads, taking into consideration the capacity of the microgrid central storage. Then, the MS that cannot be controlled, such as PV and wind unit, should be reconnected to the low voltage grid, considering the local generation and the storage capacity available. Since the controllable loads are connected firstly, the microgrid can support the connection of the MS without severe voltage and frequency deviations [12].

6. Synchronization of the microgrid with the upstream grid

The final stage of the restoration procedure consists in the synchronization and connection of the microgrid to the upstream grid, after receiving the order from the distribution system operator (DSO) [33], [54]. The transformer connecting the microgrid to the upstream grid should be energized firstly by the MV grid before the microgrid can be reconnected [12].

In [7], the microgrid restoration procedure is validated by using a multi-agent system in order to determine the most suitable restoration actions to follow during the simulation. It is shown that the utilization of the common capabilities available at microgrids can be a great improvement.

Besides being able to perform its own restoration based on local resources, the microgrid can also assist the distribution system restoration procedure by providing adequate services. Such services include [6]:

- The ability to operate in island mode, which avoids the disconnection of the low voltage consumers;
- It can provide DR strategies by adjusting the local loads in order to meet the microgrid's production availability;
- The possibility of increasing the power production in order to inject power into the MV network, thus acting as a black-start source.

In [31] the distribution system restoration using MMG is tested and validated. The tested MV grid includes several microgrids and DG units and its restoration procedure demonstrates the feasibility of the integration of microgrids in the distribution system environment, as well as the decrease of the total restoration procedure duration, when compared to the conventional power system restoration.

2.3 - Novel Approaches

In this section, a literature review regarding several novel strategies for power system restoration is presented. There have been several studies and simulations regarding strategies based on multi-agent systems (MAS), electric vehicles (EVs), stochastic methods, spanning tree search, complex network theory, firefly optimization algorithms and black-start integration of wind power [3].

The multi-agent system approach is based on an interactive set of intelligent agents, which possess a set of goals in common. These agents can recognize changes in the environment, being able to react to those changes, make decisions and help other agents in order to achieve their objectives [57]. In [58] the restoration of a smart grid system based on a distributed multi-

agent system was performed on a six bus system using Tennessee Technological University Smart Grid Laboratory.

In [59] it was proposed a multi-agent approach which was compared to the solutions obtained by using the mathematical programming approach. It was concluded that the proposed approach reaches the correct solution, the quality of the solution was similar to the solution obtained by the mathematical approach and only used local information. A Belief-Desire-Intention (BDI) agent-based approach was presented in [60]. This strategy can be adapted to any size or structure of a power system and it was shown that the approach becomes more efficient and effective as the scale of the power system expands.

EVs can be seen as flexible storage devices that can be useful in the power system restoration procedure. In [61] it was proposed a model for power system restoration which uses EVs as a support for the generators start-up procedure. This model consisted in a bi-level optimization-based network reconfiguration scheme which was solved by a particle swarm optimization algorithm. It was concluded that a centralized charging station for EVs could increase the effectiveness of the restoration process of a power system in case that there were not black-start capabilities available or the black-start generators do not provide sufficient cranking power.

A proposed strategy regarding the active integration of the EVs in the microgrid restoration procedure was presented in [33]. Here, it was described a new functionality of the EVs designated as vehicle-to-grid (V2G). This functionality enables the possibility of the EV to participate in the frequency control of the microgrid by using an active power/frequency droop control, in the vehicle inverter.

In [62] the service restoration problem in a renewable powered microgrid, operating in island mode, due to an unscheduled disconnection from the upstream grid, was addressed. The main challenges were the uncertainty of the renewable production and duration time of the disconnection from the main grid. Two methods based on stochastic information were proposed, to address the scheduling problem that can provide two efficient solutions close to the optimal solution.

Ref. [63] addressed a stochastic model that can provide support to the decision making process regarding the restoration procedure in a pre-hurricane situation. In this study, two different approaches, regarding a complete restoration and a partial restoration of the system, were provided. Moreover, a stochastic mixed integer linear method was proposed in order to verify the potential of the microgrids black-start capabilities in [64].

Regarding spanning tree search methods, a graph-theoretic strategy for the power system restoration, based on the inclusion of microgrids in the distribution system, was presented in [9]. Here, the objective was to maximize the load restoration by minimizing the number of actuations of the switching devices. The proposed algorithm was capable of determining an optimal solution in terms of network topologies.

In [65] the microgrid black-start capabilities were analyzed, and the existing microgrids in the power system were sectionalized, automatically. The unserved critical loads were then supplied by the microgrids with enough generation margins, through the application of a spanning tree search algorithm.

The increasing integration of wind power in the power systems has increased the risk of power outage occurrence, since this type of energy is naturally associated with volatility and uncertainty [3]. In terms of complex network theory approaches, associated with the integration of wind power, it is possible to find a model based on this method in [66].

In this work was proposed an improved complex network theory considering the integration of wind farms to define a model that enables the power flow analysis of a cascading power failure. Although not related with wind power integration, also in [67] was proposed an algorithm for the reconfiguration of transmission networks using complex network theory. This algorithm consisted in a self-healing restoration scheme.

Regarding the firefly optimization algorithms, and still related to the integration of wind power integration in the power system, in [68] it was presented an algorithm capable of finding the optimal sequence of the start-up of the non-black-start units, the most adequate transmission paths to be used and also the optimal sequence for the load pickup procedure, by considering and not considering the integration of wind power systems. It was concluded that the integration of the wind farms is actually beneficial since it allowed the reduction of the unserved load.

Another field of studies is the integration of wind farms in the restoration procedure by using these wind systems as a black-start unit. In [69] was presented an hybrid black-start unit which includes a combustion gas turbine, a static synchronous compensator and a wind farm. Then, a control model based on a three-level scheme was presented, which enabled the control of the active and reactive output of the unit. It was also presented a control scheme that enables the variable speed wind turbines to contribute to the frequency and voltage regulation of the system.

In Table 2.1 it is presented a taxonomy table that classifies all the consulted contributions in this presented state of the art and also in the previous chapter.

Table 2.1 - Taxonomy table.

Year	Overview	PSR Issues/Planning	Black-Start	Network configuration	Load Restoration
1991		[11]			
1995	[10]				
2006	[35], [20]	[23]			
2007					[12]
2008		[28], [29]	[15]		
2010	[22] ,[46]				[13]
2011			[31]	[17]	
2012	[45], [40], [50]	[19], [14]			
2013	[2] ,[4], [36]	[27]	[64], [33]		
2014	[1], [5], [34], [42]	[66], [21]	[55]	[60], [59], [16], [9]	[18], [58], [6]
2015	[54], [57], [48], [52]	[63]	[69], [68]	[8]	[62]
2016	[43] ,[39], [3], [49], [51]		[65], [61]	[67]	[70] ,[24]
2017	[53], [37], [41], [38], [32], [47]	[25], [26], [30], [44]	[56]		[7]

2.4 - Chapter Summary

Blackouts are characterized by not being frequent events but, when they do happen, can lead to long periods of time where the consumers will not be supplied. This can be problematic since critical consumers, such as hospitals and universities, cannot afford an extended period without electric power.

The first approach described in this chapter reviews the conventional power system restoration, in which the restoration procedure begins from the transmission system and then progresses towards the lower voltage levels. This means that the distribution system consumers will need to wait a long period of time to be supplied. This procedure is implemented by the system operator.

The second approach reviewed in the same chapter is based on the change of paradigm in the electric systems, in which several dispersed generation units and microgrids are connected to the power system. This way, it is expected that the coordination of these resources will lead to a shorter unavailability time, especially regarding the distribution system consumers, since it is based on a bottom-up procedure in which the restoration process begins in the distribution system and comprises autonomous controllers.

Furthermore, there have been new approaches that use advanced computational techniques and also new microgrid resources, such as EVs and wind farms, in order to improve the existing restoration procedures by decreasing the total restoration duration.

Chapter 3

Dynamic Modelling of Benchmark MG

In order to study the restoration procedures in a microgrid environment, it is necessary to evaluate the dynamic behavior of a LV test microgrid. This means that it is necessary to create a model of the latter. In this chapter, the dynamic models of the MS and its control architectures, are presented as well as the load and network modelling used to build the low voltage microgrid. The models of the MS include a PV array, a single-shaft microturbine, a split-shaft microturbine, a wind generator, a solid oxide fuel cell and a storage device, while the control architectures used consist in the PQ control and V/f control that are presented in Section 3.2. The simulation platform used to implement the models described is the MATLAB/Simulink.

The low voltage (LV) microgrid considered in this study consists in a three-phase system, with balanced operation that supplies a suburban residential area. However, this is not the most common situation in the current low voltage distribution grids, since single phase loads and generation units usually exist. The detailed description of the LV microgrid can be found in [71]. The microgrid is presented in Figure 3.1.

Regarding the loads, they were considered as constant impedance loads, that are characterized by depending on the voltage value, with a power factor of 0.85 and its nominal value can be found in Table 3.1. It is assumed that the consumer 3 and 5 are controllable loads in two load steps.

The LV microgrid has a circuit breaker at the low voltage bus of the substation, contrarily to what happens in the typical low voltage grids where it is common to find fuses instead. However, a circuit breaker is necessary in order to ensure the flexibility needed for enabling the islanded operation of the microgrid, by disconnecting/connecting both the microgrid and the MV grid, respectively.

The maximum power production of the microgrid is 63kW if every MS is injecting its maximum output, and its maximum active load is 98.94kW. This means that the microgrid is unable to supply all of its loads in case of islanded operation.

The microturbine displayed in Figure 3.1 is considered to be the split-shaft microturbine for single master operation and the single-shaft microturbine for multi-master operation. Furthermore, since the microgrid consists in a low voltage grid a TN-C earthing system was also considered.

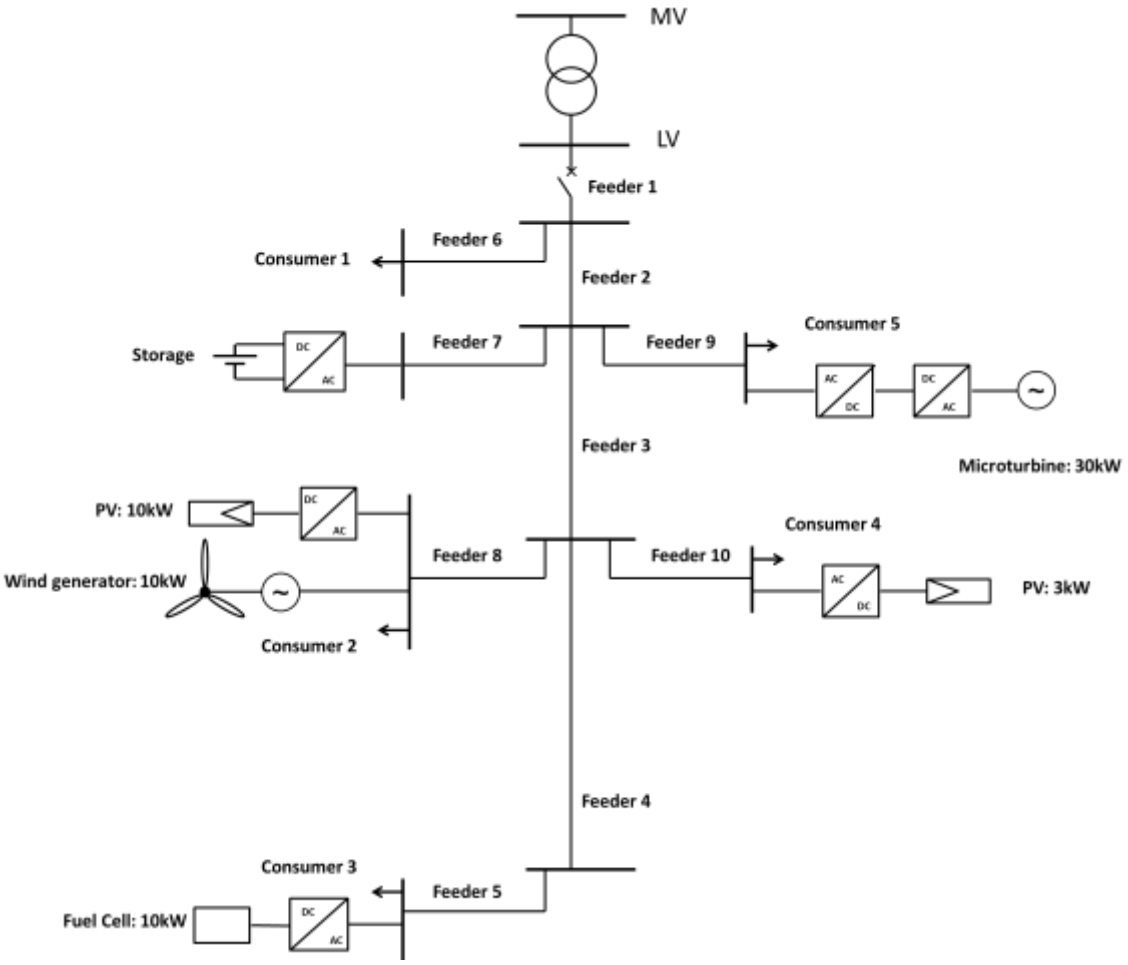

Figure 3.1 – Low voltage test microgrid.

Table 3.1 – Nominal loads.

Consumer	S (kVA)
1	5.7
2	23
3	25
4	5.7
5	57

The feeders have specific lengths and electric characteristics that can be found in Table 3.2. These were modelled as a RL series branch and for the MV grid it was considered a Thévenin equivalent of a voltage source, connected to RL series branch that is also connected to a three-phase transformer, as shown in Figure 3.2.

3.1- Microsources Dynamic Modelling

The existing MS can be divided into two categories: the controllable and non-controllable MS. The first set is related to the MS that can adjust its output power in order to meet the microgrid demand including the single-shaft, the split-shaft microturbines and also the fuel cell. The second set refers to the MS that cannot adjust its output power according to the microgrid demand, since these are dependent of external variables, such as meteorological conditions, including the PV array and the wind turbine.

Table 3.2 - Feeder characteristics.

Feeder	Lenght (m)	R (Ω)	X (Ω)
1	35	0.00994	0.002905
2	35	0.00994	0.002905
3	70	0.01988	0.00581
4	105	0.02982	0.008715
5	65	0.05134	0.005365
6	30	0.1107	0.00282
7	30	0.0414	0.00246
8	30	0.02613	0.00243
9	65	0.064485	0.01134
10	30	0.1107	0.00282

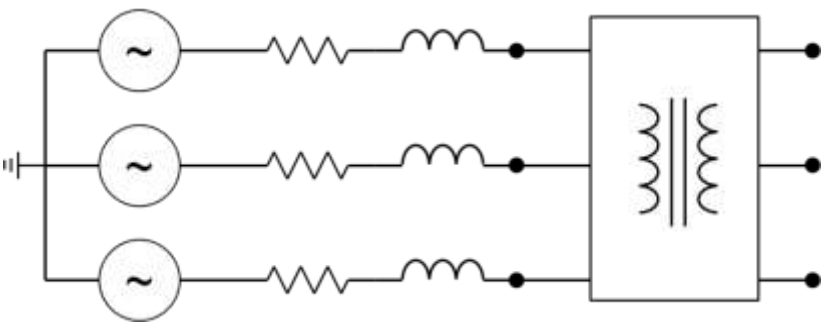

Figure 3.2 - Equivalent MV network and transformer.

3.1.1 - Photovoltaic Array

In this work a PV array was considered. The model used for the PV cell is available in [72] and it is represented in Figure 3.3. The equation regarding the current and voltage of the PV cell and the PV array are presented as follows:

$$I = I_{ph} - I_0 \cdot \left(e^{\frac{q(V+R_S \cdot I)}{A \cdot k \cdot T}} - 1\right) - \frac{V + I \cdot R_s}{R_{sh}}, \tag{3.1}$$

$$I_{sa} = N_P \cdot I_{ph} - N_P \cdot I_0 \cdot \left(e^{\frac{q}{A \cdot k \cdot T} \cdot \left(\frac{V_{sa}}{N_s} + \frac{R_S \cdot I_{sa}}{N_P}\right)} - 1\right) - \frac{N_P}{R_{sh}} \cdot \left(\frac{V_{sa}}{N_s} + \frac{I_{sa} \cdot R_s}{N_P}\right), \tag{3.2}$$

In these equations, I/I_{sa} represent the output current of the PV cell/array and V/V_{sa} correspond to the terminal voltage of the PV cell/array. The PV cell used is the "BP 585F" and its parameters can be found in Table 3.3.

Table 3.3 - PV cell characteristics.

Parameters	BP 585F
Maximum Power (W)	85
Voltage at MPP (V)	18
Current at MPP (A)	4.72
Short circuit current (A)	5
Open circuit voltage (V)	22.1
Temperature coefficient of Isc (%/°C)	(0.065±0.015)
Temperature coefficient of Voc (mV/°C)	-(80±10)
Temperature coefficient of power (%/°C)	-(0.5±0.05)
NOCT (°C)	47±2

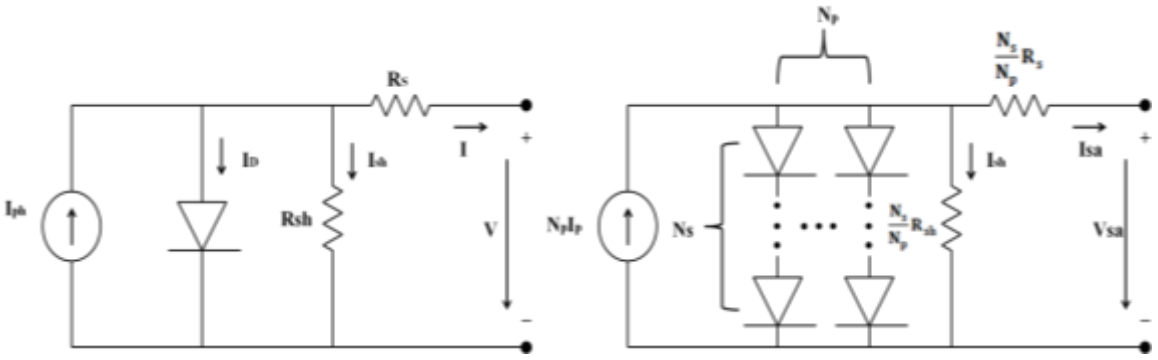

a) b)

Figure 3.3 – PV cell/array equivalent circuit a) PV cell circuit b) PV array circuit.

The PV cell "BP 585F" model is then used to build the PV array. It is assumed that the system is being operated at the maximum power point during the simulation, for determined temperature and irradiance conditions. Thus, a maximum power point tracking (MPPT) algorithm will not be considered, and the operation point of the characteristic of the PV cells will be the one presented in Figure 3.4. In [73] several MPPT algorithms are presented.

Finally, the complete PV system will include the array, a DC/AC inverter controlled using PQ control strategy which is discussed in Section 3.2, and a low pass filter in order to improve the system dynamics. This system is represented in Figure 3.5.

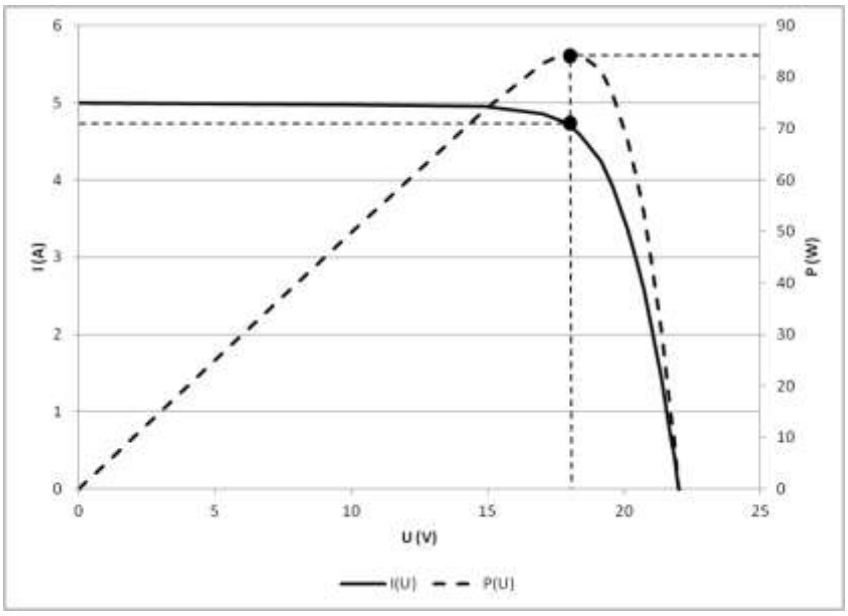

Figure 3.4 – I(V) and P(V) characteristics of the "BP 585F" PV cell.

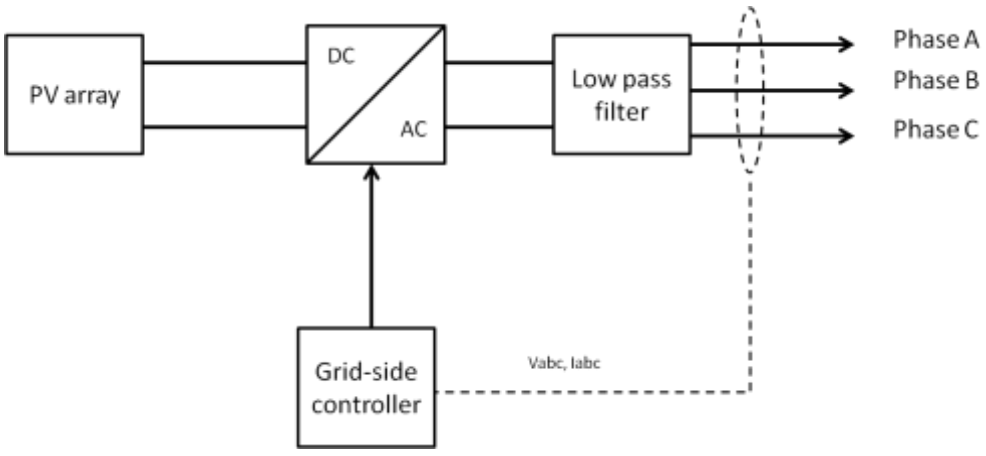

Figure 3.5 – PV system model.

3.1.2 - Microturbines

Microturbines consist in small gas turbines with a power generation capability from 25kW to 300kW. There are two possible configurations: the single-shaft microturbine and the split-shaft microturbine [74] ,[75].

The single-shaft microturbine (SSMT) is characterized by one single shaft that connects a synchronous generator, which usually consists in a permanent magnet synchronous generator (PMSG), to the turbine and to the compressor. This generator produces power at very high frequencies, usually in the range of kHz, which will require an AC/DC/AC converter in order to accommodate the frequency of the generator to the frequency of the grid [76].

The split-shaft microturbine uses two shafts, one that connects a turbine to the compressor and another that connects a different turbine to the generator, usually an induction generator, through a gearbox. This architecture does not require an electronic converter since the rotation speeds are lower that the single-shaft microturbine, usually around 3600rpm [75], [76].

In order to control the active power delivered to the grid by the microturbine, it is necessary to consider a control system based in a PI controller that has the objective of eliminating the error between the output power and its reference value [77]. This control system can be found in Figure 3.6.

In both split-shaft and single-shaft microturbine, the gas turbine (GAST) model was considered and it is available in [74]. This model considers the output power from the power control and the angular velocity as inputs and determines the mechanical power to be applied to the generator. This model is presented in Figure 3.7 and its parameters can be found in Table 3.4.

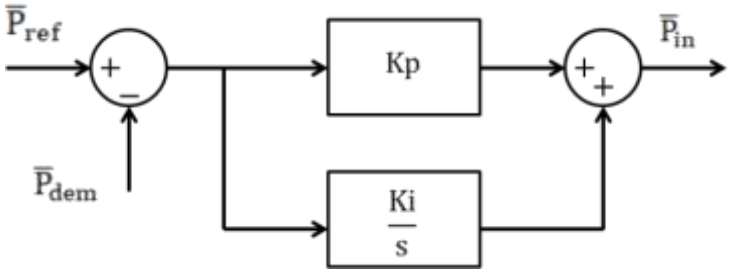

Figure 3.6 – Microturbine power control.

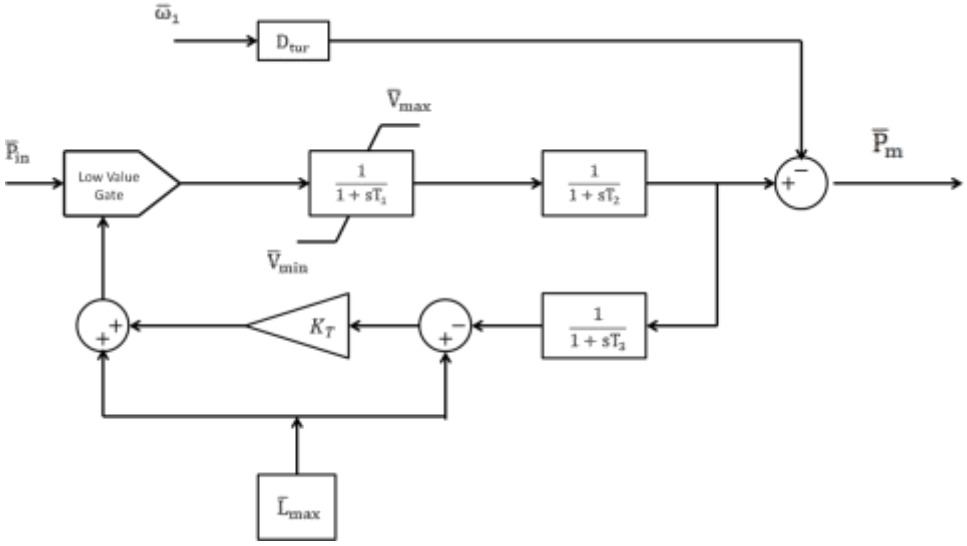

Figure 3.7 – Microturbine GAST model.

Table 3.4 – GAST model parameters.

Parameters	GAST
T_1 (s)	10
T_2 (s)	0.1
T_3 (s)	3
D_{tur}	0.03
L_{max} (pu)	1.2
V_{max} (pu)	1.2
V_{min} (pu)	-0.1
K_T	1
Kp	100
Ki	10000

From Figure 3.7, T_1 and T_2 represent the time constants of the fuel system, T_3 represents the load limit time constant, V_{max} and V_{min} consist in the maximum and minimum position of the fuel valve, respectively, and L_{max} represents the load limit parameter [77].

The split-shaft microturbine is modelled by connecting the split-shaft microturbine to an induction generator directly connected to the microgrid, as presented in Figure 3.8. This is a simple model that requires a capacitor bank, in order to avoid the excessive consumption of reactive power from the induction generator of the microturbine.

Regarding the SSMT, the generator will be a PMSG. Consequently, the power electronic interface will consist in an uncontrolled diode rectifier coupled to an inverter, which will be controlled in V/f control mode.

In order to ensure black-start capabilities, the SSMT is equipped with a storage unit at its DC link. A battery model available at the Simulink toolboxes was used, and the DC/DC regulator consists in a linear voltage regulator that increases the output voltage of the battery in order to ensure a proper value for the DC link voltage. The single-shaft microturbine diagram is presented in Figure 3.9.

3.1.3 - Wind generator

The wind generator consists in a wind turbine coupled to an induction generator, directly connected to the microgrid. Since it uses an induction generator, it will absorb reactive power which means that a capacitor bank is required. The model is presented in Figure 3.10.

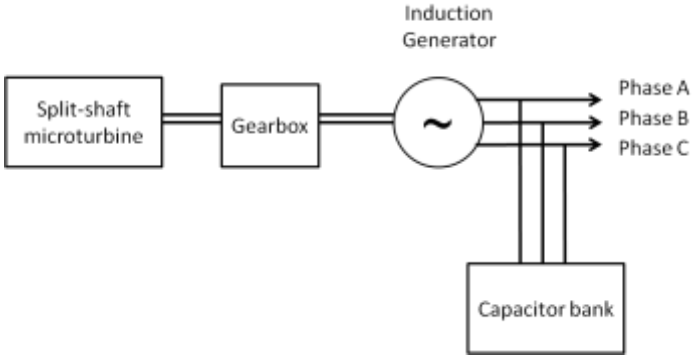

Figure 3.8 – Split-shaft microturbine model.

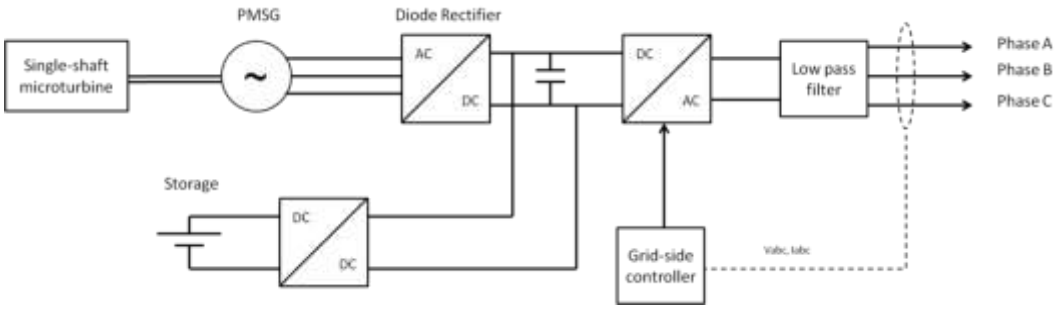

Figure 3.9 – Single-shaft microturbine model.

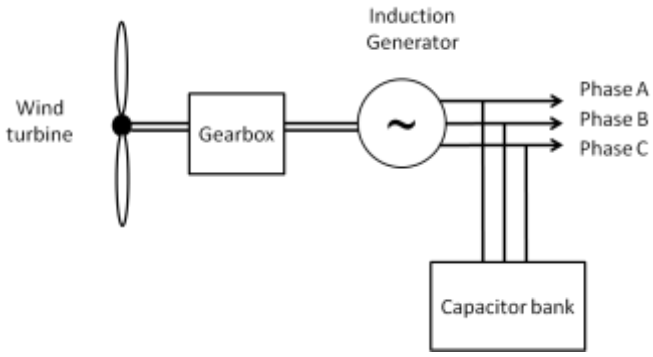

Figure 3.10 – Wind generator model.

The fundamental equation that calculates the mechanical power that can be extracted by the wind turbine is given by [78]:

$$P_m = \frac{1}{2} \cdot \rho \cdot C_P(\lambda, \beta) \cdot A \cdot V^3, \tag{3.3}$$

where P_m represents the mechanical power (W), C_P is the performance coefficient of the wind turbine, λ is the tip speed ratio (rad), β indicates the pitch angle (deg.), A represents the area swept by the blades (m^2), ρ is the air density (kg/m^3) and V is the wind speed (m/s).

The power coefficient assumes a high importance, since this variable defines the amount of energy that can be extracted from the wind kinetic energy by the wind turbine. It is a function that considers the pitch angle and the tip speed ratio, and its equation is presented as follows [78]:

$$C_P(\lambda, \beta) = 0.5176 \cdot \left(\frac{116}{\lambda_i} - 0.4 \cdot \beta - 5\right) \cdot e^{\frac{-21}{\lambda_i}} + 0.0068 \cdot \lambda, \tag{3.4}$$

where λ_i can be calculated as [78]:

$$\frac{1}{\lambda_i} = \frac{1}{\lambda + 0.08 \cdot \beta} - \frac{0.035}{\beta^3 + 1}, \tag{3.5}$$

Regarding the pitch angle, it was considered to be zero in order to obtain the maximum mechanical power from the wind turbine.

3.1.4 - Solid Oxide Fuel Cell

A fuel cell consists in a device that can produce electrical energy from a chemical reaction. This device is constituted by two electrodes: an anode (negative charge) and a cathode (positive charge). A electrolyte layer also exist, being responsible for enabling the circulation of electrons between the anode and the cathode [77].

There are two major steps in the operation of the fuel cell. In the first place, an oxidation reaction occurs in the anode which is responsible for separating the hydrogen atoms into negative charged electrons and positive charged protons. Secondly, a reduction reaction

occurs at the cathode as a result of the combination between the oxygen atoms, the protons and the electrons [77].

There are several types of fuel cells that are classified according to the type of electrolyte used. Proton exchange membrane fuel cell (PEMFC), alkaline fuel cells (AFC), direct methanol fuel cells (DMFC), molten carbonate fuel cells (MCFC), phosphoric acid fuel cell (PAFC), and solid oxide fuel cells (SOFC) are the most common types of fuel cells [79].

The fuel cell model parameters can be found in Table 3.5. The SOFC was considered and its model is presented in Figure 3.11. More details are available in [74]. This type of fuel cell is characterized by operating at high temperatures (700ºC – 1000ºC). This means that the start-up time of this particular fuel cell in order to reach the required temperature can be significantly high, between 30 and 50 minutes [77], [80].

The partial pressure of hydrogen (p_{H_2}), the partial pressure of water (p_{H_2O}) and the partial pressure of oxygen (p_{O_2}) can be calculated as follows, all measured in atm:

$$p_{H_2} = \frac{\frac{1}{K_{H_2}}}{1 + \tau_{H_2} \cdot s} \cdot \left({q_{H_2}}^{in} - 2 \cdot K_r \cdot I \right), \tag{3.6}$$

$$p_{H_2O} = \frac{\frac{1}{K_{H_2O}}}{1 + \tau_{H_2O} \cdot s} \cdot 2 \cdot K_r \cdot I, \tag{3.7}$$

$$p_{O_2} = \frac{\frac{1}{K_{O_2}}}{1 + \tau_{O_2} \cdot s} \cdot \left({q_{O_2}}^{in} - K_r \cdot I \right), \tag{3.8}$$

where K_{H_2}, K_{H_2O}, K_{O_2}, represent the valve molar constant of hydrogen, of water and oxygen respectively, τ_{H_2}, τ_{H_2O}, τ_{O_2}, stand for the response time for hydrogen flow of hydrogen, water and oxygen, respectively.

An important parameter to be considered consist in the fuel utilization parameter, which corresponds to the ratio between the fuel flow which reacts inside the stack and the input fuel flow. This parameter can be calculated as follows [77]:

$$U_f = \frac{{q_{H_2}}^{in} - {q_{H_2}}^{out}}{{q_{H_2}}^{in}} = \frac{{q_{H_2}}^{r}}{{q_{H_2}}^{in}} = \frac{2 \cdot K_r}{{q_{H_2}}^{in}} \tag{3.9}$$

The output current must be kept between a predefined limit, because for $U_f < 80\%$, the voltage would increase rapidly (under-used condition) and for $U_f > 90\%$ a permanent damage of the fuel cell could be a consequence, by fuel starvation (over-used condition) [77], [74]:

$$\frac{0.8 \cdot {q_{H_2}}^{in}}{2 \cdot K_r} \leq I \leq \frac{0.9 \cdot {q_{H_2}}^{in}}{2 \cdot K_r} \tag{3.10}$$

The hydrogen input flow (kmol/s) can be calculated as follows:

$${q_{H_2}}^{in} = \frac{2 \cdot K_r \cdot I}{U_{opt}}, \tag{3.11}$$

The open circuit voltage can be calculated using Nerst equation, presented below [77]:

$$E = N_0 \cdot \left(E_0 + \frac{R \cdot T}{2 \cdot F} \cdot \ln\left(\frac{p_{H_2} \cdot \sqrt{p_{O_2}}}{p_{H_2O}} \right) \right), \tag{3.12}$$

where N_0 is the number of cells in series, E_0 is the ideal standard potential (V), F is the Faraday's constant (96487C/mol), T is the absolute temperature (1273K) and R is the universal gas constant (8314J/(kmol.K)).

After calculating the open circuit voltage of the stack of cells, the output voltage is then calculated by using Ohm's law [77]:

$$V = E - r \cdot I, \tag{3.13}$$

where r stands for the ohmic losses (Ω/per cell) in the fuel cell stack and I represents the output current of the fuel cell (A).

Table 3.5 - SOFC model parameters.

Parameters	GAST
T (K)	1273
F (C/mol)	96487
R (J/(kmol.K))	8314
E_0 (V)	1.18
N_0	1020
U_{max}	0.9
U_{min}	0.8
U_{opt}	0.85
K_{H2}	8.43×10^{-4}
K_{H2O}	2.81×10^{-4}
K_{O2}	2.52×10^{-3}
τ_{H2} (s)	26.1
τ_{H2O} (s)	78.3
τ_{O2} (s)	2.91
r (Ω/per cell)	3.2813×10^{-4}
T_e (s)	0.8
T_f (s)	5
r_{H_O}	1.145

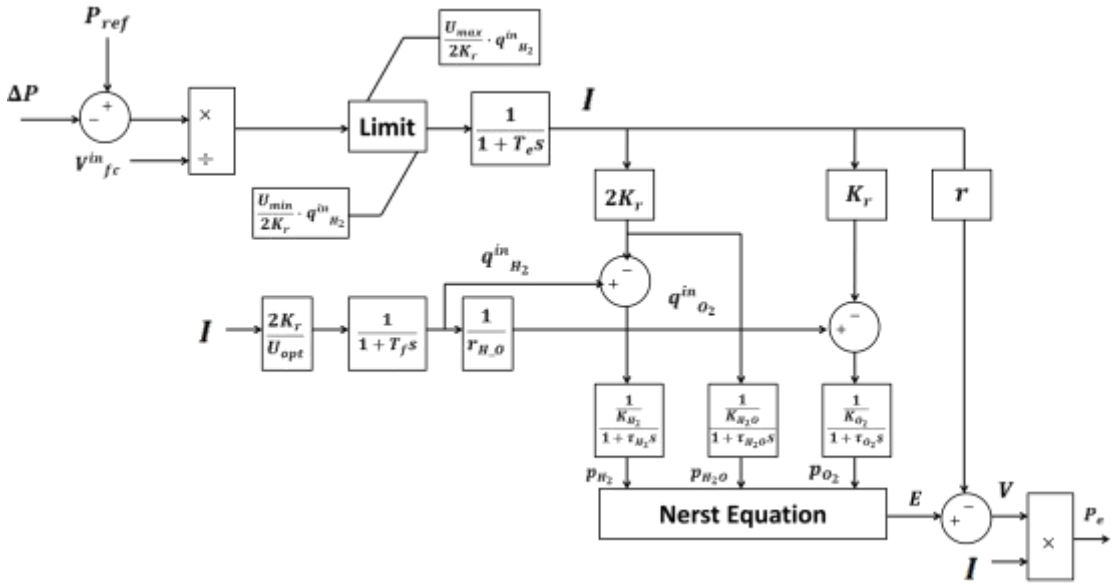

Figure 3.11 – Solid Oxide Fuel Cell (SOFC) model.

3.1.5 - Storage device

Storage devices are a crucial part of the microgrid specially when operating in island mode, disconnected from the upstream grid. These devices provide a fast response in terms of primary control by stabilizing the frequency deviations usually caused by the connection/disconnection of loads and generation units in the microgrid.

The storage device was modelled using a storage model available at Simulink libraries connected to a linear DC/DC converter that maintains the voltage at the DC link at its adequate value, coupled to a converter operated in V/f control mode and its diagram can be found in Figure 3.12.

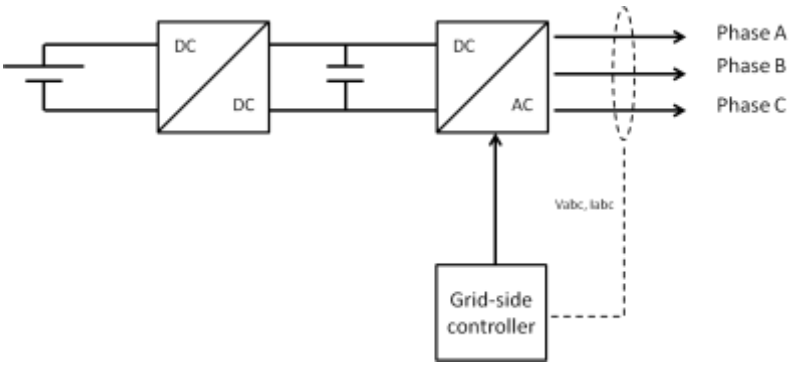

Figure 3.12 – Storage model.

3.2- Inverter Modelling

The MS of the microgrid will possess inverters that need to be controlled under specific control modes. There are two control modes in which these inverters can be operated [4]:

- PQ control

In this type of control, the inverter will inject a pre-defined set-point of active and reactive power, of the MS, into the microgrid. This set-point can be specified locally or centrally, through the MGCC [12]. This inverter is commonly used in PV or wind generation units [81]. According to [82], the principle behind this method is based on the PQ decoupling current control scheme. This method is based on the following dynamic equations of the converter:

$$\begin{cases} E_d = U_d + i_d \cdot R + L \cdot \dfrac{di_d}{dt} - \omega \cdot L \cdot i_q \\ E_q = U_q + i_q \cdot R + L \cdot \dfrac{di_q}{dt} + \omega \cdot L \cdot i_d \end{cases} \tag{3.14}$$

In order to ensure the proper decoupling of the active and reactive power, it is necessary to control the current on the d and q axis, separately. This is done by using a feedforward compensation [82]:

$$\begin{cases} E_d = U_d + K_{p,id} \cdot (i_{d\,ref} - i_d) + K_{i,id} \cdot \int (i_{d\,ref} - i_d)\, dt - \omega \cdot L \cdot i_q \\ E_q = U_q + K_{p,iq} \cdot \left(i_{q\,ref} - i_q\right) + K_{i,iq} \cdot \int \left(i_{q\,ref} - i_q\right) dt + \omega \cdot L \cdot i_d \end{cases} \tag{3.15}$$

The external inputs of the PQ controller consist in the reference values of the active and reactive power to be injected into the grid while the output of the PQ controller consists in the voltage signal (u_{abc}) to apply to the pulse width modulation (PWM). The block diagram associated to this type of control is presented in Figure 3.13, adapted from [81].

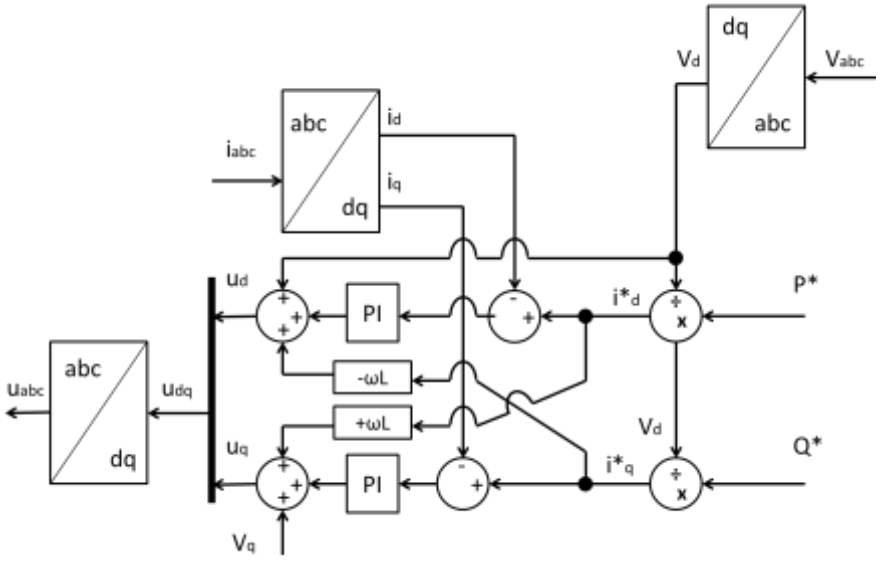

Figure 3.13 - PQ control of a MS converter.

- Voltage/frequency (V/f) control

In V/f control, the voltage source inverter (VSI) allows the control of the voltage magnitude and also the frequency, in the AC side of the inverter, thus simulating the behavior of a synchronous machine. In order to ensure this independence, the control scheme is based on the following droop equations [12]:

$$\omega = \omega_0 - k_P \times P, \tag{3.16}$$

$$V = V_0 - k_Q \times Q, \tag{3.17}$$

In this case, the active power output will be proportional to the frequency deviation of the microgrid. The inputs of the converter will be both voltage and current at the connection point of the MS with the microgrid. The output will be the voltage signal (u_{abc}) to be applied to the pulse with modulation (PWM). The block diagram that demonstrates the principle behind this type of control is presented in Figure 3.14, adapted from [7].

It can be seen that two different control blocks exist: the voltage control loop and the current control loop. These blocks were modelled by considering the "*Generalized theory of the instantaneous reactive power in three phase circuits*" also known simply as p-q theory and it is available in [83]. This theory consists in an algebraic transformation of the *a-b-c* coordinate system, which is a three-dimension vector, to a *α-β-0* coordinate system, with only two dimensions. The coordinate *0* only exists in unbalanced power systems with neutral wire. The voltage and current transformation can be obtained by applying the following equations [83], [84]:

$$\begin{bmatrix} v_0 \\ v_\alpha \\ v_\beta \end{bmatrix} = T \cdot \begin{bmatrix} v_a \\ v_b \\ v_c \end{bmatrix}, \tag{3.18}$$

$$\begin{bmatrix} i_0 \\ i_\alpha \\ i_\beta \end{bmatrix} = T \cdot \begin{bmatrix} i_a \\ i_b \\ i_c \end{bmatrix}, \tag{3.19}$$

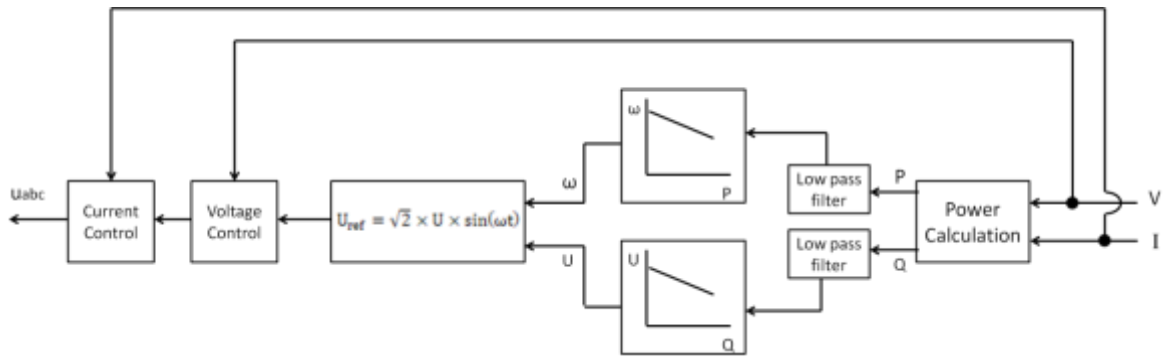

Figure 3.14 - V/f control of a MS converter.

where:

$$T = \sqrt{\frac{2}{3}} \cdot \begin{bmatrix} \frac{1}{\sqrt{2}} & \frac{1}{\sqrt{2}} & \frac{1}{\sqrt{2}} \\ 1 & -\frac{1}{2} & -\frac{1}{2} \\ 0 & \frac{\sqrt{3}}{2} & -\frac{\sqrt{3}}{2} \end{bmatrix}, \tag{3.20}$$

3.3- Chapter Summary

In this chapter, the low voltage benchmark microgrid is presented as well as its loads, its production units and its electrical features. Then, the dynamic models of all the MS and storage unit are described. The models of the inverters that connect these units to the microgrid are also described. These MS are of extreme importance when it comes to the emergency operation of the microgrid, when it is disconnected from the MV grid, and also in case of a restoration scheme after a blackout.

It can be concluded that the primary control will be ensured by the storage device in order to stabilize the frequency deviation and the secondary control will be a responsibility of the fuel cell and microturbine. It is also important to note that the single-shaft microturbine will also participate in the primary frequency control when considering the multi-master operation, however the latter is not applied to the split-shaft microturbine in single-master operation since it does not possess a VSI.

Chapter 4

Model Validation, MG Islanded Operation

In this chapter, the simulations presented in [35] were tested. The modelled microgrid is validated by considering two different scenarios: a single master operation (SMO) and a multi-master operation (MMO). In the SMO, a low load scenario and a high load scenario were tested while in the MMO case only a high load scenario was tested. The dynamic behaviour of the microgrid is then assessed in order to evaluate the feasibility of its operation in emergency mode.

4.1- Single Master Operation

In the SMO, it is assumed that only one VSI exists in the microgrid and it is responsible for controlling the storage device power output. This VSI will also be responsible for establishing the voltage reference. The remaining MS will be controlled in PQ mode and its reactive power set-points are assumed to be zero.

The existing VSI in the microgrid, in this type of operation, is the storage unit and when in island mode, its purpose is to stabilize the frequency below or above 50Hz depending on the load connection/disconnection to the microgrid. This device has a limited storage capacity, which means that it should only inject or absorb power during transient periods. So, in order to make sure that the storage returns its power output to zero, it is necessary to consider an appropriate secondary frequency control. There are two possibilities: a local secondary control, located at every controllable MS, or a centralized secondary control coordinated by the MGCC.

In these simulations a centralized secondary frequency control was considered where the MGCC sends a signal to the fuel cell and split-shaft microturbine in order to reduce or increase its production, depending on the frequency value by establishing a new active power set-point. For this purpose, a PI controller was used with a proportional gain of 0.5 and an integral gain of 5 for the low load case, and for the high load case an integral gain of 7 was considered. This secondary control is presented in Figure 4.1.

It is considered that the microgrid is operated and interconnected with the MV grid, in the first stage. For the low load case, it was assumed that at 15 seconds of the simulation, a symmetrical three-phase short-circuit occurs at the MV grid which leads to the disconnection of the microgrid from the MV grid. It is assumed that the circuit breaker that connects the MG to the MV grid acts 100ms after the fault occurrence (at 15.1 seconds).

In the high load case, it was considered that the short-circuit occurs at 5 seconds, then the circuit breaker acts at 5.1 seconds and finally at 5.6 seconds the MGCC sends a signal to the controllable loads to reduce the microgrid's consumption (load shedding scheme), thus stabilizing the frequency deviation at 50Hz.

Besides the frequency control, the microgrid also needs to maintain its voltage at the rated 400V value. To accomplish this requirement, a secondary voltage control scheme was modelled at the storage VSI. This control scheme can be found in Figure 4.2.

4.1.1- Low Load Case

In this scenario, it is considered a total load of 50.49kW and a total of 63kW of active production of the MS. The active load distribution before the fault occurrence can be found in Table 4.1. The results are presented from Figure 4.3 to Figure 4.9, respectively.

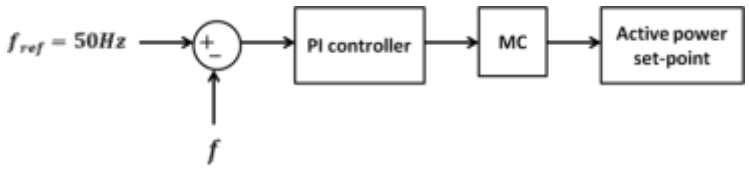

Figure 4.1 - Secondary frequency control scheme.

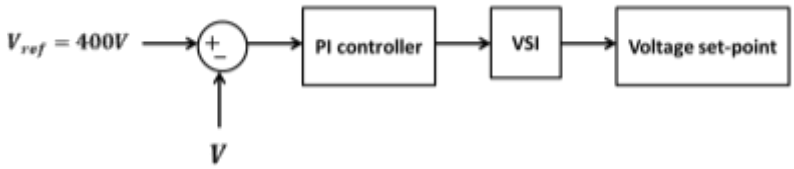

Figure 4.2 - Secondary voltage control scheme.

Table 4.1 - Active power distribution: loads and production units.

Consumer	Active load (kW)	Microsource	P (kW)
1	4.845	PV1	10
2	19.55	PV2	3
3	21.25	Wind Gen.	10
4	4.845	Fuel Cell	10
5	-	Split-shaft MT	30
Total	50.49	Total	63

Since the microgrid's production is higher than its consumption after the fault elimination, it is expected that the storage unit will absorb active power to stabilize the microgrid's frequency. Then, the controllable MS should decrease its production due to the centralized secondary frequency control.

The results were divided into two different time spans: short-term (from 14 to 18 seconds) and long-term (from 13 to 80 seconds). The first one has the purpose of analysing the transient behaviour of the MS. The second one is used to verify if the results converge to the expected solution due to the action of the secondary control scheme.

According to Figure 4.3.a, it can be observed that at 15 seconds due to the fault occurrence, the frequency starts to increase rapidly. At 15.1 seconds the circuit breaker at the low voltage side of the substation will act, and thus the frequency will start to stabilize at around 50.3Hz.

Since the frequency tends to increase after the initial transient, the storage unit will start absorbing a determined amount of power, accordingly to the droop control parameters to stabilize the frequency, as shown in Figure 4.4.a. In Figure 4.4.c, it is possible to see that during the initial transient the storage unit will increase the current magnitude significantly, about 5 times the initial value. This can cause an inverter overload. One way to overcome this problem is to select an up-rated VSI, that can sustain an overload for a determined period of time [35].

It can be seen at Figure 4.6.a and Figure 4.6.b that the PV units decrease its production considerably at 15 seconds, although this effect has more impact in the 10kW PV unit than in the 3kW PV unit. After the actuation of the circuit breaker, these units can restore its output, prior to the fault, almost instantaneously. The same behaviour can be seen in the fuel cell active output in Figure 4.5.b. The wind generator has a more significant transient (see Figure 4.5.c) since it was modelled as an asynchronous generator which will contribute to the short-circuit current.

It can also be seen that for about 0.1 seconds, the wind generator acts as a motor, but after the actuation of the circuit breaker, this MS can recover its active output in less than 0.5 seconds, since the storage unit is able to provide enough reactive power so that the generator can recover. This phenomenon can be found in Figure 4.4.b, where after 15.1 seconds the storage unit will inject a significant amount of reactive power until the stabilization of the induction generators. The same behaviour can be seen in the split-shaft active output in Figure 4.5.a, for exactly the same reasons.

Another important aspect regards the voltage at the storage unit terminals (see Figure 4.3.b). It can be seen that the short-circuit causes a significant voltage drop, which is a normal behaviour. After the fault elimination at 15.1 seconds, the voltage will be restored in about 0.5 seconds due to its local secondary voltage control scheme.

Regarding the long-term results, these are presented from Figure 4.7 to Figure 4.9. Firstly, it can be observed that the frequency will return to its nominal value of 50Hz due to the action of the centralized secondary frequency control at the MGCC. This secondary control sends new active power set-points to the controlled MS (fuel cell and split-shaft microturbine) in order to reduce its active power output (see Figure 4.7.a, Figure 4.7.c and Figure 4.8.a). At the same time, the storage active output will start to decrease in absolute value, returning its value to zero as shown in Figure 4.7.b. It can also be observed that the time that the secondary frequency control takes to act is considerable. This can be explained by the relatively high time constants of the controllable MS that leads to a slow process [35].

Finally, the non-controllable MS (PV units and wind generator) are able to maintain its active power output, which is very helpful during the islanded operation, since it enables the stabilization of the frequency in the microgrid (see Figure 4.8.c and Figure 4.9). The storage unit will be injecting reactive power into the microgrid, to feed the excitation requirements of the induction generators of the wind generator and split-shaft microturbine, as shown in Figure 4.8.b.

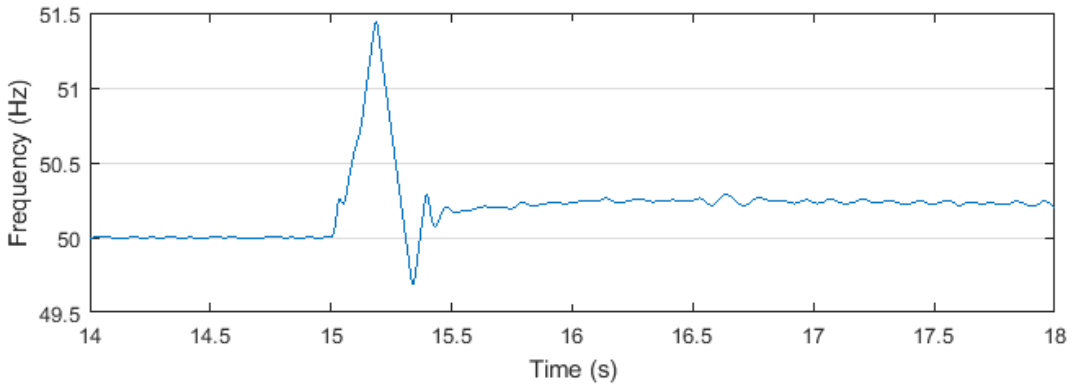

a)

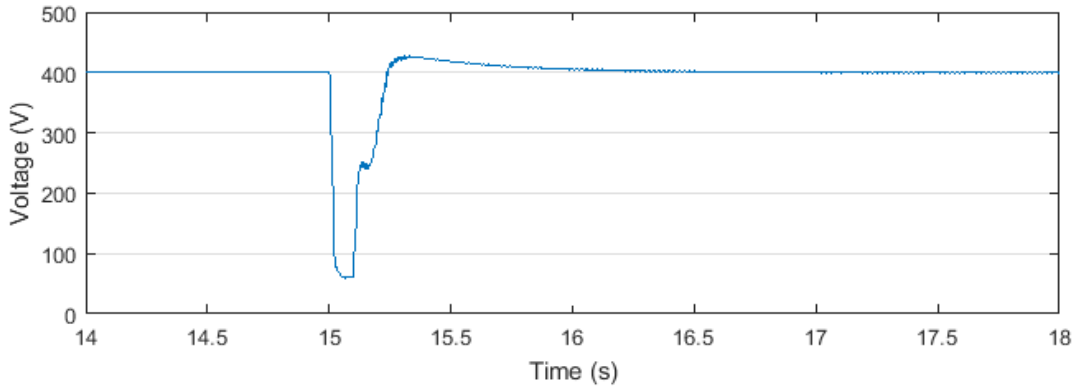

b)

Figure 4.3 - Short-term results: a) Frequency b) Storage voltage.

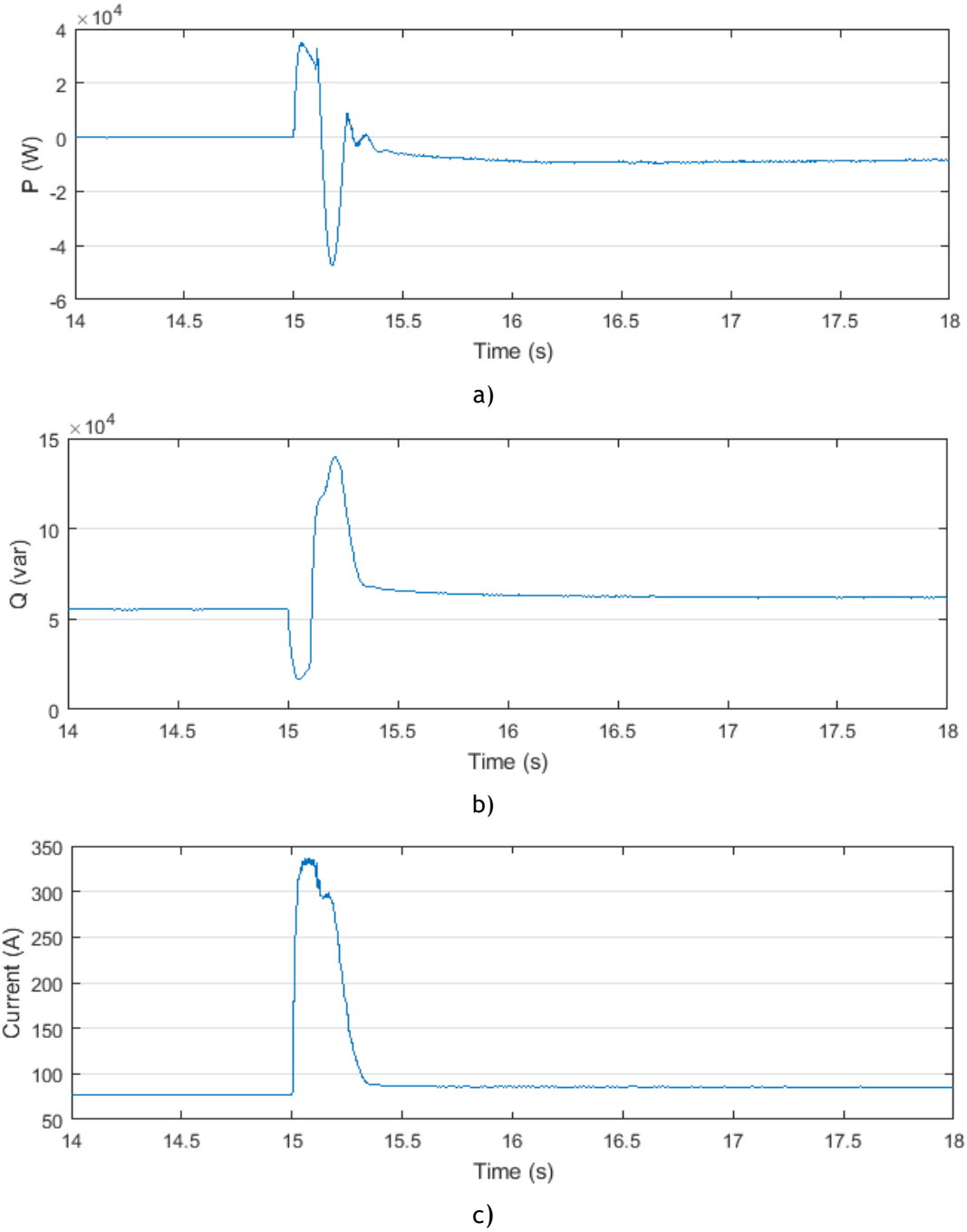

Figure 4.4 - Short-term results: a) Storage active output b) Storage reactive output c) Storage root mean square (RMS) current.

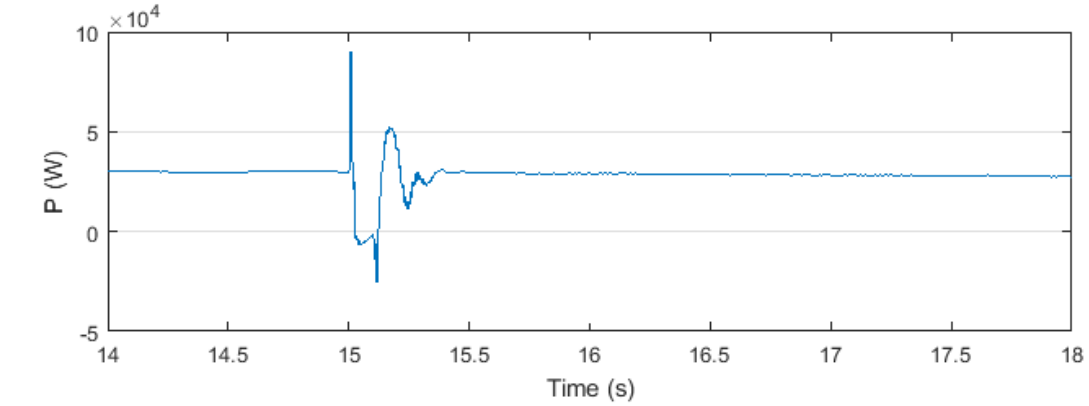

a)

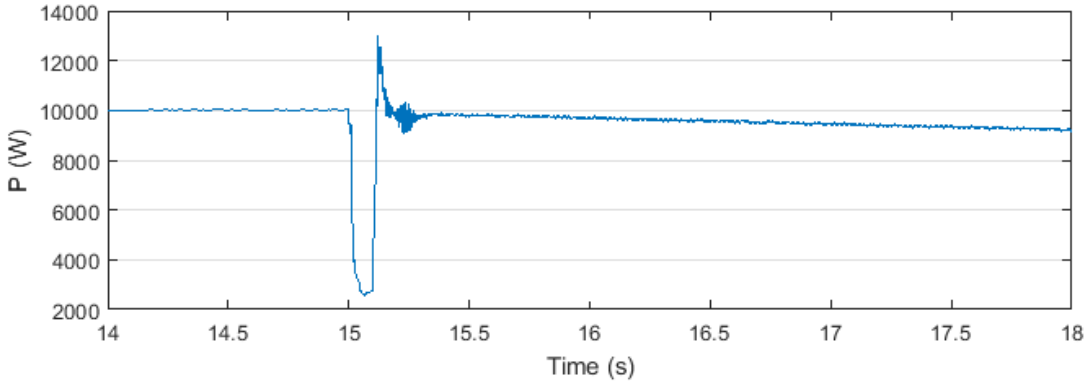

b)

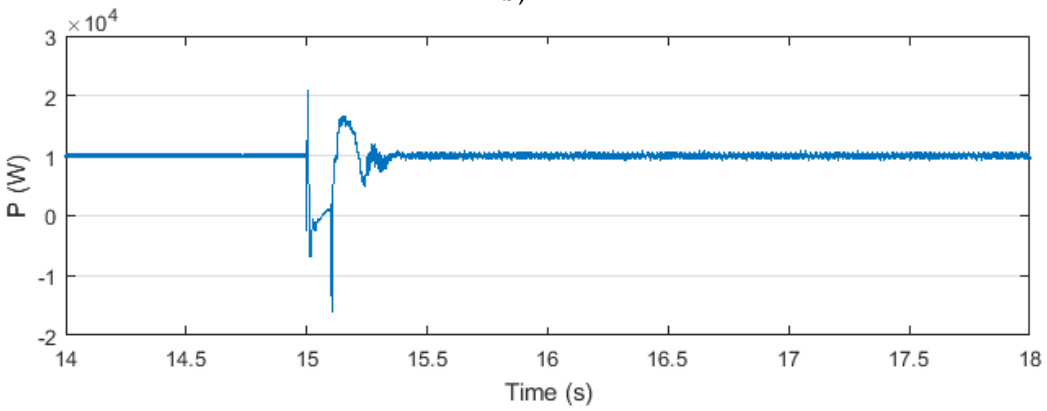

c)

Figure 4.5 - Short-term results: a) Split-shaft microturbine active output b) Fuel cell active output c) Wind generator active output.

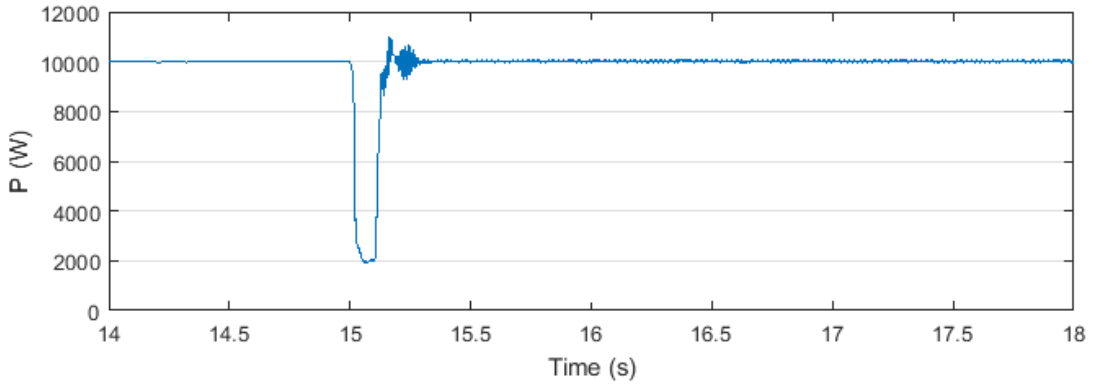

a)

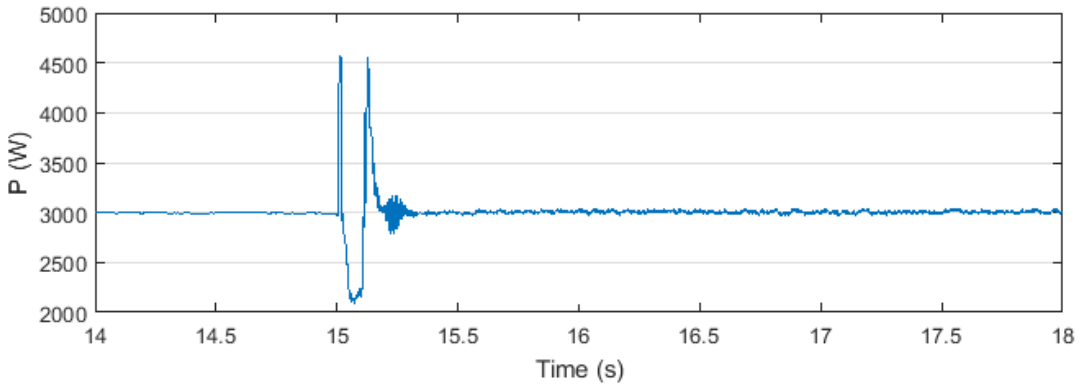

b)

Figure 4.6 - Short-term results: a) 10kW PV active output b) 3kW PV active output.

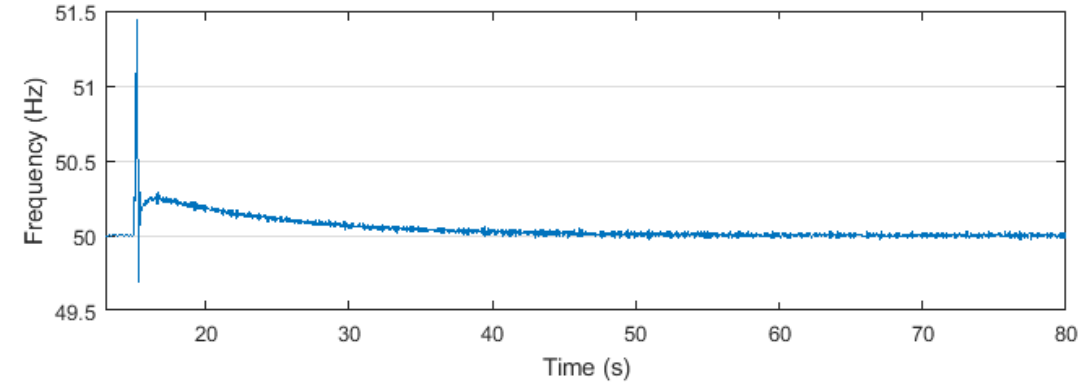

a)

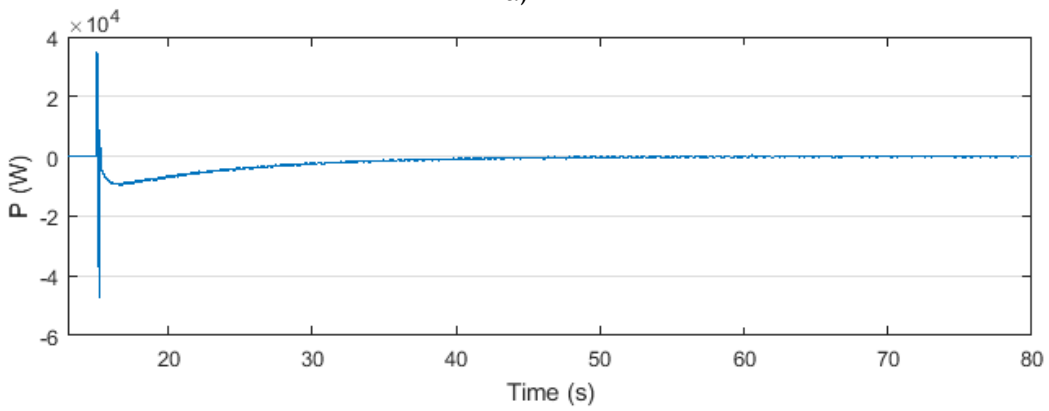

b)

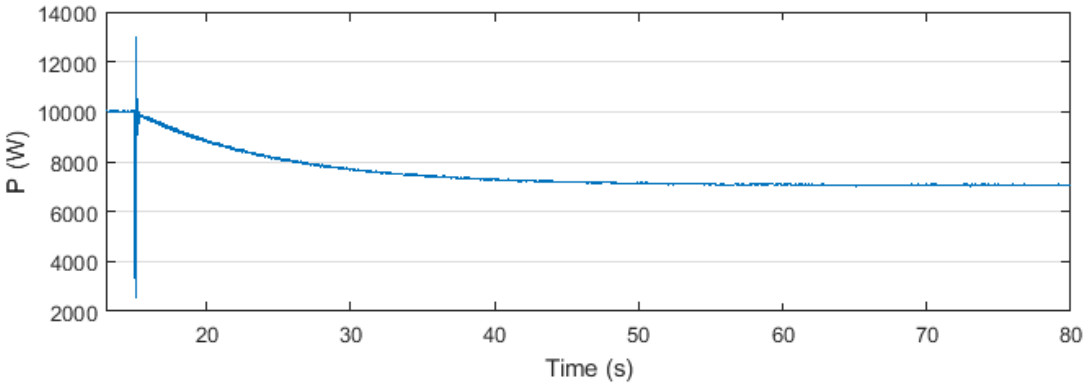

c)

Figure 4.7 - Long-term results: a) Frequency b) Storage active output c) Fuel cell active output.

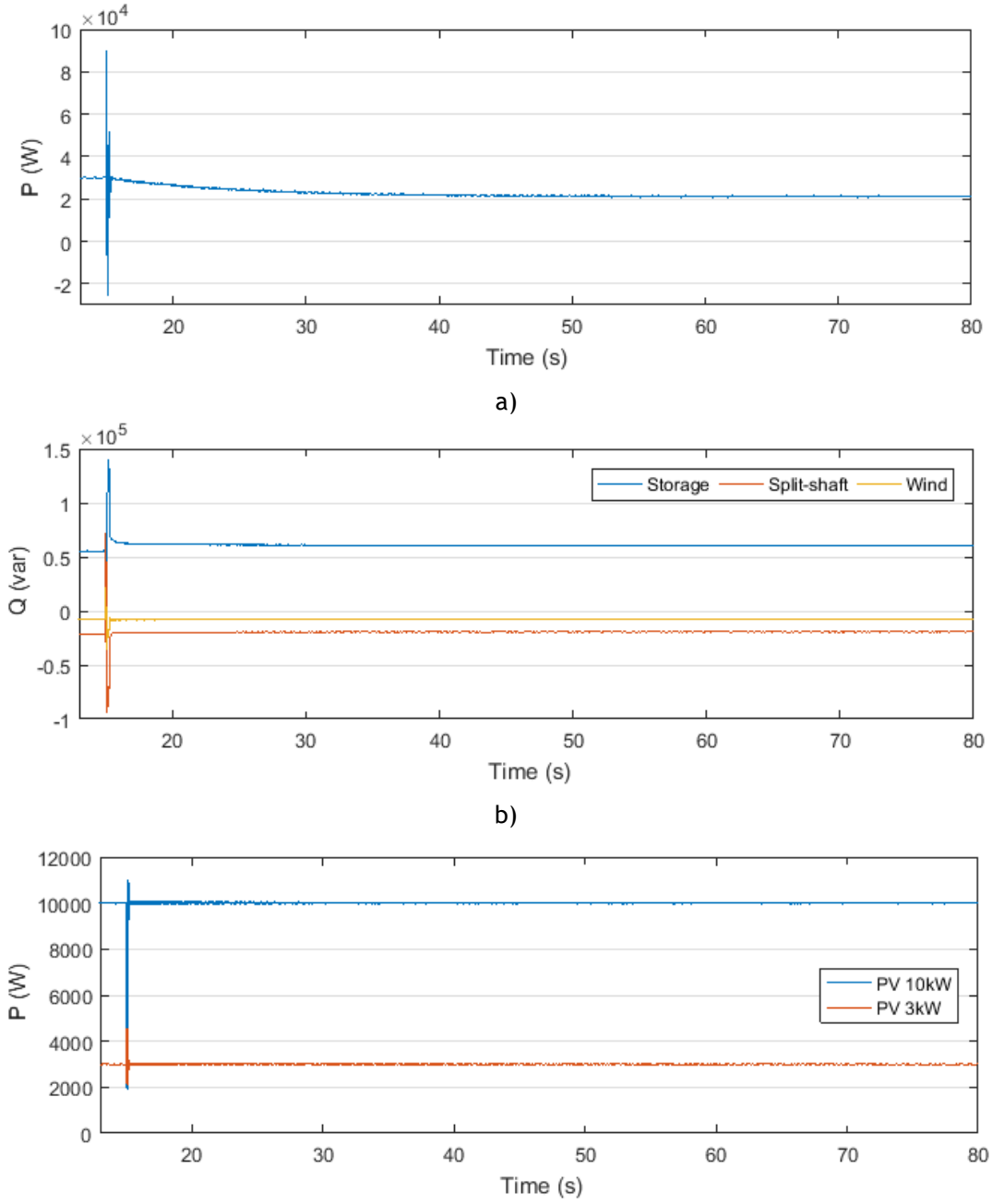

Figure 4.8 - Long-term results: Split-shaft microturbine active output b) Storage, split-shaft microturbine and wind generator reactive output c) PV units active output.

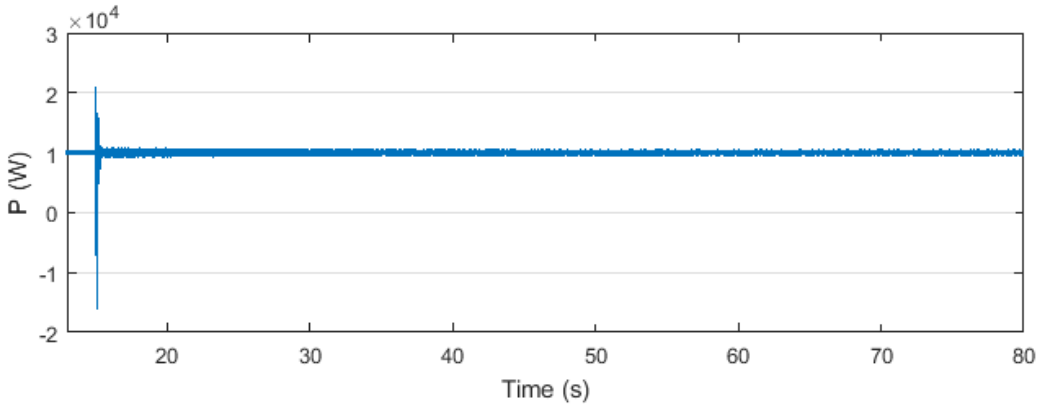

Figure 4.9 - Long-term result: Wind generator active output.

4.1.2- High load case

In the high load case, before the disconnection of the microgrid, it is considered that its total load is 88.315kW and its total production is 43kW. So, in this case there is not enough local production to supply the local load demand. The total active power consumption and production before the islanding procedure can be found in Table 4.2.

Since the local production is not enough for the current demand, it is expected that the microgrid's frequency will decrease, which means that firstly it is necessary to stabilize it. In order to do so, some of the controllable loads will be shed (consumer 1, 3, 4 and one step of consumer 5) in order to balance the local production and the local demand. This type of functionality is introduced as an emergency DR service presented in Section 2.2.3. It is possible to find the information regarding the load scenario immediately after the islanding procedure, and in the end of the simulation, in Table 4.3 and Table 4.4, respectively.

Similarly to the low load case, two time spans were considered: short-term (from 4 to 8 seconds) and long-term (from 3 to 60 seconds). The results can be found from Figure 4.10 to figure Figure 4.16.

Table 4.2 - Initial active power distribution: loads and production units.

Consumer	Active load (kW)	Microsource	P (kW)
1	4.845	PV1	10
2	19.55	PV2	3
3	21.25/2	Wind Gen.	10
4	4.845	Fuel Cell	6
5	48.45	Split-shaft MT	14
Total	88.315	Total	43

Table 4.3 – Active power load scenario immediately after islanding.

Consumer	Active load (kW)
1	-
2	19.55
3	-
4	-
5	48.45/2
Total	43.775

Table 4.4 – Active power load scenario in the final stage of the islanding operation.

Consumer	Active load (kW)
1	4.845
2	19.55
3	21.25/2
4	-
5	48.45/2
Total	59.245

According to Figure 4.10.a, it can be seen that the disconnection of the microgrid leads to a significant frequency deviation, due to the power production and consumption mismatch that needs to be compensated by enabling the load shedding functionality. By shedding some of the controllable loads indicated above (in this case loads 1, 3, 4 and a step of load in load 5), the frequency is able to return to its nominal value.

As expected, the voltage at the storage terminals will drop due to the fault occurrence (see Figure 4.10.b), but the local secondary voltage control is able to restore it in about 0.5 seconds. At 5.6 seconds the load shedding occurs, which will also cause a small voltage deviation that is also eliminated. The PV units show a similar behaviour of the low load case (see Figure 4.13).

The same phenomenon that occurred at the low load case regarding the induction machine behaviour is present in this scenario (see Figure 4.12.a and Figure 4.12.c). The split-shaft microturbine is generating around half of the power that was generating in the low load case, which means that the reactive power provided by the storage unit to enable the excitation of the induction machines will be less than in the low load case, as shown in Figure 4.11.b.

The storage unit's fast response can be verified in Figure 4.11.a where it can be seen that when the fault occurs (at 5 seconds) its active output increases almost instantaneously. Then, at 5.1 seconds when the circuit breaker provides the islanding of the microgrid its output increases again since the demand is much higher than the generation. Finally, at 5.6 seconds after the load shedding scheme, it returns to approximately zero.

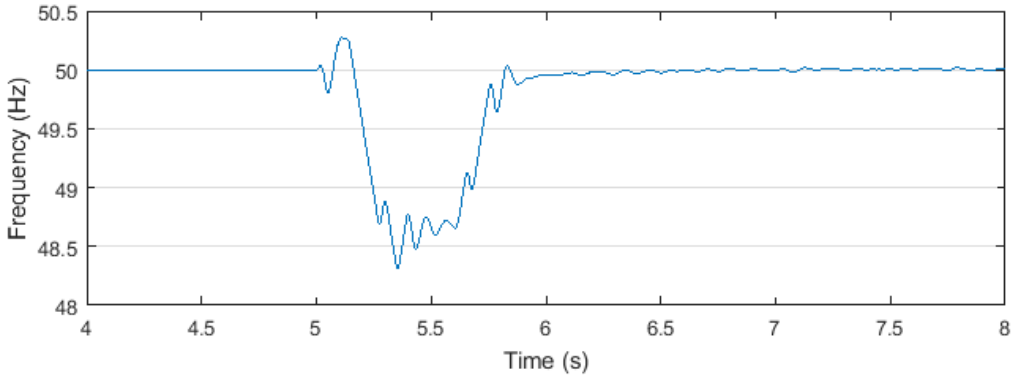

a)

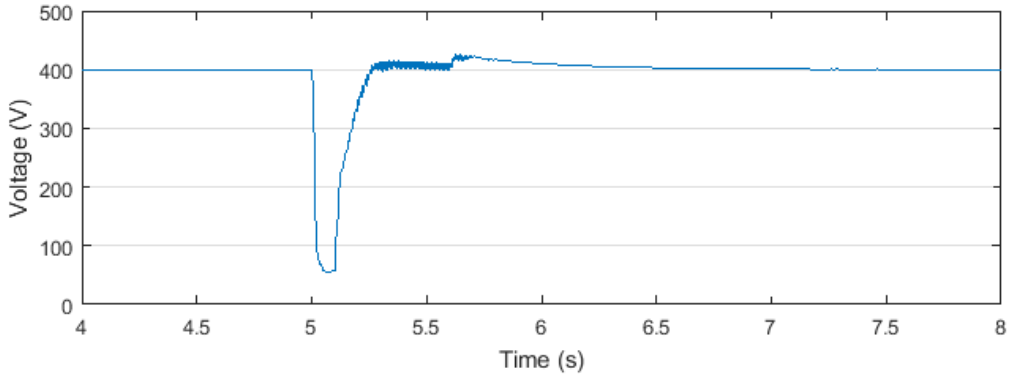

b)

Figure 4.10 - Short-term results: a) Frequency b) Storage voltage.

The fuel cell will have a similar behaviour to the low load case during the transient period, however after this period, its active output will tend to increase, due to the action of the secondary frequency control (see Figure 4.12.b). The storage will also inject a high current during this transient period, which is very similar to the low load case, as shown in Figure 4.11.c, in terms of amplitude.

Regarding the long-term time span, the frequency evolution is presented in Figure 4.14.a. There, it can be seen that the controllable loads are reconnected at 11 seconds (a step of load 3) and at 35 seconds (load 1), which causes the frequency to drop. However, this deviation is eliminated by the secondary frequency control of the microgrid. It can also be seen that the MS that ensure secondary control (fuel cell and split-shaft microturbine), increase its active power output in order to meet the power consumption and thus eliminate the frequency deviation, as shown in Figure 4.14.c and Figure 4.15.a.

This is the opposite behaviour than the one in the low load case. Besides, the remaining units (PV arrays and the wind generator) maintain its power output, which is very helpful in the frequency restoration process (see Figure 4.15.c and Figure 4.16.b). It is also important to notice that in the low load case, the initial frequency deviation is positive and in this high load

case, it is negative due to the different load and production scenarios before the islanding procedure.

The storage increases its active power output every time a load is connected to stabilize the frequency deviation and, as the controllable MS increase their production (fuel cell and split-shaft microturbine), the storage output decreases (see Figure 4.14.b). This way it is possible to ensure that the storage only acts during transient periods, thus managing its state of charge (SOC).

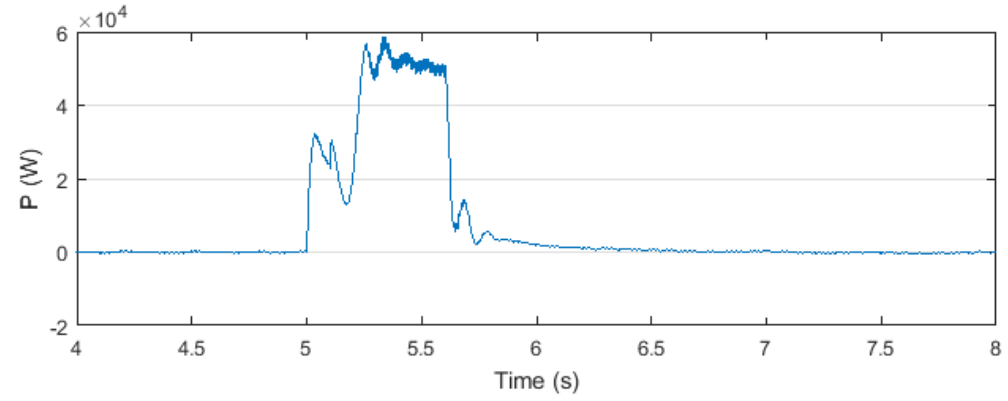

a)

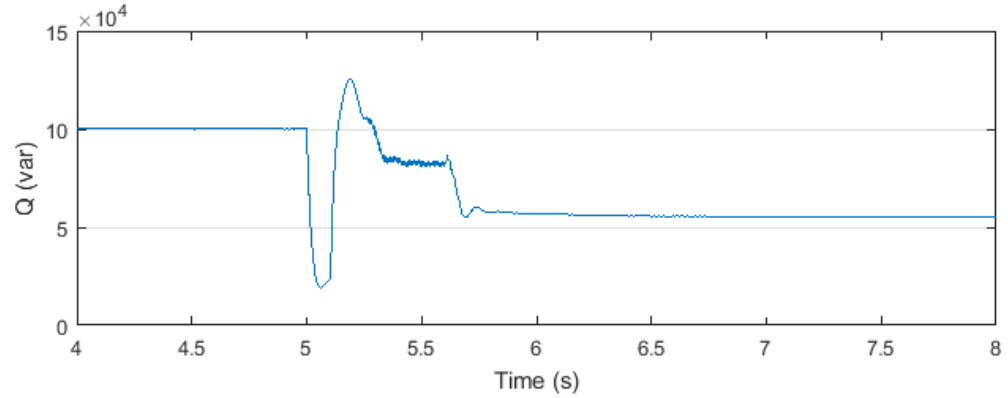

b)

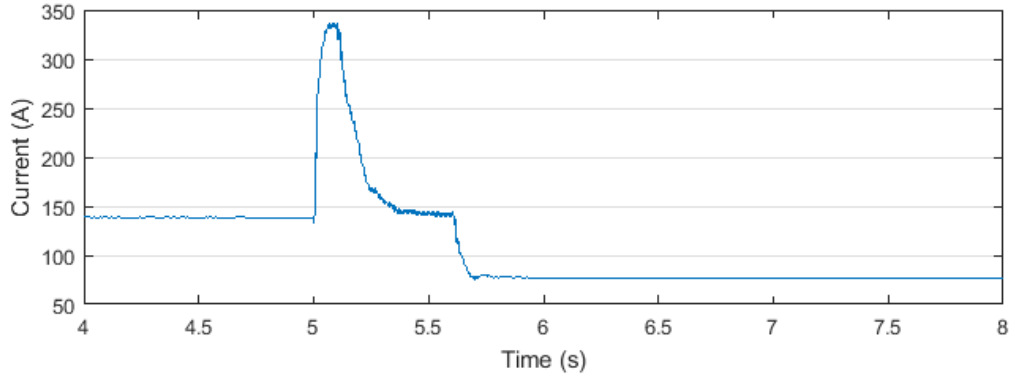

c)

Figure 4.11 - Short-term results: a) Storage active output b) Storage reactive output c) Storage RMS current.

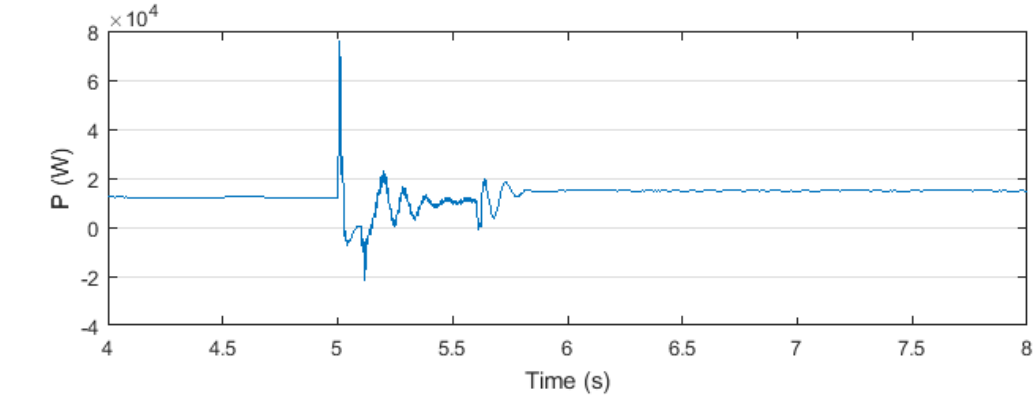

a)

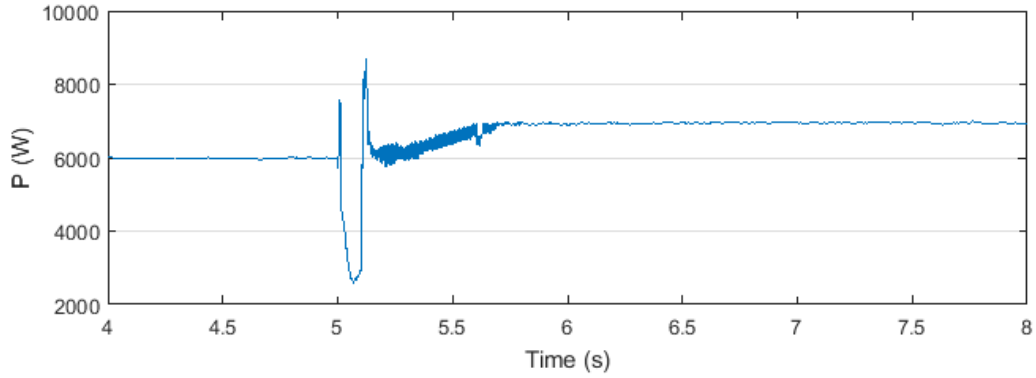

b)

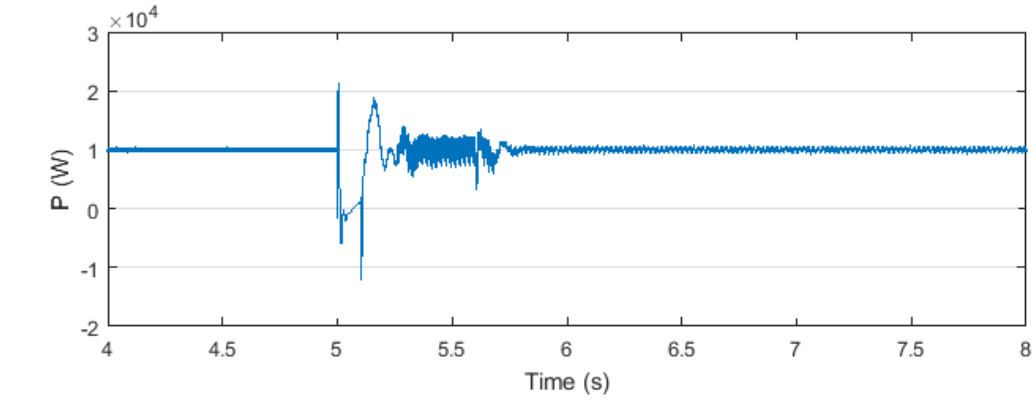

c)

Figure 4.12 - Short-term results: a) Split-shaft microturbine active output b) Fuel cell active output c) Wind generator active output.

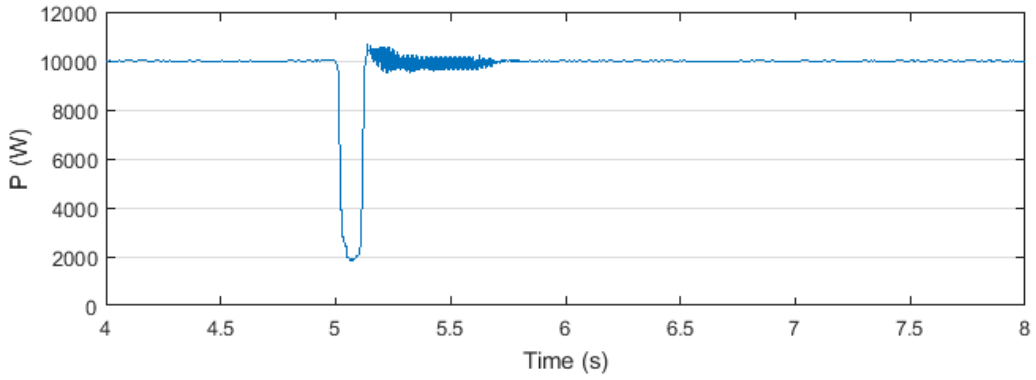

a)

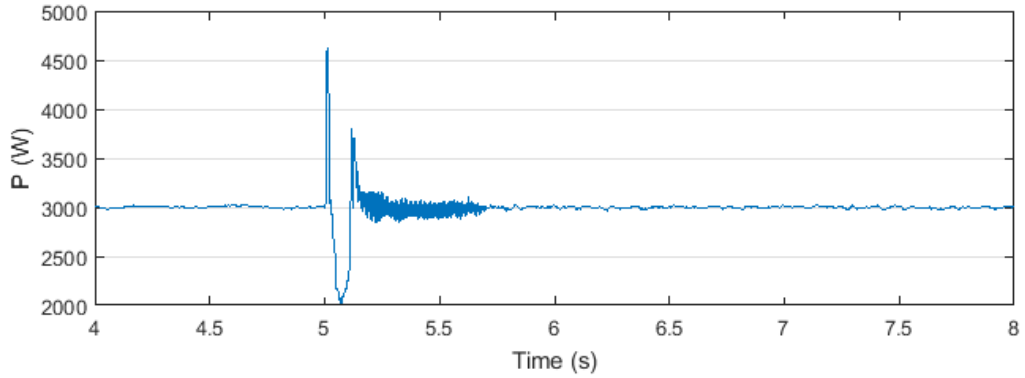

b)

Figure 4.13 - Short-term results: a) 10kW PV active output b) 3kW PV active output.

In terms of voltage, every time a load is connected the voltage drops, although not significantly. This effect can be seen in Figure 4.16.a, at 11 and 35 seconds. The storage unit will increase its reactive power output in two steps, which corresponds to the load connections made at the abovementioned instants, as shown in Figure 4.15.b.

In Figure 4.14.c, it is possible to check that the fuel cell, which starts from a 6kW active power output, will increase its output power in order to correct the frequency deviation, due to the secondary frequency control. However, at around 38 seconds the fuel cell reaches its capacity, which means that from this instant, only the split-shaft microturbine will be responsible for the frequency restoration process, as shown in Figure 4.15.a.

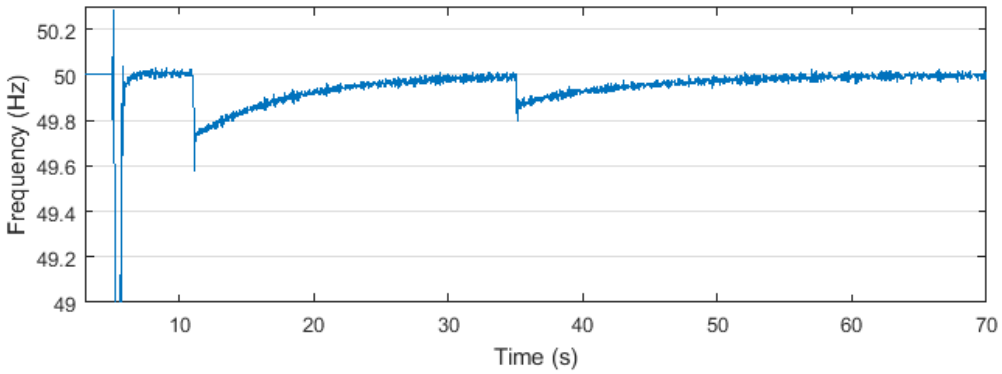

a)

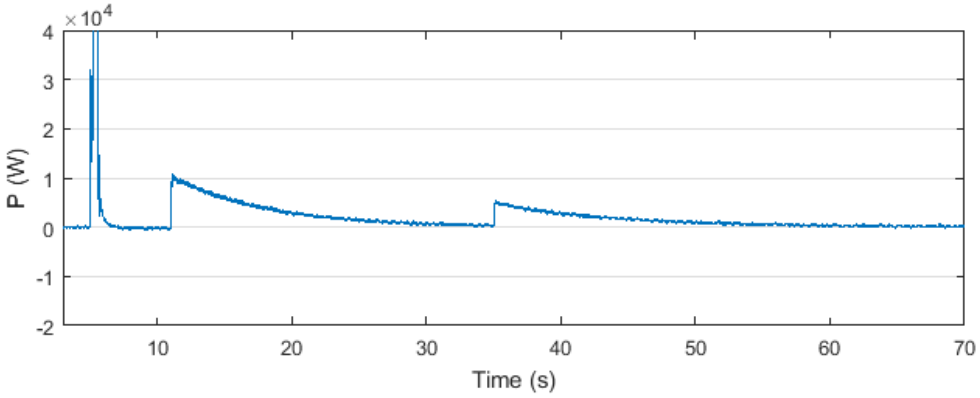

b)

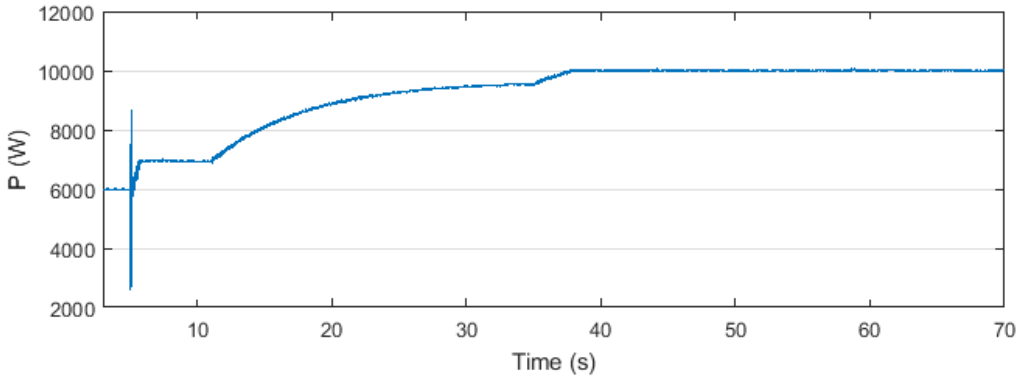

c)

Figure 4.14 - Long-term results: a) Frequency b) Storage active output c) Fuel cell active output.

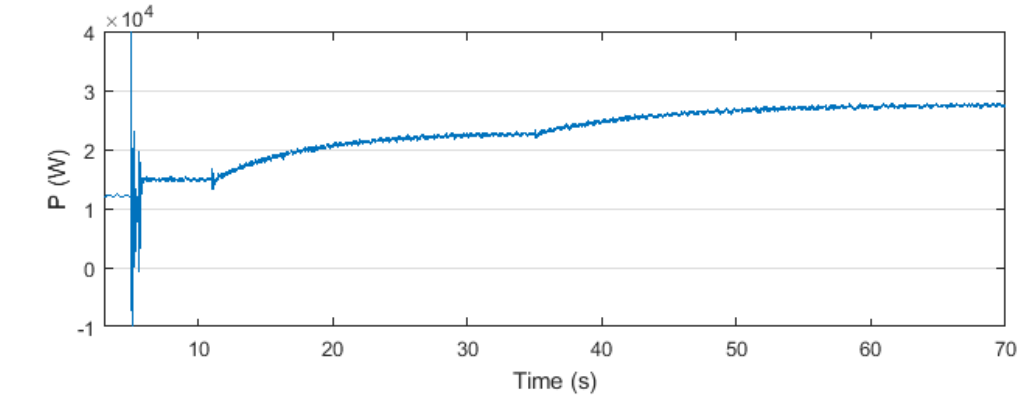

a)

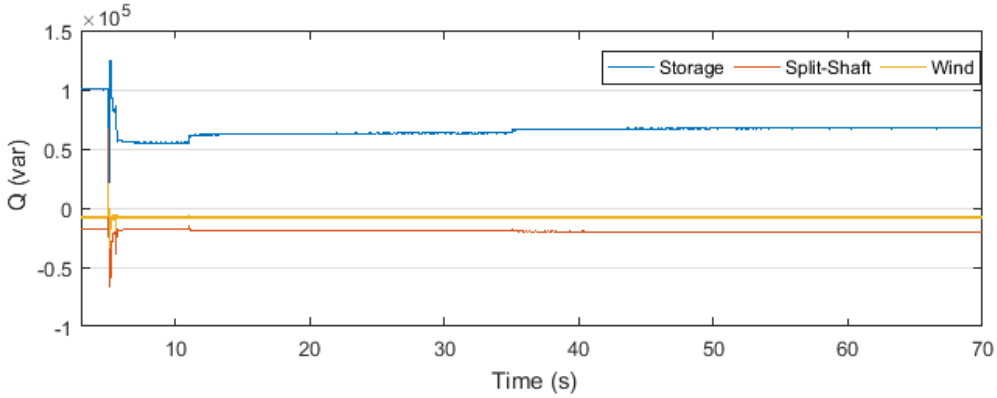

b)

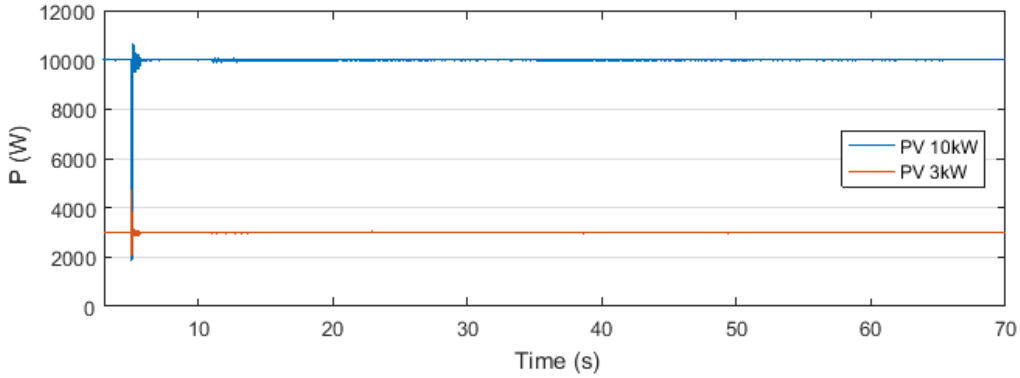

c)

Figure 4.15 - Long-term results: **a)** Split-shaft active output b) Storage, Split-shaft microturbine and wind generator reactive output c) PV units active output.

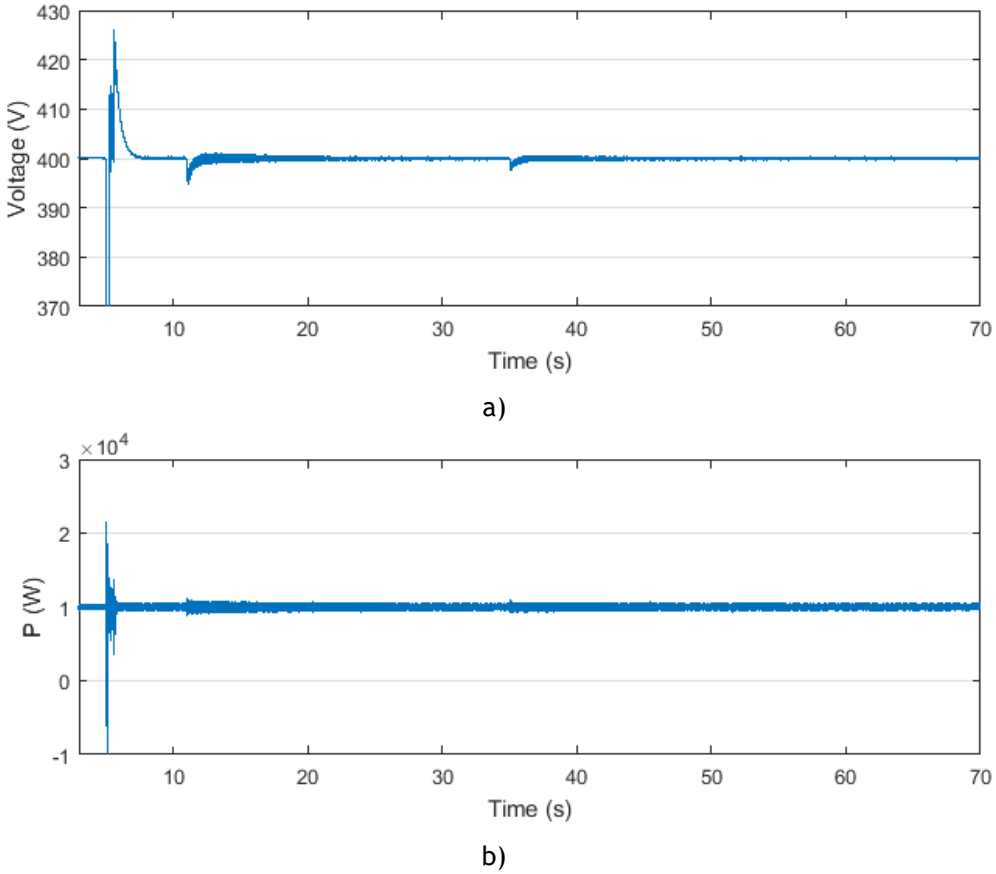

Figure 4.16 - Long-term results: a) Storage voltage b) Wind generator active output.

4.2- Multi-Master Operation

In the MMO, it is assumed that instead of using a split-shaft microturbine, a single-shaft microturbine (SSMT) is used, and both the storage device and the latter are operating with a coupled VSI. The remaining MS will be controlled in PQ mode. In this case, the SSMT will be responsible not only for the primary frequency control but also the secondary frequency control. Since it is operated in V/f control mode, the MGCC will send a signal with new frequency set-points to the VSI that, consequently, adjust the SSMT active output to meet the microgrid's needs, as shown in Figure 4.17. The fuel cell active output will act according to the same secondary control scheme, as presented in Figure 4.1. It was assumed that only the storage unit possesses a local secondary voltage regulator.

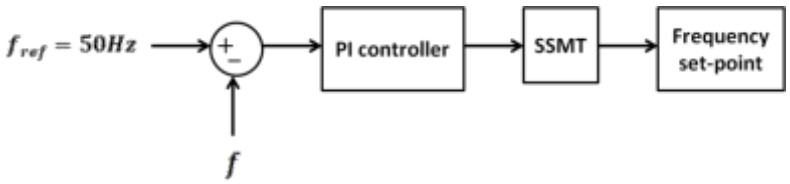

Figure 4.17 - Secondary frequency control scheme applied to the SSMT.

4.2.1- High load case

In this case, the same operating conditions such as fault occurrence and disconnection times assumed in SMO were considered. In this operation mode, since there is a higher storage capacity available at the microgrid, its frequency can be restored to 50Hz faster than in SMO scenario [35]. It was considered that the SSMT active output increases in three steps.

The first and third steps are due to the connection of loads at 11 seconds and at 15 seconds. The second step is defined in advance by considering the load and production knowledge within the microgrid before its islanding procedure, and occurs at 13 seconds, since it is assumed that the MGCC sends a signal to the VSI of the SSMT with a new frequency set-point, that will cause an active power output increase.

At 5.1 seconds, it is assumed that the microgrid is disconnected from the upstream MV grid. This causes a frequency transient, as shown in Figure 4.18.a. At 5.5 seconds, the frequency stabilizes at around 49.3Hz, which is a smaller deviation when compared to the SMO, where the frequency stabilized at around 48.6Hz and it was less constant. This is caused since there is more output power available at the primary frequency control level of the microgrid.

At 5.6 seconds, the under-frequency relays will activate the load shedding functionality, thus disconnecting the same loads considered in the SMO scenario. This will help to avoid large frequency transients that may compromise the microgrid operation and lead to inverter overload. As shown in Figure 4.18.a, the load shedding scheme adopted will cause the frequency to stabilize at 50Hz.

Another important topic to discuss is that the voltage drop at the storage terminals is smaller (although the difference is of only a few Volts) and it is restored faster than in the single master operation scenario (see Figure 4.18.b). This can be explained by the fact that in MMO two VSI exist in this simulation, which ensures a higher primary voltage control capacity. The remaining power outputs of the MS can be found in Figure 4.19 and Figure 4.20.

After the initial transient period, the next step will be to reconnect the maximum amount of load that the local production of the microgrid is able to supply. At 11 seconds and 15 seconds, the load is incremented which causes the frequency to drop (see Figure 4.21.a). After the loads are connected, the fuel cell and SSMT will increase its output due to the secondary frequency control, as shown in Figure 4.21.b and Figure 4.21.c, respectively. At 13 seconds, the MGCC sends a signal to the VSI of the SSMT with a new frequency set-point that allows the frequency to reach around 49.9Hz, thus enabling the possibility of connecting the remaining load at 15 seconds.

Comparing the time that this process takes to complete with the SMO it can be seen that in MMO, the frequency is completely restored in approximately 45 seconds while in the SMO the frequency takes almost 65 seconds to be restored. This means that the MMO scenario is more suitable to cope with frequency restoration processes. The voltage drops, due to the load

connections, can be found in Figure 4.22.b. The storage active output has the same behaviour as in SMO, although it returns to zero faster (see Figure 4.22.a).

The current injected by the storage unit can be found in Figure 4.23.a, and it can be seen that every time a load is connected, the current increases in a step. In terms of the reactive power of the storage unit and the SSMT, it can be seen that, since the only existent voltage regulator is located at the storage unit, when a load is connected the storage increases its reactive output, while the SSMT decreases it (see Figure 4.22.c). Regarding the non-controllable MS (PV units and wind generator), in Figure 4.23.b and Figure 4.23.c it is possible to find their active power output, where it is possible to see that these units are able to maintain it after the initial transient.

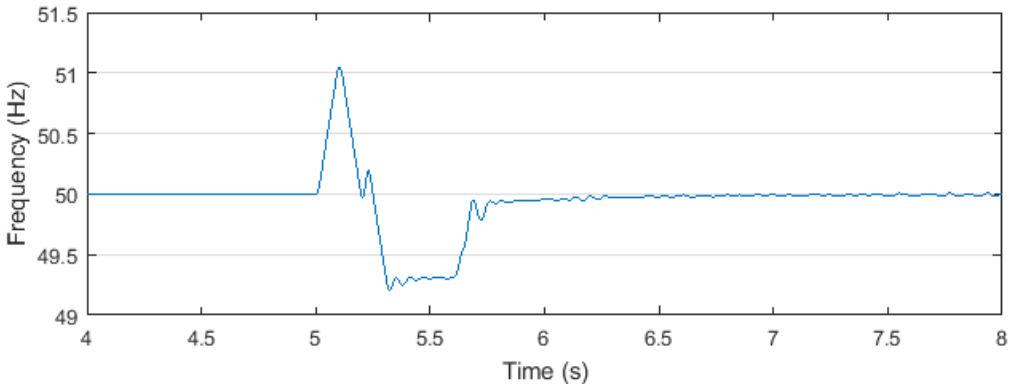

a)

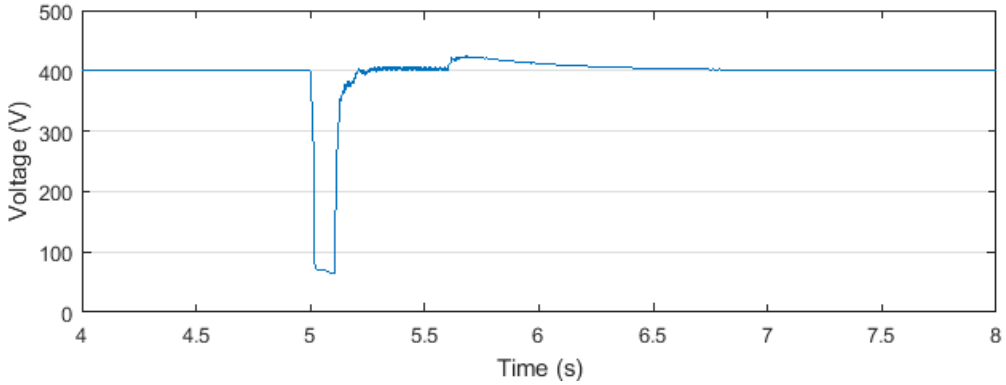

b)

Figure 4.18 - Short-term results: a) Frequency b) Storage voltage.

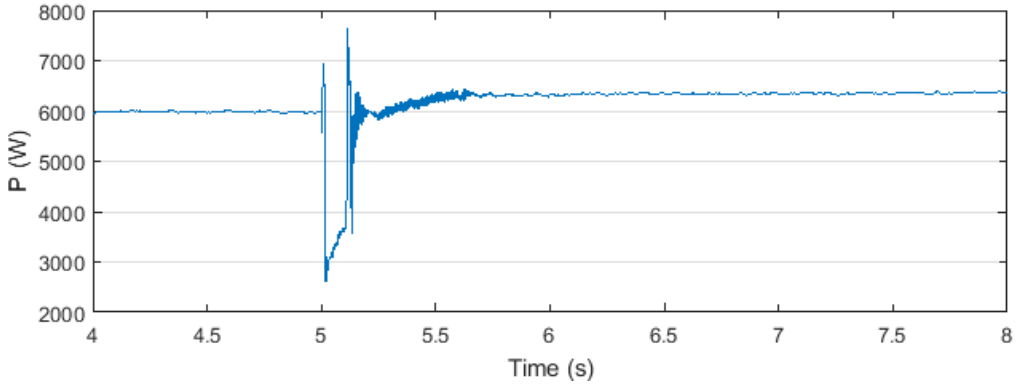

a)

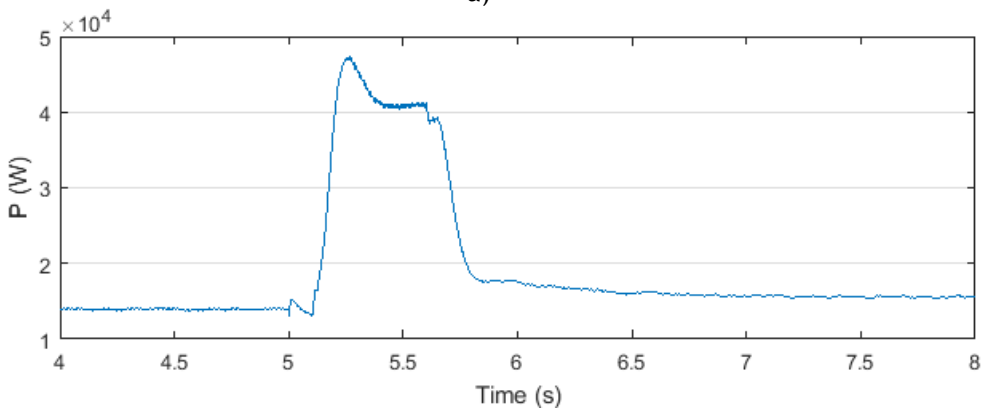

b)

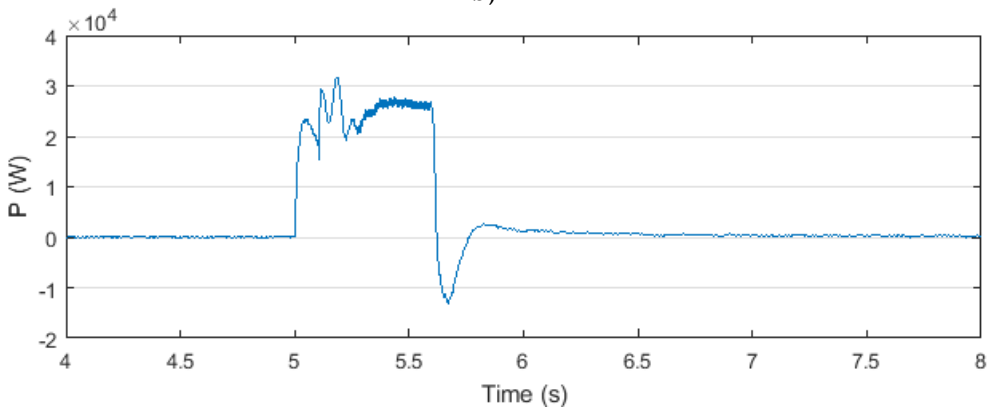

c)

Figure 4.19 - Short-term results: a) Fuel cell active output b) SSMT active output c) Storage active output.

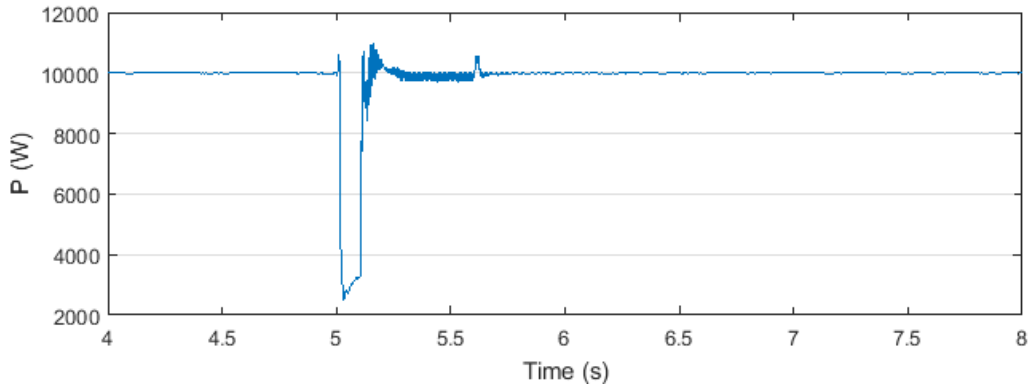

a)

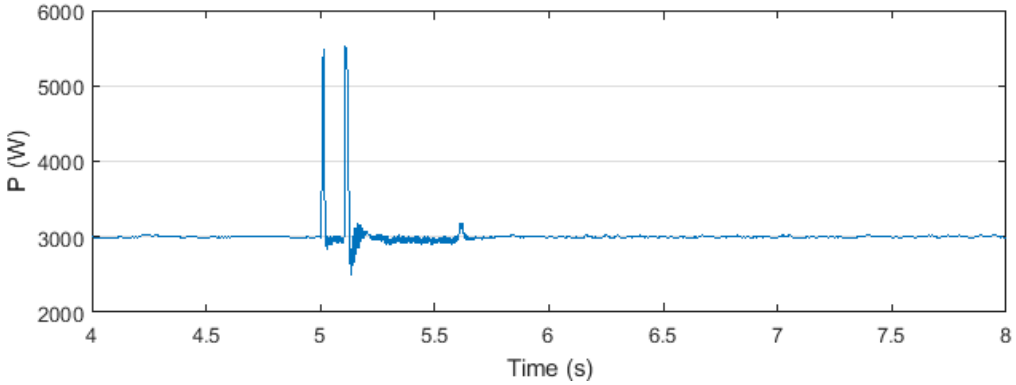

b)

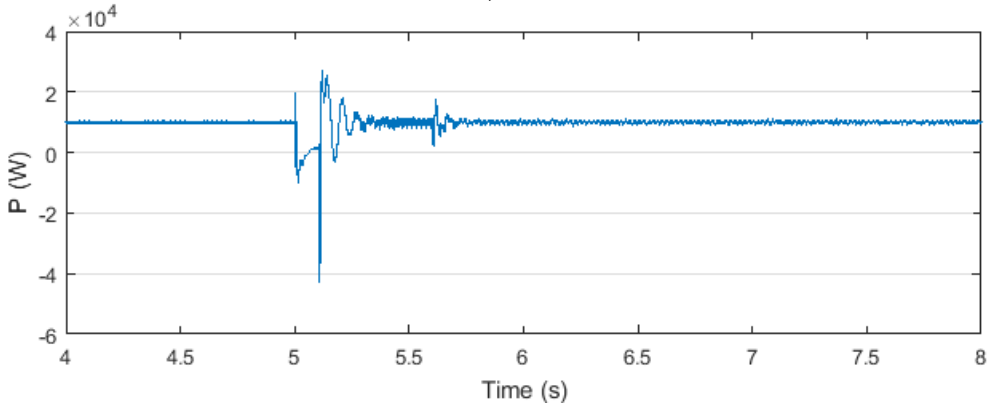

c)

Figure 4.20 - Long-term results: a) PV 10kW active output b) PV 3kW active output c) Wind generator active output.

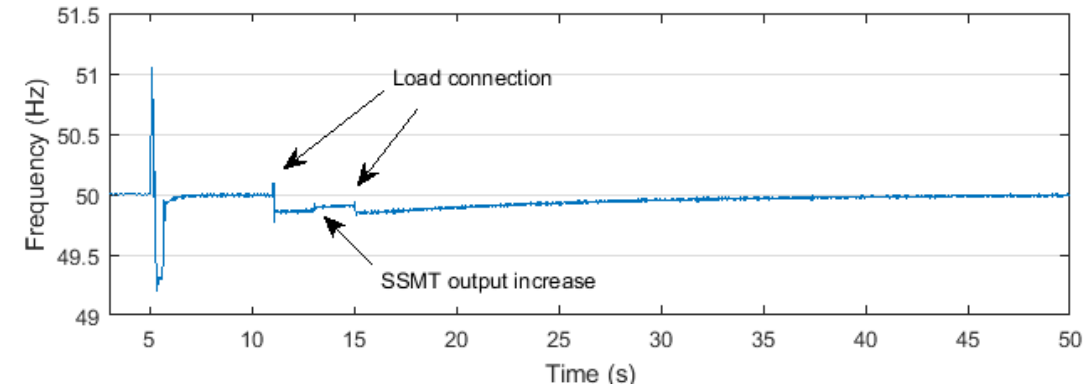

a)

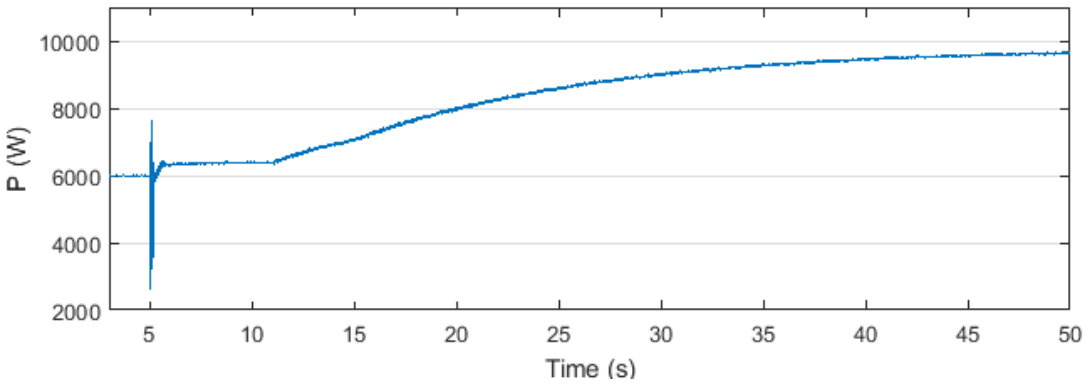

b)

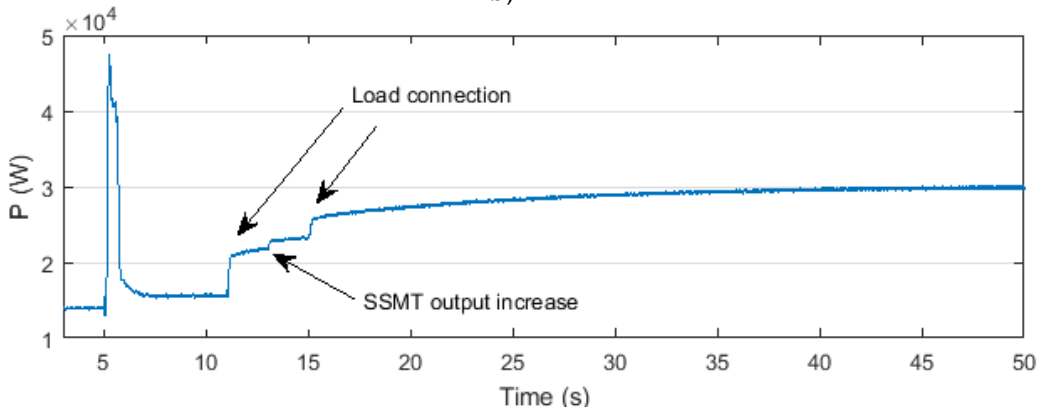

c)

Figure 4.21 - Long-term results: a) Frequency b) Fuel cell active output c) SSMT active output.

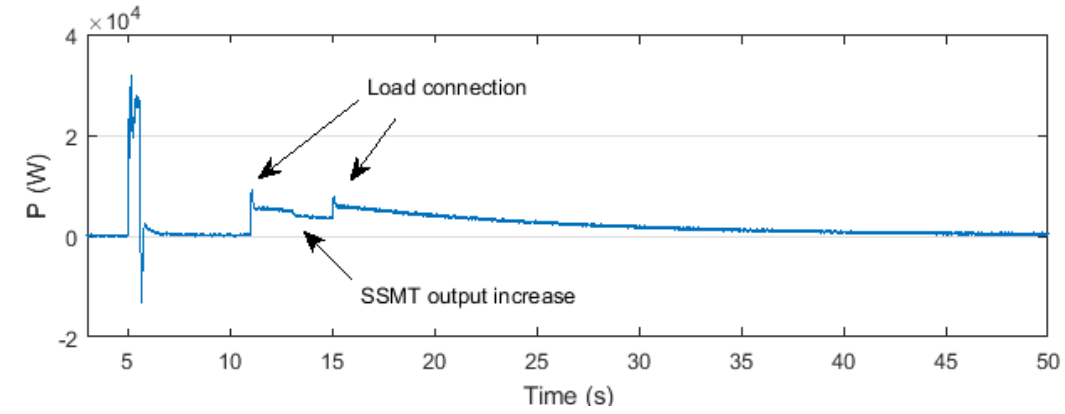

a)

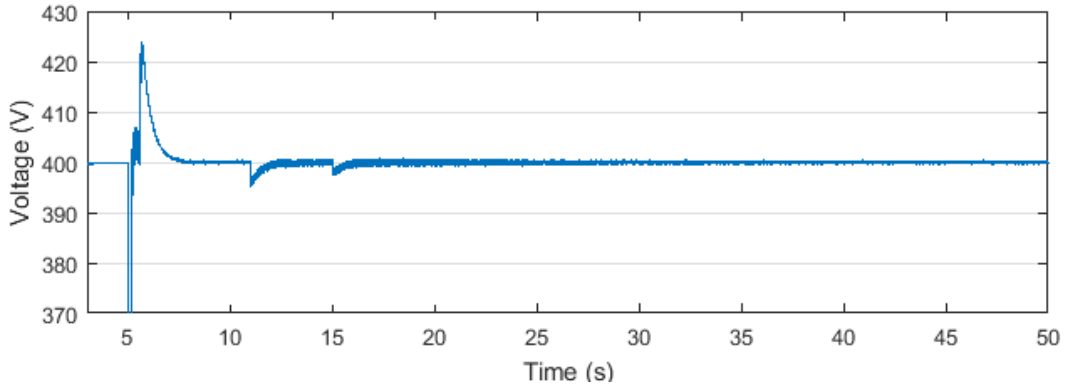

b)

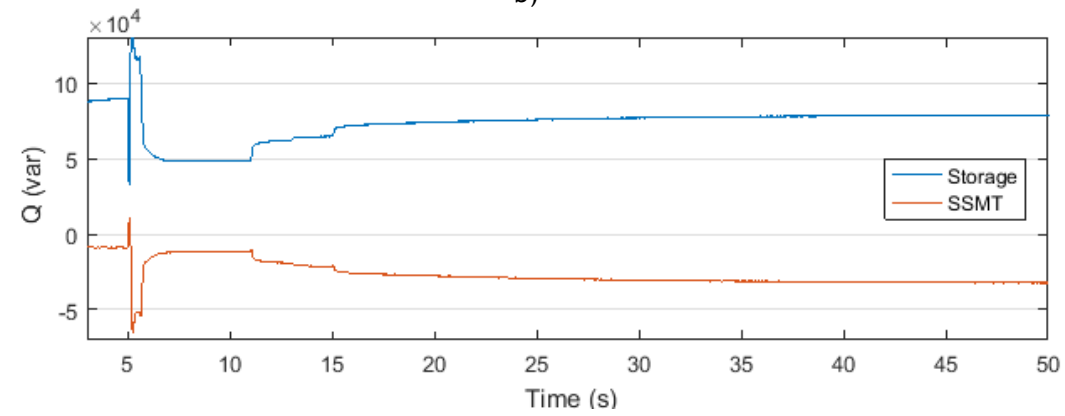

c)

Figure 4.22 - Long-term results: a) Storage active output b) Storage voltage c) Storage and SSMT reactive output.

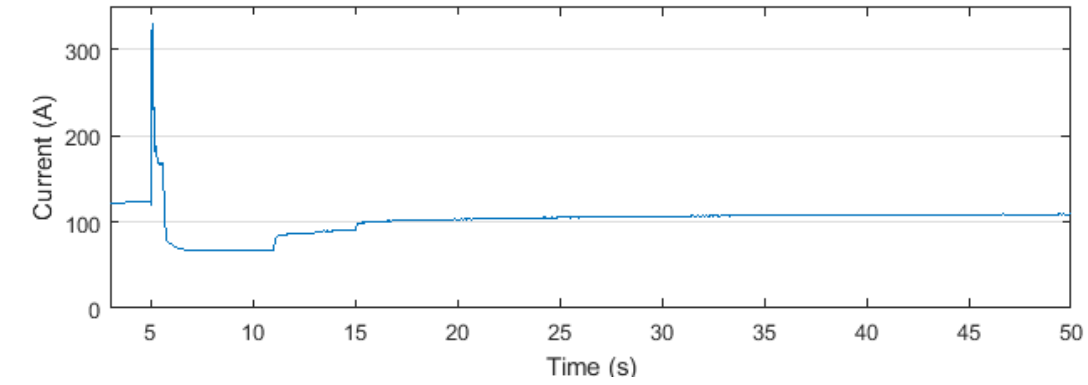

a)

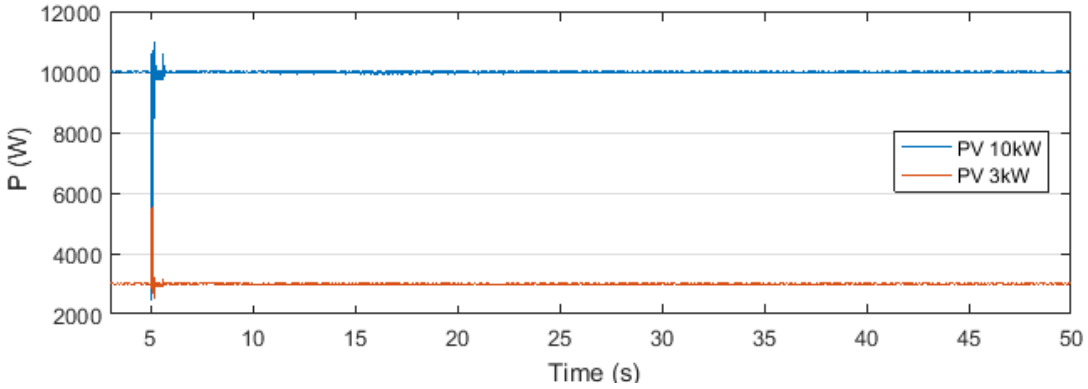

b)

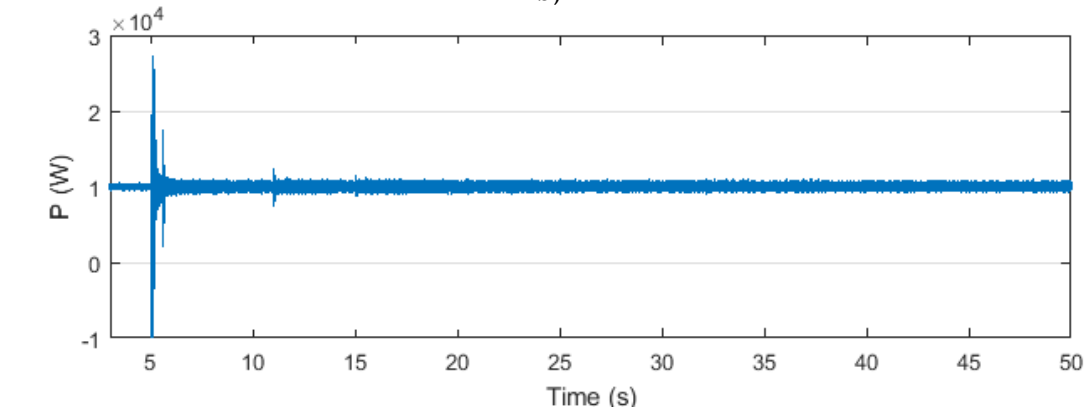

c)

Figure 4.23 - Long-term results: a) Storage RMS current b) PV units active output c) Wind generator active output.

4.3- Chapter summary

In this chapter, the feasibility of the microgrid islanded operation is validated by considering two different control strategies: the SMO and the MMO. It is shown that both schemes are appropriate for the microgrid operation in islanding conditions, caused by the unplanned disconnection of the MV grid, and ensure that the microgrid operates in a stable and effective way. Since the transients caused by the disconnection of the microgrid and by the connection/disconnection of loads are less significant, and the frequency can be restored faster in the MMO than in SMO, it can be concluded that MMO is more suitable for the microgrid islanded operation, since the primary frequency control has more power injection capacity. One important note is that the storage device is the most critical device in this type of operation, because it is the responsible for the primary frequency and voltage control. However, it requires an appropriate management due to its limited storage capacity.

Chapter 5

Microgrid Restoration Procedure

In this chapter, a restoration scheme for the microgrid, modelled and tested in the previous chapters, is proposed. It was assumed that the microgrid is operating under a MMO scheme since it was demonstrated in the previous chapter that it is more suitable for the microgrid islanded operation. Differently from the previous chapter, in these simulations the PI coefficients from the secondary control scheme were changed in order to promote a faster frequency restoration, it was assumed that the fuel cell did not possess secondary frequency control, thus producing its maximum output. Moreover, it was considered that the load 3 and load 5 can both be adjusted in three equal load steps, instead of two, and finally it was assumed that the consumer 1 consists in a 5kW motor load, which was also modelled as an asynchronous machine directly connected to the microgrid, in order to assess the impact of connecting this motor load to the microgrid, while in islanded operation.

5.1- General Assumptions

The restoration procedure of the microgrid is assumed to be centrally directed by the MGCC. This controller is responsible for checking a proper set of conditions that need to be assessed at every single step of the restoration procedure. These conditions are important when connecting the MS or loads, according to the values of frequency, voltage and standing phase angles [12].

In order to ensure the proper restoration of the microgrid, it is necessary that the MGCC receives information regarding all the MS and loads, such as the available generation and consumption. This particular information will be used to determine the best sequence of actions to employ. The DMS should also send information to the MGCC. It is important to assess when the MV grid is restored and capable of being connected again with the microgrid. It can

be seen that an important part of the restoration procedure relies on the communication infrastructures that enable the information sharing between all the controllers.

As determined in the previous chapter, the most suitable islanded operation for the microgrid is the MMO, which is used in the next section. The storage unit and the SSMT are used as the two black-start resources of the microgrid. The secondary frequency control will be applied only in the SSMT, contrarily to what was considered in Chapter 4, in which the fuel cell would also participate. This means that the latter, when connected, it will inject its maximum capacity of 10kW. Regarding the secondary voltage control, it was assumed that only the storage unit was contributing. Finally, it was considered a complete blackout, where every single load and generation unit were disconnected from the microgrid.

5.2- Restoration Procedure

The beginning of the restoration procedure in a microgrid is similar to the conventional power system restoration, in which islands with black-start units supplying local loads are created and then connected together, building a bigger and more stable grid. So, the first step of the restoration procedure is to create two islands: in one of them, the storage unit will be used to energize all the feeders of the microgrid, without connecting any load or generation unit, and in the other, the SSMT will be black-started since there is a battery at its DC link and will be supplying a local load. There is no secondary voltage control at the SSMT, which means that the voltage in this island will be lower than its nominal value, due to the load connection.

It can be seen from Figure 5.1 that the frequency in the storage island is a bit below 50Hz due to the lines impedances. Also in the same figure, at 2 seconds the MGCC sends a signal to the circuit breaker of the SSMT in order to connect a local load, which causes a frequency drop, being then corrected by the secondary frequency control in the island of the SSMT. After the frequency is stabilized, the MGCC sends a signal to the SSMT with a new frequency set-point that causes a slight decrease of its production, thus leading to a small frequency deviation of -0.4Hz. At this moment the secondary frequency control of the SSMT is deactivated, by the MGCC, to maintain the frequency deviation. At 6 seconds, the MGCC sends a signal to check the synchronization conditions, which are validated at 6.5 seconds. At this instant, the MGCC sends another signal to the circuit breaker to connect them together.

For this purpose, a synchronization block was modelled (see Figure 5.2) that measured the voltage magnitude difference, and the phase difference between the two three phase sinusoidal signals, and then compared these values to specified limits (2 Volts for the voltage magnitude difference and 0.2 rad for the phase difference). If the measured differences are less than the limit values, then the synchronization block will act. The resulting frequency and power output transients are very small which indicates that the synchronization procedure was successful (see Figure 5.3.a and Figure 5.3.c). The voltage has a very small transient, and after

this transient it just increases to a value close to the nominal value and then, the secondary voltage control on the storage will restore the voltage to exactly 400V (see Figure 5.3.b).

After synchronizing the two islands, the next step is to build a larger and more stable grid, so it is necessary to connect the maximum amount of load that can be supplied by the existing resources in the microgrid. The proposed sequence of actions is the following:

1. At 11 seconds, one load step of the consumer 3 is connected;
2. At 15 seconds, the fuel cell is connected, producing 10kW;
3. At 20 seconds, consumer 4 is connected;
4. At 25 seconds, the 3kW PV unit is connected;
5. At 30 seconds, the 10kW PV unit is connected;
6. At 35 seconds, one step of the consumer 2 is connected;
7. At 40 seconds, the wind generator its connected;
8. At 45 seconds, the consumer 1 (motor load) is connected.

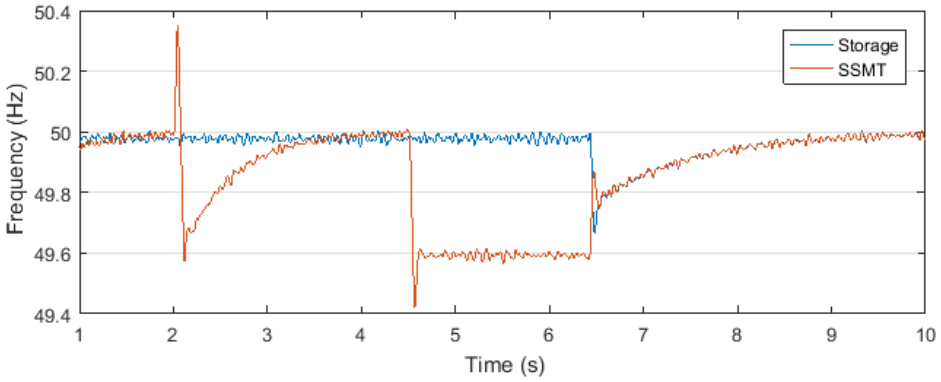

Figure 5.1 - Synchronization time span: Frequency in storage island and in SSMT island.

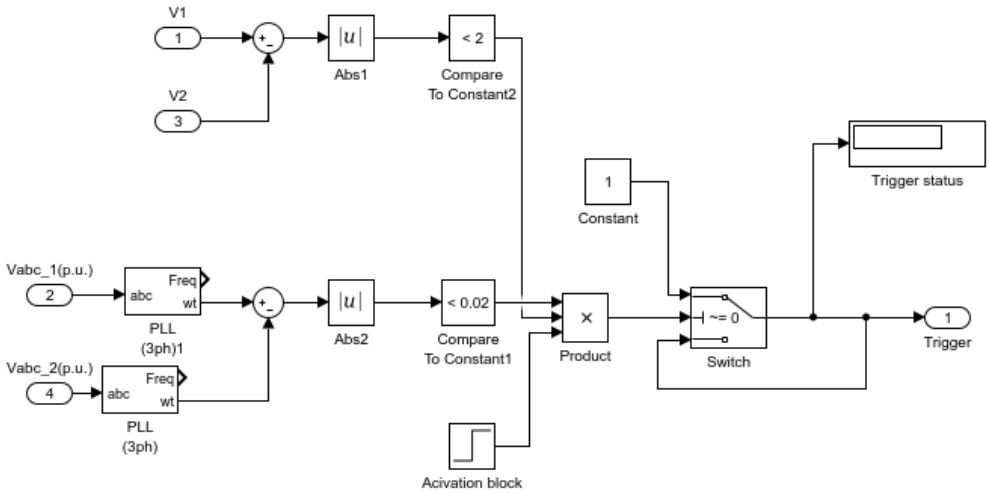

Figure 5.2 - Synchronization block modelled in MATLAB/Simulink.

This sequence of actions is characterized by an alternating MS and load connection pattern (after a load is connected, a MS is connected). This alternating procedure helps to conserve the SOC of the storage unit. For example, if four loads were connected one after the other, the storage output would increase to values that could make the SOC run out much faster.

In Figure 5.4.a and Figure 5.4.c, it can be seen that when a load is connected, the frequency drops being corrected by the secondary control applied to the SSMT, increasing its production. The contrary situation happens when a generation unit is connected since the frequency increases, and so the microturbine will decrease its production, so that the frequency is restored to its nominal value.

Besides, the motor load and the wind generator connections are the ones that cause the most significant frequency transients, because they use an asynchronous machine that is characterized by absorbing high currents in its start-up procedure. The voltage transients are also more significant is these cases, as shown in Figure 5.5.a. The storage unit is responsible for stabilizing the frequency so, it only absorbs or injects power during the frequency restoration periods, thus returning its output to zero (see Figure 5.4.b). The remaining MS outputs can be found in Figure 5.5.b, Figure 5.5.c and Figure 5.6.

After the maximum amount of load and generation units are connected, the microgrid becomes more stable which means that the next step is to connect it to the upstream MV grid, in order to be possible to supply the remaining loads that the microgrid cannot supply due to lack of local production.

In order to synchronize both grids, the same conditions need to be checked. Since the scope of this work is on microgrid restoration and the synchronisation procedure was already done for synchronizing the storage and SSMT islands, the reconnection of the microgrid to the MV grid is not simulated.

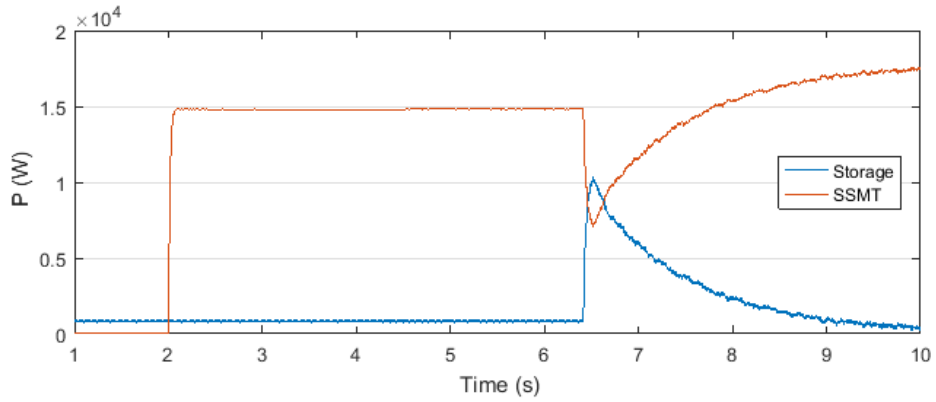

a)

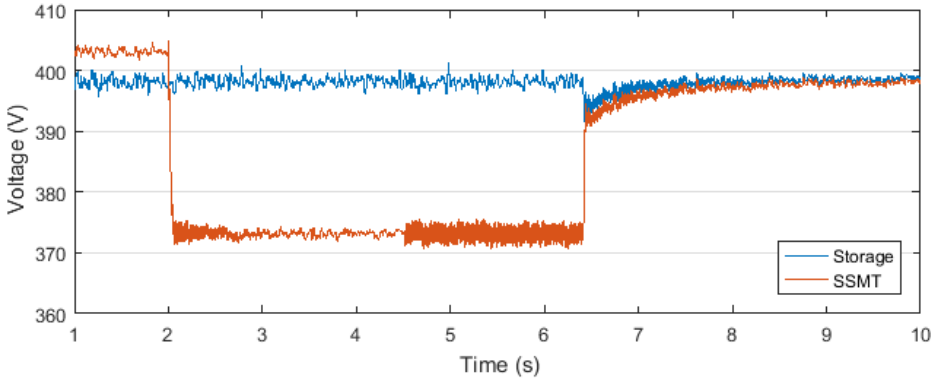

b)

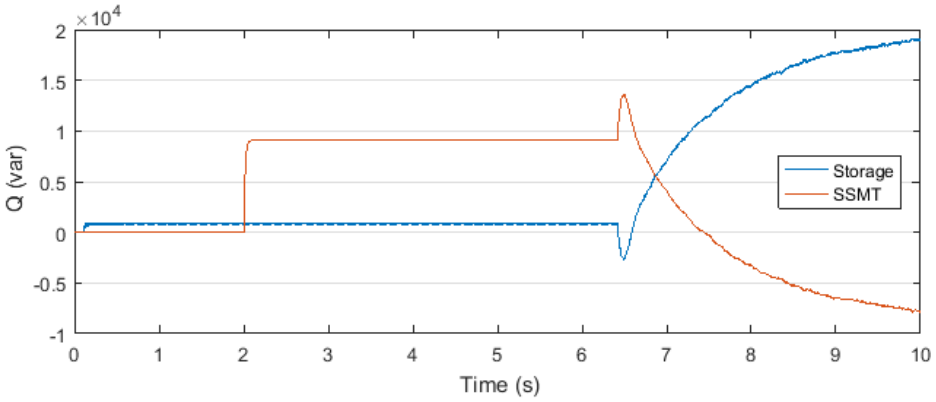

c)

Figure 5.3 – Synchronization time span: a) Storage and SSMT active power output b) Storage and SSMT voltage c) Storage and SSMT reactive output.

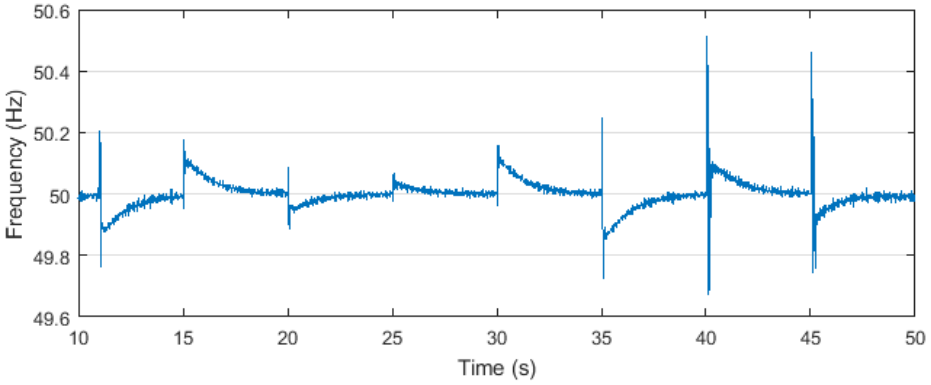

a)

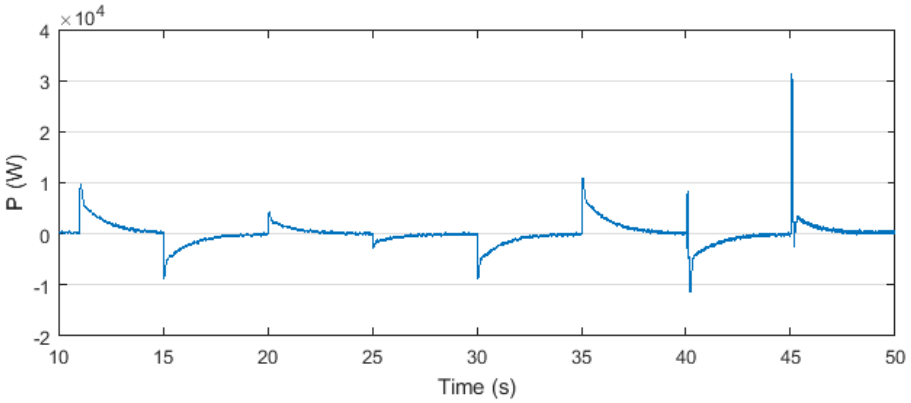

b)

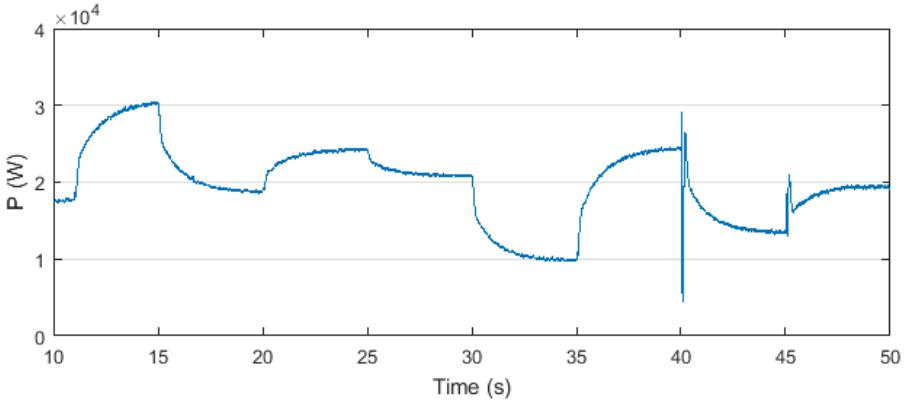

c)

Figure 5.4 - Load connection time span: a) Frequency b) Storage active output c) SSMT active output.

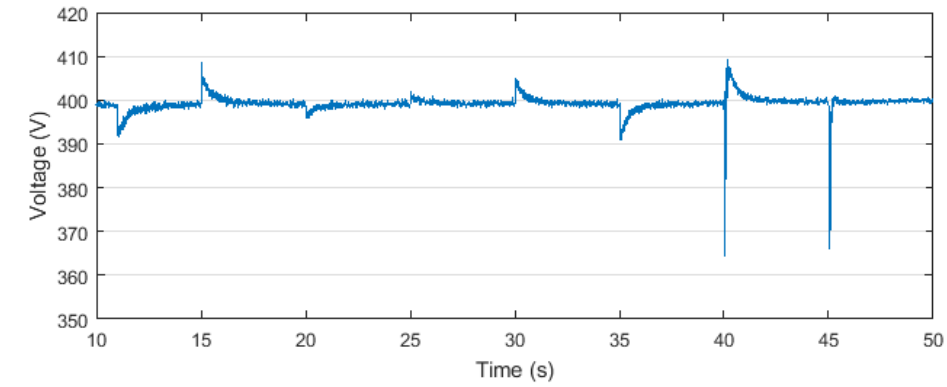

a)

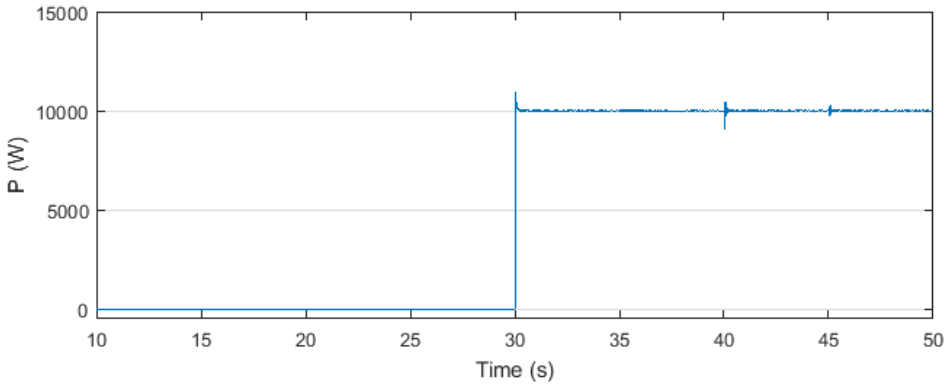

b)

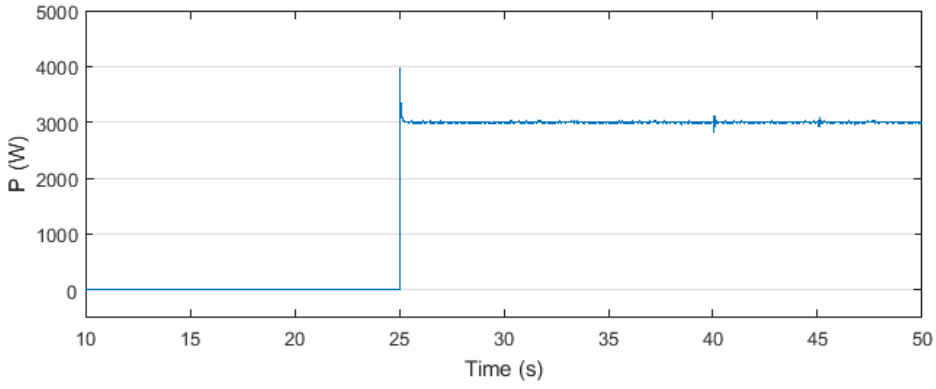

c)

Figure 5.5 – Load connection time span: a) Storage voltage b) 10kW PV active output c) 3kW PV active output.

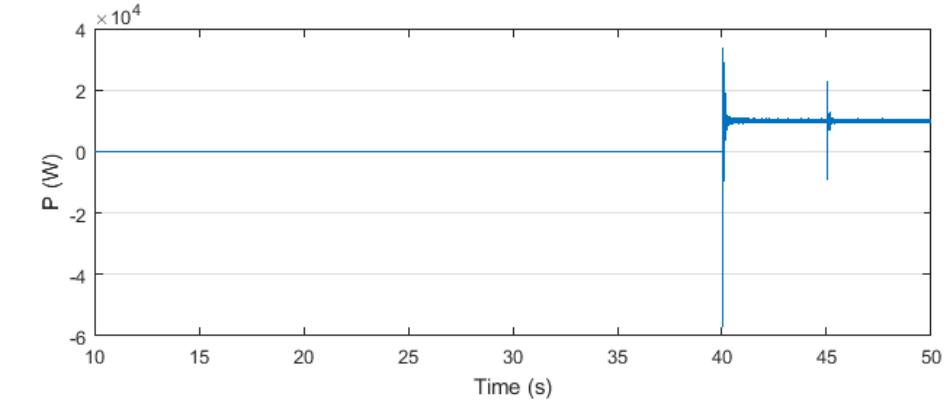

a)

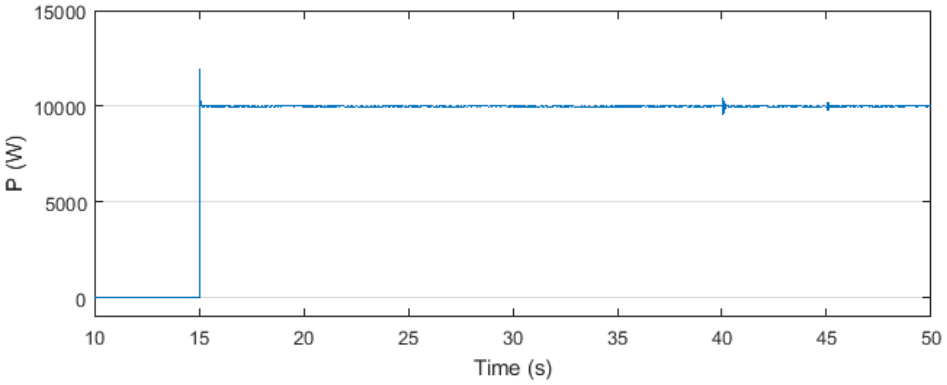

b)

Figure 5.6 - Load connection time span: a) Wind generator active output b) Fuel cell active output.

5.3- Chapter summary

In this chapter, the microgrid restoration is approached and assessed. It can be concluded that it is possible to successfully restore the modelled microgrid without any synchronous machine, and using only power electronic converters ensuring the stability of the microgrid. It can be seen that the storage unit is the most important element in this procedure, specially if the microgrid is operated in SMO since there are no other MS under a V/f control scheme.

Considering a power system that is already fully developed with several microgrids, if there is a fault in the MV grid, automatically the microgrid starts working on islanded mode, which means that is very unlikely that the latter will be in complete blackout. However, these studies are needed for two specific reasons:

- Considering a low voltage microgrid that is being created. It is necessary to connect the MS to the grid but this cannot be done all at the same time. So in this case, the connection of the MS to the microgrid will be similar to the restoration procedure presented in this chapter;
- Another reason is related to the fact that the microgrid is built, so that it can be operated successfully in island mode. This means that the microgrid is considered to be a small power system. So, assuming that the MV grid is not available for some hours or even days, the microgrid will be operating in island mode during this time period, which means that it is subjected to the occurrence of faults that may lead to an internal blackout.

It is possible to implement a restoration scheme based on several operational constraints, for example according to the loads pre-defined priority, minimizing the total restoration time by finding the most suitable network configuration, among others. This creates some opportunities for the research in this field of studies.

Chapter 6

MAS for Decentralized MG Restoration

In this chapter, the major contribution consists in a decentralized multi-agent based system (MAS), proposed for the microgrid restoration problem assuming a complete blackout, in which the loads and MS are assigned to specific agents. These agents are responsible for updating their information based on local measurements and for communicating with the remaining agents to exchange its information.

Then, after the agents exchange their information, they will be able to make a decision. In this work, it is considered that the agents will solve a 0/1 Knapsack problem to determine the loads that should be reconnected to the microgrid based on their priority and the SSMT's reserve. This problem will be solved by all the agents every time a load is connected.

Also in this chapter, the same MAS will be used in a different case study in which only a partial blackout occurred in the microgrid. This case study has the purpose of assessing the feasibility of the EDRP, to help the restoration procedure, using the developed MAS.

Regarding the benchmark low voltage microgrid tested in this work, it was considered that the consumer 1 is now a single residential consumer, instead of the motor load considered in Chapter 5. This means that all of the loads are considered to be residential, and these are also classified in this chapter according to its maximum off-time. The benchmark microgrid can be found in Figure 6.1.

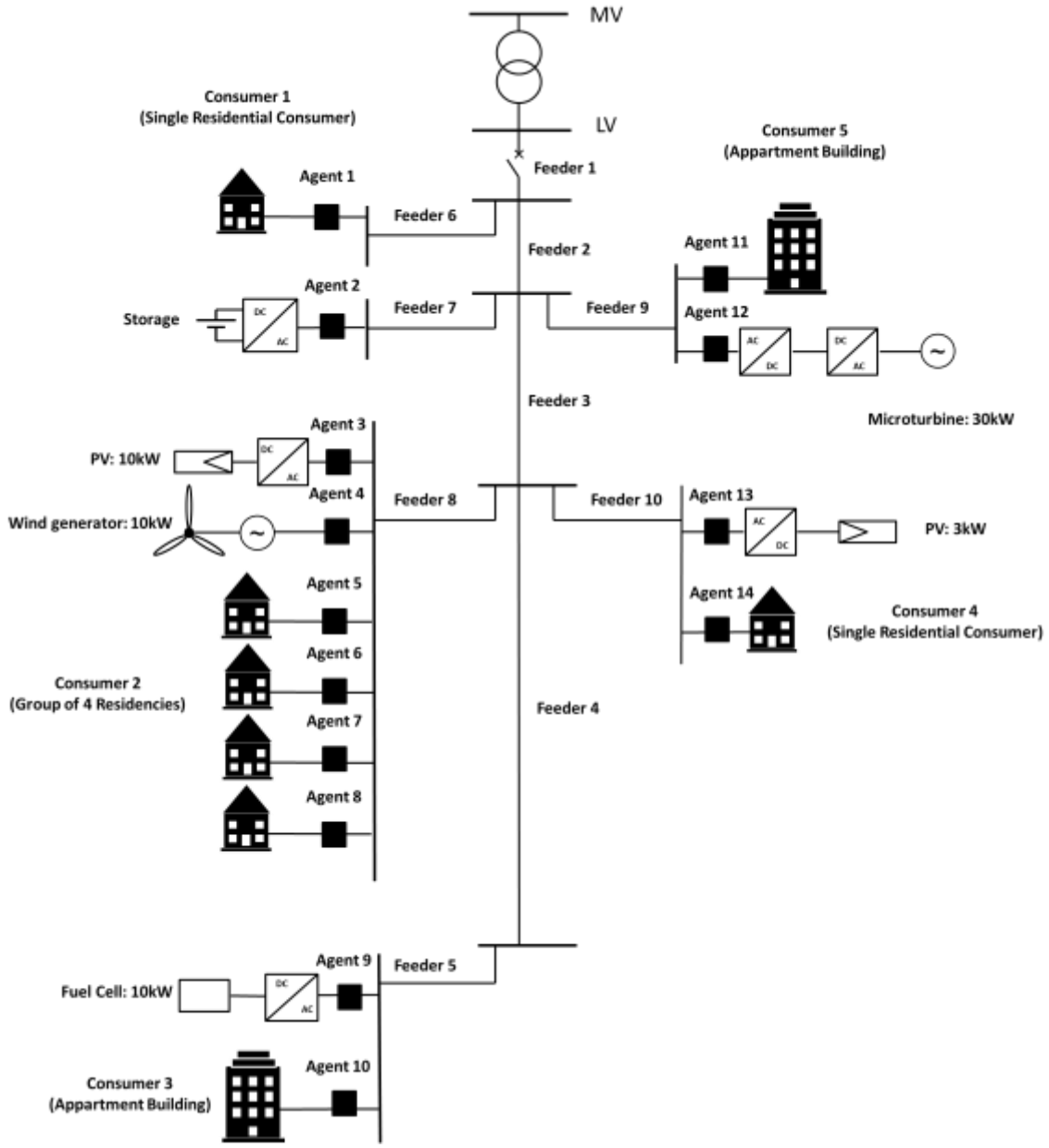

Figure 6.1 – Benchmark low voltage microgrid.

6.1- Multi-Agent System (MAS)

A multi-agent system is composed by different agents. Accordingly to [85], an agent is software/hardware system that is inserted in a proper environment and has the capability to react to changes in the latter. Besides, the agent must be able to change and observe a part of the current environment.

In the case of a microgrid, or a general power system, the environment will be physical, and consists in the power grid that can be observable by the agent through sensor measurements, and the latter may also change this environment, for example by

opening/closing a circuit breaker thus reconfiguring the network. In a microgrid environment an agent must have three key features:

- **Reactivity:** the agent needs to be able to be aware and react to changes that may occur in its environment (which is the microgrid), this includes load changes, generation changes, network reconfiguration, among others;
- **Pro-activeness:** an agent needs to be pro-active, which means that in case that the connection between two agents is lost for some reason then, both of them need to adapt and search for another connection with a different agent that ensures the same objectives. Besides, the agents must operate in order to achieve a common goal;
- **Social ability:** every agent must communicate with the others to obtain the information required to achieve the proposed goals. But the communication must be goal oriented, which requires the cooperation between agents.

For the studied microgrid with the goal of its own restoration, the MAS will have the structure depicted in Figure 6.2. Here the LC and the MC will be assigned to different agents with different information. For example, in the case of the LC agent, an important information will be the load value, while in the case of the MC agent will be the available production. For the case of the SSMT, the available generation will correspond to its active power reserve, while in the PQ controlled MS, the available generation will correspond to the maximum active power that these units may provide.

The communication time between agents is verified in [7] by using a consensus algorithm. It concludes that this communication time is so small (less than 0.01 seconds) that for the time periods considered in this microgrid (around 5 seconds between the connection of loads and MS), this communication time can be neglected. It was assumed that the communication between agents follows the abovementioned consensus algorithm.

Regarding the DER of the microgrid, these can be controlled using a centralized or decentralized approach during the microgrid restoration procedure. In the centralized approach a central controller, the MGCC, will be responsible for sending new production/frequency set-points to the dispatchable MS, and also the control commands to the controllable loads for DR purposes [42].

This is an hierarchical control scheme, where the occurrence of potential conflicts can be minimized since all the decisions are made in the highest control layer of the hierarchy [86]. However, the main drawback of this centralized control scheme is when one or more communication channels are lost, or the restoration module of the MGCC fails, then the entire control system may be compromised [87]. In the case of decentralized control schemes, the objective is to enable a high degree of autonomy of the different loads and MS, and so every load and generation unit will possess an agent associated that will be able to communicate

with their neighbors, thus exchanging their information [42]. This way it is not necessary the existence of a central controller [86].

Contrary to the centralized control scheme, if one communication path is lost in the decentralized approach, the system still works because the agents are all connected between each other through other communication links, which is its main advantage. However, the implementation of the local controllers and the implementation of control schemes that require high levels of coordination is harder to achieve [87], [88].

6.2- 0/1 Knapsack Problem Formulation

The Knapsack problem consists in a combinatorial optimization problem, very common to find in the decision making situations encountered every day [89], [90]. Considering N items, the objective is to place a subset of these items in a knapsack with a defined capacity of W, knowing that each item has a determined weight (w_i) and value (v_i), by maximizing the total value in the knapsack such that the sum of the weights is less than, or equal to its capacity.

This problem is known for considering that the decisions are binary (*yes or no*) and independent, by selecting an item the capacity will decrease, and during the decision time, there are no changes in the problem inputs [91]. The mathematical formulation is presented below [92]:

Objective function:

$$max\, f(x) = \sum_{i \in N} v_i \cdot x_i \tag{6.1}$$

Subject to:

$$\sum_{i \in N} w_i \cdot x_i \leq W \tag{6.2}$$

where v_i corresponds to the value of the item, x_i represents a binary variable that indicates if the item is included or not (1 or 0, respectively), and w_i is the weight of the item i [93].

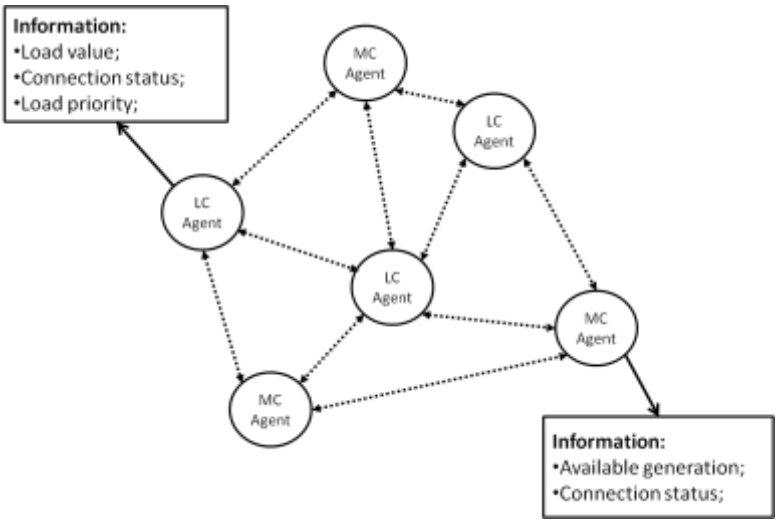

Figure 6.2 - Multi-agent system structure.

This problem can be easily adapted to the conditions of the microgrid restoration problem. By considering that v_{ij} corresponds to the priority of the load j of the consumer i, x_{ij} corresponds to the same binary variable which indicates if the load is connected or not, L is the sum of the weights and w_{ij} corresponds to the active power load value, the following problem can be formulated:

Objective function:
$$max\, f(x) = \sum_{i \in N} \sum_{j \in L} v_{ij} \cdot x_{ij} \tag{6.3}$$

Subject to:
$$\sum_{i \in N} \sum_{j \in L} w_{ij} \cdot x_{ij} \leq W \tag{6.4}$$

where W will represent the microgrid's active power reserve. This reserve will correspond to the reserve of the SSMT, since this MS is the only one that operates in V/f control and is supposed to be continuously operating, contrarily to the storage unit that should only inject/absorb power during the transient periods.

The proposed strategy consists in solving the Knapsack problem every time a new load is connected. This problem will be solved by every agent. The agents will possess the structure presented in Figure 6.3. Assuming that the SSMT and storage unit were already synchronized together, the algorithm followed by the agents will be:

1. Update W with the available active power reserve of the SSMT;
2. Solve the 0/1 Knapsack problem and determine the loads to connect based on their priority;
3. Remove the loads that were connected from the inputs of the algorithm, in order to consider only the ones that are not connected already;
4. Then, connect the MS with the most available capacity. If there are more than one with the same capacity, choose randomly between those units;
5. Update W. This value will always be the SSMT reserve, because this MS is operated in V/f control. This means that after a MS is connected, the SSMT will decrease its output in order to maintain a frequency of 50Hz, thus increasing its reserve. The contrary situation happens when a load is connected;
6. Repeat step 2 to 5 until there are no more MS to connect and the SSMT reserve is not enough to connect more loads.

It should be noted that the storage is not considered as a MS with reserve, since it is supposed to act only during transient periods, thus returning its active power production to zero.

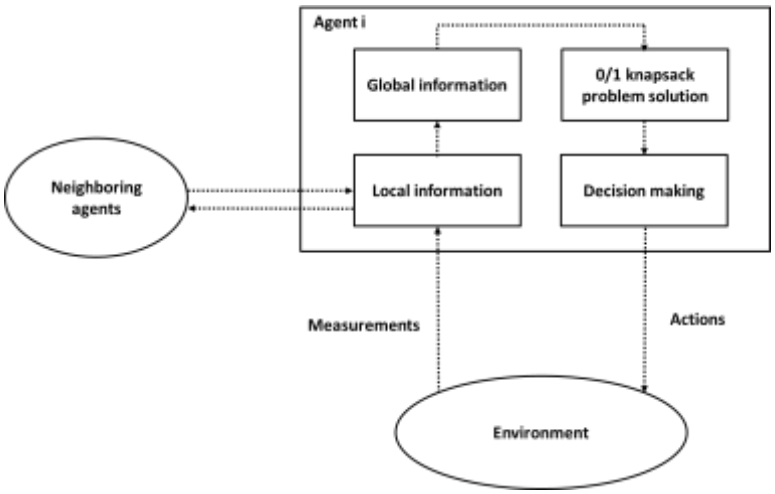

Figure 6.3 – Structure of an agent for the MG restoration problem.

6.3- Dynamic Programming

In order to solve the 0/1 Knapsack problem, the table-based dynamic programming approach was used. The table-based dynamic programming algorithm is based on the following Bellman equation, adapted from [89]:

$$f_i(j) = \max(v_i + f_{i-1}(j - w_i), f_{i-1}(j)) \tag{6.5}$$

where, considering the Knapsack problem, $f_i(j)$ corresponds to the maximum value that results from the objective function of the Knapsack problem. More information and examples regarding this method can be found in [89].

Basically, the table-based dynamic programming is a method that solves sub-problems of the main problem and then records the solutions in a table. This table will be filled and, from the analysis of the latter, the final solution can be obtained [90].

This method requires that all the coefficients are integers, and that the items are sorted in an ascending order by the weights. Considering an example, for the application of dynamic programming to the 0/1 Knapsack problem, with a capacity of 6, the inputs can be found in Table 6.1.

Table 6.1 – Example of the inputs regarding the 0/1 Knapsack problem.

Item	Weight	Value
A	1	1
B	3	4
C	4	5
D	5	7
E	2	4

The first step is to organize the items in ascending order regarding its weights, as presented in Table 6.2. The objective is to maximize the sum of the values of each object. So, in the first place it is necessary to build the table that is the base of the dynamic programming algorithm, which can be found in Table 6.3. This table can be seen as a matrix with $N \times (W + 1)$ dimensions, and the calculation of the values is done according to the following steps:

- If the weight of the item i is greater than the sum of the weights then the matrix value in the position (i, j) will be equal to the value immediately above: $M(i, j) = M(i - 1, j)$. This means that there is not enough capacity for including item i. In the case of the first row, since there are no rows above, the value for this condition should be the value of the item in the first row: $M(1, j) = Value(1)$;
- If the weight of the item i is less than or equal to the sum of the weights, then the matrix value in the position (i, j) will be calculated according to Bellman's equation (6.5). If $v_i + f_{i-1}(j - w_i) > f_{i-1}(j)$, then by including the new weight, the total value is higher than excluding the latter. If the contrary situation occurs, $v_i + f_{i-1}(j - w_j) < f_{i-1}(j)$, then the value in the Knapsack is maximized by excluding the new weight.

Table 6.2 - Inputs sorted by ascending order.

Item	Weight	Value
A	1	1
E	2	4
B	3	4
C	4	5
D	5	7

Table 6.3 - Dynamic programming table.

Item	Value	Weight	Sum of the weights						
			0	1	2	3	4	5	6
A	1	1	0	1	1	1	1	1	1
E	4	2	0	1	4	5	5	5	5
B	4	3	0	1	4	5	5	8	9
C	5	4	0	1	4	5	5	8	9
D	7	5	0	1	4	5	5	8	9

After completing the matrix then, the next step is to identify the items that were chosen. The best value will be located at the right lower corner, which in this case is 9. Then, if this value is equal to the above row, it means that the item in the last row was not included, which is the case. It can be seen that the number 9 appears three times for the items B, C and D. It can be concluded that the items C and D are not included since in the above row there is an equal value, which is 9.

The item B is included because in the above row, there is not a value 9. Then, it is necessary to subtract to the sum of the weights, the weight of the value B, which gives a sum of weights of 3 ($6 - 3 = 3$). In column 3 and line 2, the value is 5, which added to the value of the item B gives the value 9. Since in the above row there is not the value 5, it can be assumed that item E was also included. The same procedure can be followed, and it can be seen that item A was also included. So, the final solution would be that the items chosen are A, E and B, which gives a total value of 9 and a total sum of weights of 6.

6.4- Load Priority

The first step is to make a description of every type of residential loads existent in the microgrid. In [94], it is possible to find the most common groups of home appliances in residential loads. Besides, each group has a maximum off-time, which consists in the maximum time that these devices can be turned off without causing discomfort to the consumers. So, in order to minimize the consumers' discomfort, it was assumed that the loads with smaller maximum time off will have higher priorities than the ones with higher maximum time off. These considerations were adopted and can be found in [95]. The load characterization can be found in Table 6.4, Table 6.5 and Table 6.6. From here on, load $i.j$ corresponds to the group of loads j of the consumer i.

Table 6.4 - Individual domestic load groups with the respective maximum off-time and priority.

Group	Description	Maximum off-time	Priority
1	Electric space and water heaters, refrigerators, freezers	5 minutes	1
2	Washing machines, tumble dryers	3.5 minutes	2
3	Cooking appliances	2 minutes	3
4	In line heaters	15 seconds	4
5	Lighting loads	4 seconds	5

Table 6.5 – Distribution of load for every group of each consumer.

Consumer	Group 1	Group 2	Group 3	Group 4	Group 5
1	60%	11%	12%	9%	8%
2	59%	12%	11%	9%	9%
3	62%	10%	9%	10%	9%
4	63%	9%	10%	8%	10%
5	65%	9%	8%	8%	10%

Table 6.6 – Amount of load in each group of the respective consumer.

Consumer	Total (kW)	Group 1 (kW)	Group 2 (kW)	Group 3 (kW)	Group 4 (kW)	Group 5 (kW)
1	4.845	2.907	0.53295	0.5814	0.43605	0.3876
2	19.55	11.5345	2.346	2.1505	1.7595	1.7595
3	21.25	13.175	2.125	1.9125	2.125	1.9125
4	4.845	3.05235	0.43605	0.4845	0.3876	0.4845
5	48.45	31.4925	4.3605	3.876	3.876	4.845

Since the SSMT will be supplying a local load, and this MS is in the same bus as the consumer 5, the loads 5.2, 5.3, 5.4 and 5.5 will be supplied due to their higher priority, so these will not be considered by the algorithm because they are already connected. The load 5.1 will not be supplied as well since the SSMT as a limited capacity of 30kW and so it is not possible to supply this load.

It was assumed that the storage unit will be responsible for supplying the lighting loads due to its maximum time off which is the lowest, thus having the highest priority. Since the lighting loads are not too high, the storage will stabilize the frequency below 50Hz, not equal to. In the other island, the SSMT will have the secondary control activated so, contrarily to the previous chapter, in which the MGCC would send a signal to the SSMT with a new frequency set-point, there is no need for that in this case since the storage also has a deviation in frequency.

6.5- Results and Discussion

Since the focus of this contribution is on the load connection during the microgrid restoration procedure, the connection of the microgrid with the MV grid is not simulated in this chapter.

The first steps in the microgrid restoration procedure are the following: the storage unit should energize the feeders of the microgrid and supply only the critical loads (loads with the least maximum off-time), and the SSMT should be black-started and supply a local load, thus creating two different islands. Then, the two islands should be synchronized. It is assumed that the MGCC is responsible for these steps.

In Figure 6.4 the synchronization procedure can be found. This procedure is similar to the one presented in the previous chapter. However, since the storage will be supplying the lighting loads in the microgrid (see Figure 6.4.b), its frequency will be stabilized at 49.85Hz, due to the lack of secondary frequency control, which is less than 50Hz, the nominal frequency (see Figure 6.4.a).

At 2.5 seconds, the lighting loads in the storage island and the local loads in the SSMT island are connected, since the MGCC sends a signal to the respective circuit breakers, giving the order to close. The SSMT has secondary frequency control, which corrects the frequency value back to 50Hz. It was assumed that the SSMT does not have a secondary voltage control, so the voltage will stabilize at around 370V (see Figure 6.4.c).

At 4.5 seconds, the MGCC sends a signal verify the synchronization conditions between the existent islands. At 5 seconds, these conditions are met, thus the MGCC sends another signal to the circuit breaker between the islands, so that it closes, and finally the synchronization occurs. After a small transient, the microgrid is stabilized. In the load connection time span it was assumed that between the connection of MS or loads a 5 second window has passed, thus enabling the complete frequency restoration.

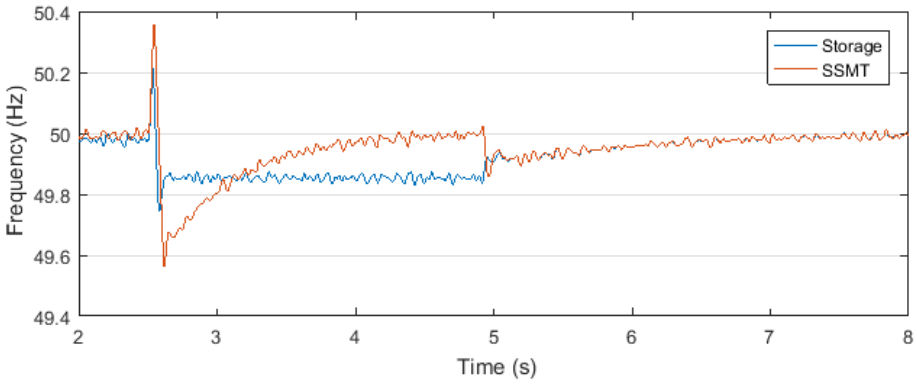

a)

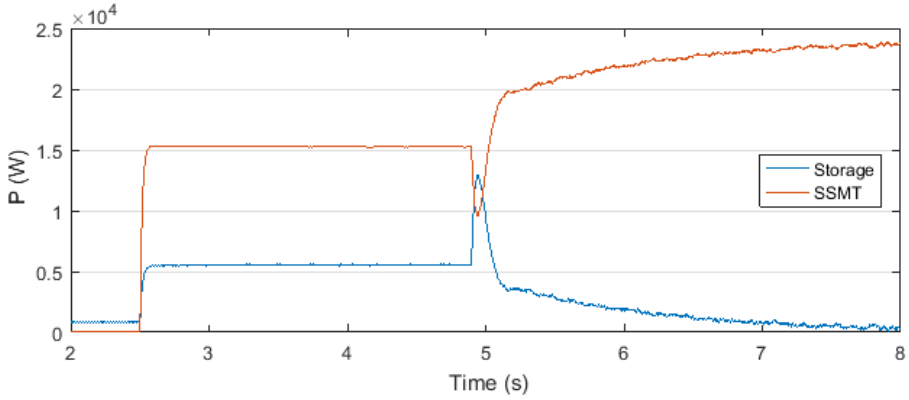

b)

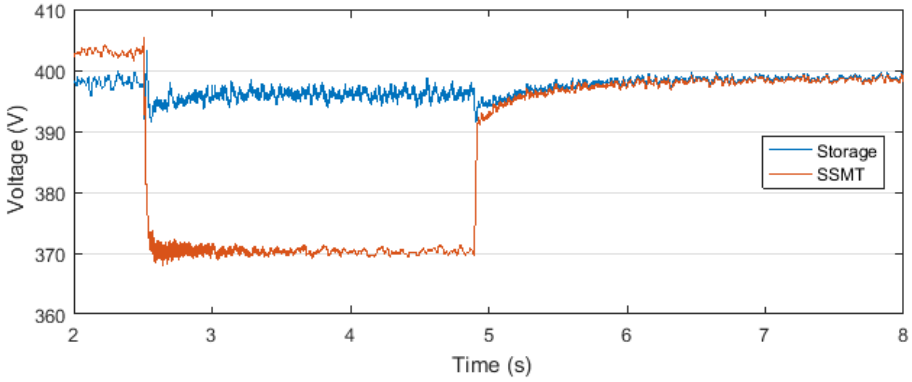

c)

Figure 6.4 - Synchronization time span: a) Frequency b) Storage and SSMT active power c) Storage and SSMT voltage.

After the synchronization of both islands, the next step is to use the proposed decentralized MAS to solve the load connection problem. Immediately after the synchronization, the SSMT active power reserve is calculated by its corresponding agent, which at 9 seconds, is around 6kW. Then, all the agents exchange the information depicted in Figure 6.2, and solve the 0/1 Knapsack problem.

The selected loads, which give a total of 6kW, are connected and the microturbine should reach exactly a 30kW output, however it overcomes this value. This effect is caused by the losses, which can be observed in Figure 6.6.c. This is a normal behaviour, since usually in the low voltage grids the factor R/X is much greater than 1, which means that this kind of grids are predominately resistive. However, since this overload in the SSMT is not very significant and only lasts a few seconds, it is not a problematic situation, and therefore can be neglected.

By observing Figure 6.6.a, it can be seen that the frequency decreases when a load is connected and increases when a MS is connected and, due to the action of the SSMT secondary frequency control, stabilizes at its nominal value of 50Hz, which is the expected behaviour. Regarding the storage unit active output, it can be found in Figure 6.6.b.

At 14 seconds, the fuel cell is connected (see Figure 6.7.c) because the SSMT does not have enough reserve. This MS is chosen according to the criteria mentioned in Section 6.2. The SSMT active output decreases as expected to around 20kW, which gives a total reserve of 10kW. This procedure is repeated until there isn't enough available reserve and all the MS are already connected.

At 34 seconds, the 3kW PV is connected (see Figure 6.7.b). However, the available reserve after its connection is not enough to connect any more loads. This means that it is necessary to connect another MS if available. The wind turbine is connected at 39 seconds, as shown in Figure 6.5, and then the reserve is sufficient to connect more loads. The Knapsack problem is solved by the agents and the selected loads are connected at 44 seconds.

This steps can be observed in Figure 6.6.c. The voltage behaviour can be found in Figure 6.7.a. In Table 6.7, the solutions obtained every time the 0/1 Knapsack problem is solved by the agents are presented, and it can be seen that the loads with higher priority are connected in the first two steps, as expected.

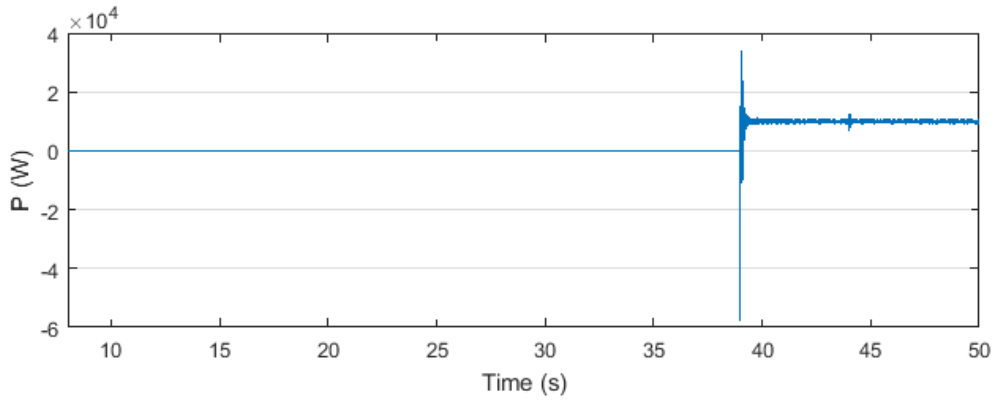

Figure 6.5 - Load connection time span: Wind generator active output.

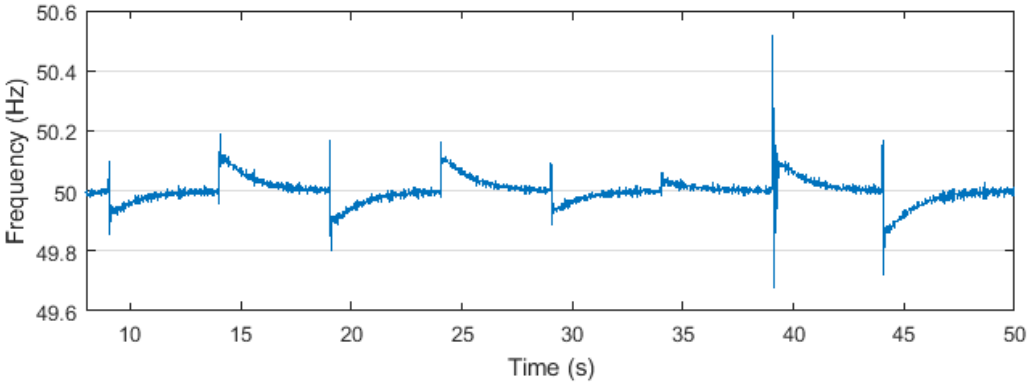

a)

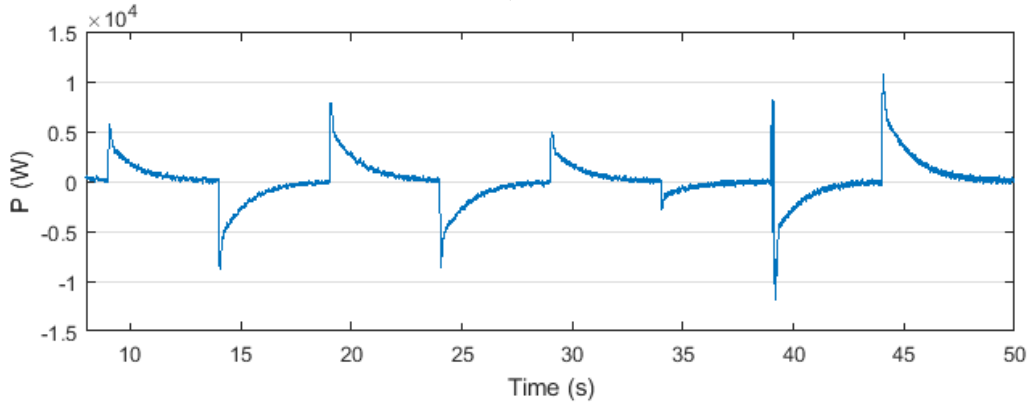

b)

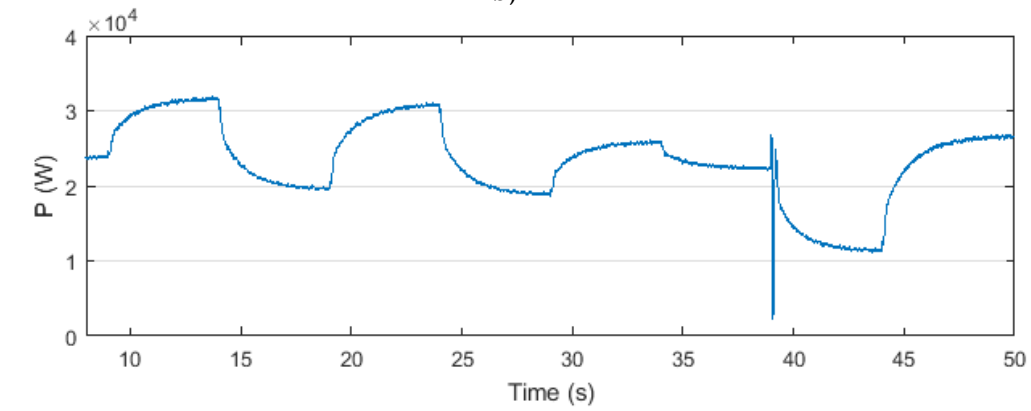

c)

Figure 6.6 - Load connection time span: a) Frequency b) Storage active power c) SSMT active power.

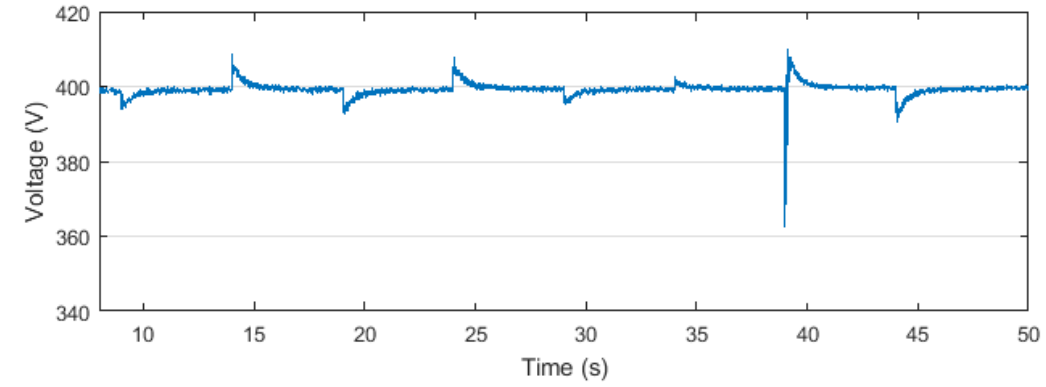

a)

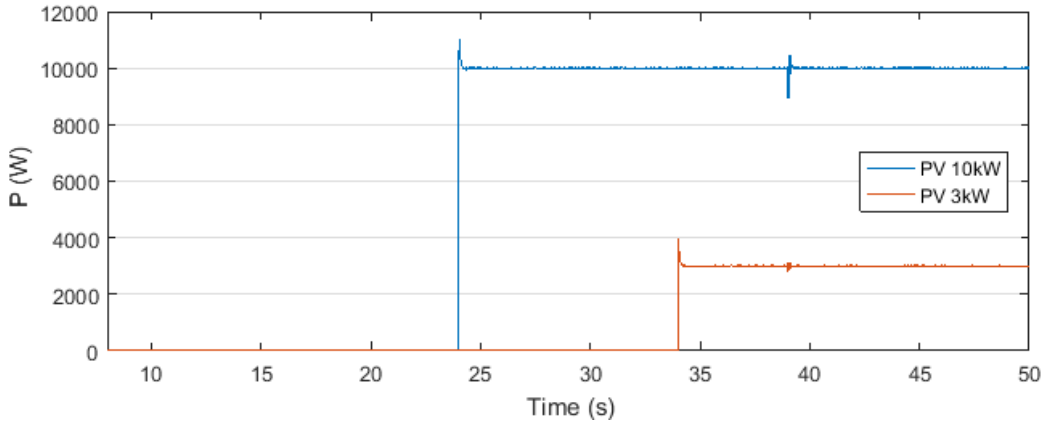

b)

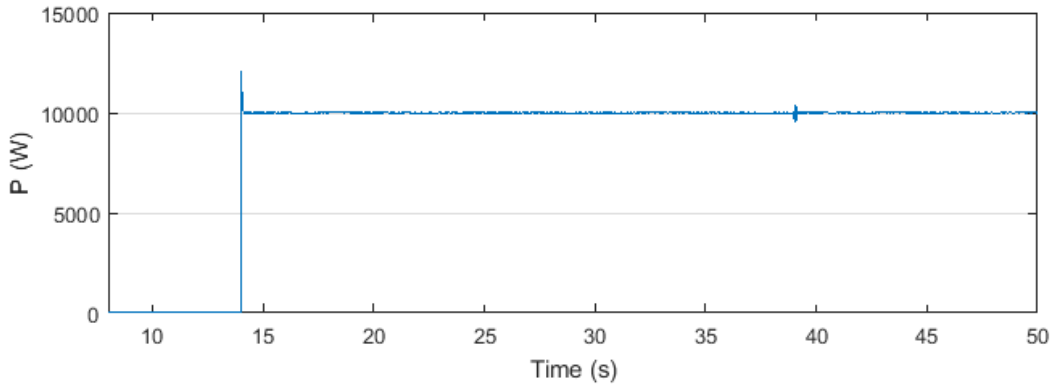

c)

Figure 6.7 - Load connection time span: a) Storage voltage b) PV units' active output c) Fuel cell active output.

Table 6.7 – SSMT's reserve, loads to be connected and sum of the loads connected, for every solved 0/1 Knapsack problem.

Step	Reserve	Loads	Sum of loads
Step 1	6kW	4.4/1.4/4.2/4.3/1.3/2.4/3.3	6kW
Step 2	10kW	1.2/2.3/3.4/3.2/2.2	9.28kW
Step 3	10kW	1.1/4.1	5.96kW
Step 4	18kW	3.1	13.18kW

6.6- MAS Applied to Partial MG Blackout

The multi-agent system developed in the previous section is used in this section in order to assess its operation during a partial blackout in the microgrid. It is assumed that the microgrid was restored, as stated in the previous section, and it is operating in islanded mode since the MV grid is not available to be reconnected.

In these conditions, it is simulated a fault in feeder 8, which leads to a partial blackout in the microgrid due to the actuation of the circuit breaker in that feeder to eliminate the fault. This means that 20kW of production (PV and wind generator) and 8.02kW of load are lost. In general, the microgrid will lose 11.98kW of generation (20-8.02kW), which means that the agents will solve a Knapsack problem to determine which loads should be disconnected, in order to maintain the balance in the microgrid.

This scheme is associated with EDRP, that will react to the frequency variations and will disconnected non-critical loads if necessary. This DR program is only applied to the consumers that sign contracts, in which they specify the amount of power that can be shed and also their revenues for the interruption. It was assumed that every consumer in the microgrid is available for EDRP and the non-critical loads were considered to be the groups 1, 2, and 3 due to its maximum off-time. Consequently, only these were the ones considered for the load shedding scheme.

The Knapsack problem considered for the load disconnection situation was the same used for the load connection procedure in the previous section. The only change that was required to do, because the Knapsack problem is a maximization problem, was to change the load priorities. For instance, in the previous section, priority 3 was assumed to be higher than priority 1, but in this scenario priority 1 was considered to be higher than priority 3, so the same maximization problem can be considered.

The problem's restriction (sum of the active power of the loads is less or equal to the capacity of the SSMT) is also valid to apply in this situation, since the objective is to shed the least amount of load possible. So, the agents will solve the Knapsack problem and then, if the SSMT capacity is still exceeded, the agents solve the Knapsack problem again. Considering that the SSMT has reached its capacity, the fact that the losses are considerable in a low voltage microgrid will actually cause that when for example 5kW of loads are disconnected, the SSMT

capacity will have a reserve of more than 5kW since it was supplying the 5kW plus losses. So, both the main load and losses contribute to the decrease of the SSMT output.

It was considered a short-circuit at the wind generator terminals at 52 seconds, which causes the circuit breaker in branch 8 to act, at 52.1 seconds. Then, at 52.6 seconds, the load shedding occurs. In Figure 6.8 it can be seen the short-term analysis of the short-circuit.

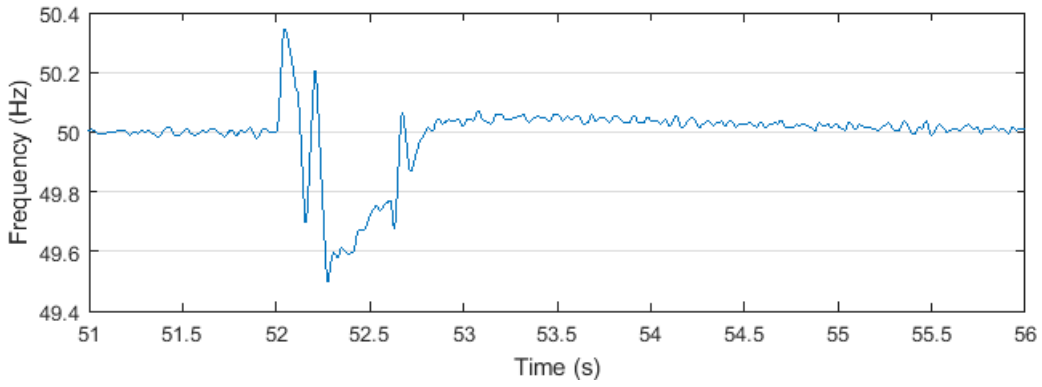

a)

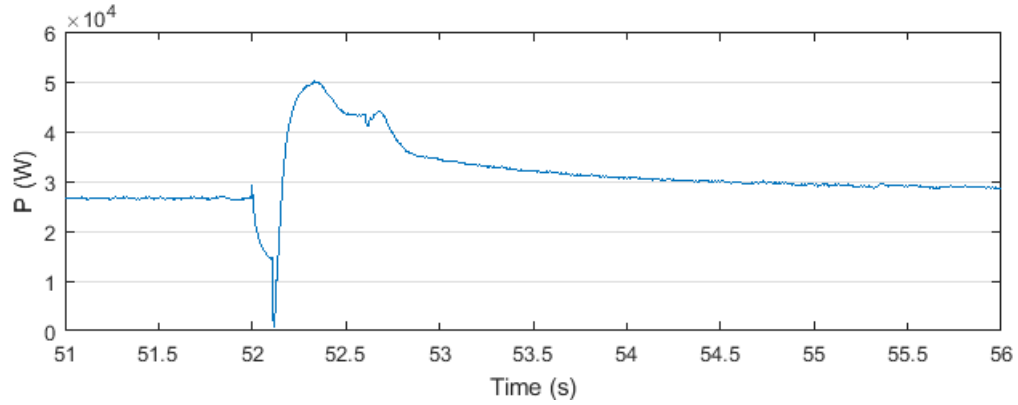

b)

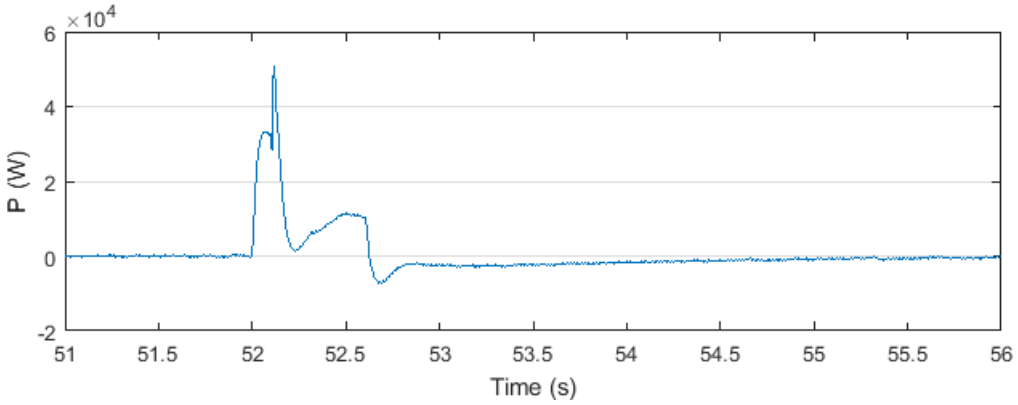

c)

Figure 6.8 - Short term: a) Frequency b) SSMT active output c) Storage active output.

Immediately before the short-circuit the SSMT is producing around 27kW. The agents will solve the Knapsack problem in order to try to maintain this output. At 50.1 seconds the agents determine the amount of load that needs to be shed in order to maintain the SSMT's output. The selected loads can be found in Table 6.8. It can be seen that the amount of load that is shed (11.88kW) is less than the necessary amount (11.98kW). This is due to the Knapsack problem and its restriction. If the SSMT's output was still above the maximum capacity, the agents would solve the Knapsack problem again. However, this is not the case. The frequency returns to its nominal value after the load shedding scheme, as presented in Figure 6.8.a.

In Figure 6.9, the long-term analysis is presented. After the short-circuit, the selected loads by the agents after solving the Knapsack problem are curtailed. Then, the process is equal to the one in the previous section. At 60 seconds, the agents detect that there are 1.5kW of free capacity in the SSMT, so they solve a Knapsack problem and connect 1.45kW, thus the SSMT reaches its capacity. Then, at 65 seconds, the 10kW PV is connected. At 70 seconds, the Knapsack problem is solved again by the agents and the selected loads are connected. Finally, at 75 seconds, the wind generator is connected and at 80 seconds, the selected loads by the agents are also connected. In Table 6.9, it is possible to find the loads to be connected in every step of the restoration procedure.

Table 6.8 - Loads to be disconnected after the short circuit.

Loads	Sum of loads
4.2/4.3/1.2/1.3/3.2/1.1/4.1	11.88kW

Table 6.9 - Loads to be connected.

Step	Reserve	Loads	Sum of loads
Step 1	1.5kW	4.2/4.3/1.2	1.45kW
Step 2	11kW	1.3/2.4/2.5/3.2/2.3/2.2	10.72kW
Step 3	10kW	3.1	5.96kW

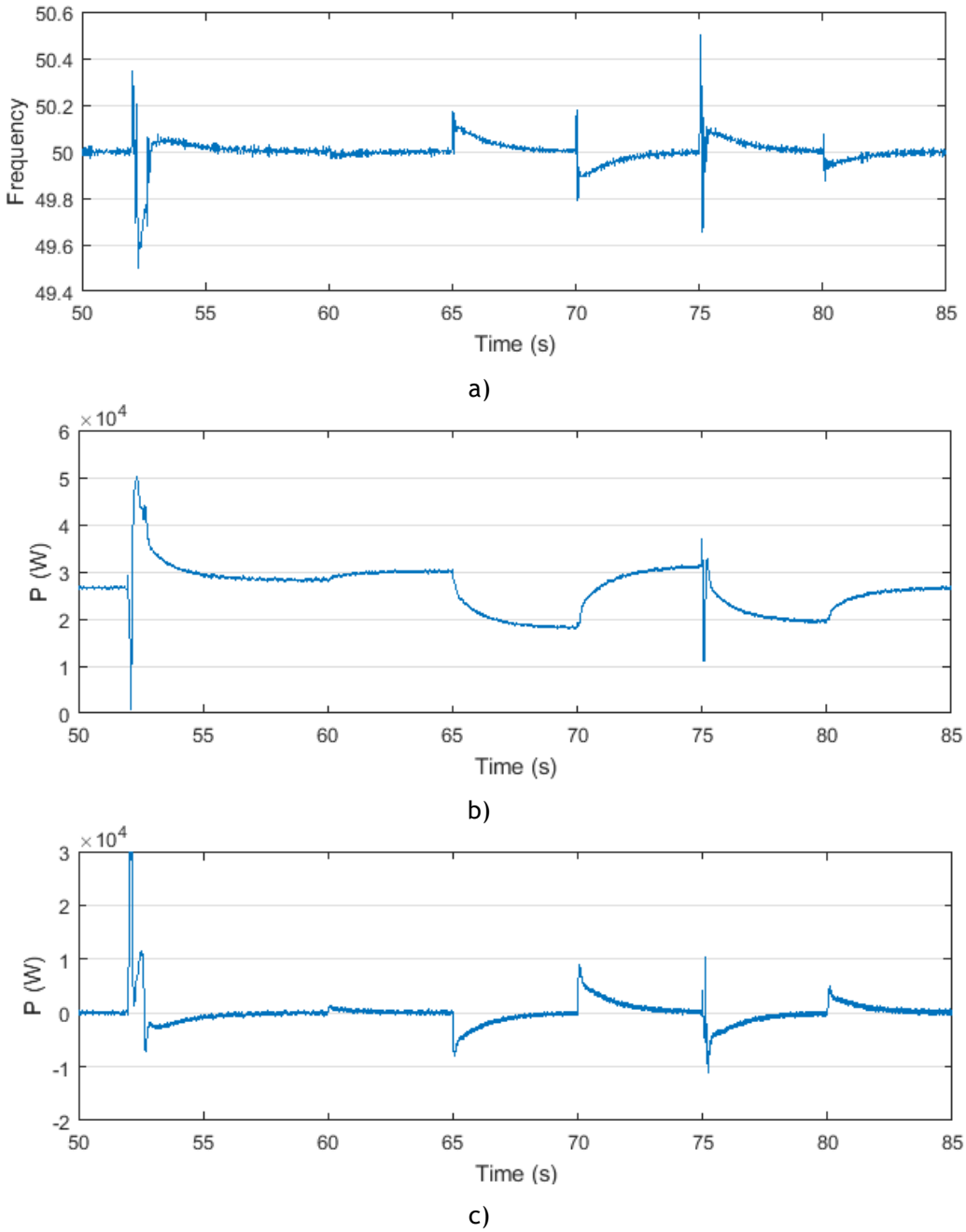

Figure 6.9 - Long term: a) Frequency b) SSMT active output c) Storage active output.

6.7- Chapter Summary

In this chapter, a decentralized MAS for microgrid restoration is proposed. In this restoration scheme it is assumed that the MGCC coordinates the first steps of the restoration procedure, and then the MAS is responsible for the load connection sequence throughout the entire procedure. The agents communicate their local information between each other and then, reach a common decision regarding the loads that should be connected in every stage. The main advantage between this decentralized scheme and the conventional centralized scheme relies on the ability to survive single-point failure.

The simulations were carried out in MATLAB/Simulink environment and the results show that the proposed MAS is able to perform the restoration procedure without endangering the entire procedure. The effect of the losses in the LV microgrid can be observed, however it is not a significant matter since they only influence the results in time periods of few seconds.

The MAS can be easily adapted to a load shedding situation caused by a fault in the microgrid that leads to a partial blackout, and the load restoration after the fault elimination can be carried out exactly like the case of the total blackout scenario.

Chapter 7

Conclusions and Future work

In this chapter the main conclusions taken from this work, regarding the utilization of a decentralized MAS, for dealing with microgrid restoration, are presented. Moreover, possible suggestions regarding the future works based on this dissertation are also identified, as well as the scientific contributions that resulted from this work.

7.1- Conclusions

It can be seen that the microgrid restoration procedure is very similar to the conventional power system restoration process, however there are also some differences. For instance, in the conventional restoration, depending on the cylinder's temperature of the conventional thermal units these can take several hours until they are able to start. This means that the black-start strategy may need to be adapted. However, in microgrids the production units do not have this time constant restriction, so its start-up procedure is much faster.

Regarding the microgrid restoration procedure, it is necessary to have a proper control system, which ensures that the procedure is performed efficiently and correctly, where the MGCC is the highest control level in this control scheme, being responsible for the coordination between the energy resources.

The response time of the inverters connected to the MS in the microgrid, will have a strong impact in the total restoration duration. This means that, if during the connection of loads and MS, the frequency stabilizes closer to its nominal value and the secondary control acts faster, then the total restoration time will decrease.

The MGCC is responsible for several tasks, among them the restoration procedure of the microgrid. By considering a decentralized restoration scheme, it is possible to free some resources of the MGCC, thus becoming more fast and efficient when it comes to other decision-making processes.

This dissertation presented a decentralized multi-agent system for microgrid restoration where the agents were responsible for exchanging their local information and then, based on the latter, these would solve a 0/1 Knapsack problem to reach a common decision.

The proposed model uses the table-based dynamic programming algorithm to solve the 0/1 Knapsack problem, thus resulting in an optimization problem which consists in determining the best load connection sequence during the microgrid restoration procedure, considering the SSMT active power reserve as well as the MS active power output, and also the previously defined load priority.

The work was develop using a MATLAB/Simulink environment where the benchmark microgrid to be tested was modelled, and then two different simulations where carried out considering a total blackout and a partial blackout.

The results show that the utilization of this decentralized scheme can effectively result in the proper restoration of the microgrid, taking the most of the DER controllability and is able to survive a single-point failure, contrary to what happens in the centralized restoration scheme.

Regarding the total blackout scenario, by analysing the results it can be seen that the loads with higher priority are connected in the first steps of the restoration process, while the remaining ones are only connected in the final steps, which is the desired behaviour.

The effect of the losses in the LV grid can also be found, in the first load connection of the total blackout case study, since for a reserve of 6kW, another 6kW of load are connected which means that the SSMT should reach exactly its maximum capacity. However, the SSMT exceeds its capacity. Since this effect only lasts a few seconds and the overload is not very significant, it can be neglected.

Besides being able to determine the loads to connect during the restoration procedure of the microgrid, in the partial blackout case study it can be seen that the algorithm is also able to determine the amount of load to be disconnected, for emergency demand response purposes, only by changing the priorities of the loads.

Another important topic to be addressed is that since the loads are discrete values, the algorithm may or may not find a solution that uses the total available reserve of the SSMT. In Table 6.7, this effect can be observed. In the first step, the SSMT's reserve is 6kW, and the algorithm is able to find 6kW of load to connect however, in the next steps, this does not happen.

7.2- Future Work

Regarding future works related to the proposed multi-agent scheme, four main opportunities can be identified:

- Implement the decentralized MAS on a physical microgrid and obtain the experimental results;
- Building on the proposed scheme, use a fully decentralized scheme where every circuit breaker is associated to an agent as well, thus dismissing the use of the MGCC during the first stages of the restoration procedure;
- Focus on the communication protocol between the agents;
- Investigate the use of the decentralized MAS in a MMG environment.

7.3- Publications

The work developed in this dissertation resulted in two scientific papers, which are presented below:

- J.P.P. Carvalho, M. Shafie-khah, G. Osório, E. Rokrok, J.P.S. Catalão, 'Multi-Agent System for Renewable Based Microgrid Restoration', in: Proceedings of the International Conference on Smart Energy Systems and Technologies — SEST 2018, Sevilla, Spain, 10-12 September, 2018 (**accepted**);
- J.P.P. Carvalho, M. Shafie-khah, G. Osório, E. Rokrok, J.P.S. Catalão, 'Decentralized Multi-Agent System Applied to the Decision Making Process of the Microgrid Restoration Procedure towards Sustainability', in: Proceedings of the 52nd Hawaii International Conference on System Sciences — HICSS 2019 (technically co-sponsored by IEEE), Maui, Hawaii, USA, January 8-11, 2019 (**submitted**).

References

[1] E. H. Allen, R. B. Stuart, and T. E. Wiedman, 'No Light in August: Power System Restoration Following the 2003 North American Blackout', *IEEE Power Energy Mag.*, vol. 12, no. 1, pp. 24–33, Jan. 2014.

[2] Y. Xue and S. Xiao, 'Generalized congestion of power systems: insights from the massive blackouts in India', *J. Mod. Power Syst. Clean Energy*, vol. 1, no. 2, pp. 91–100, Sep. 2013.

[3] Y. Liu, R. Fan, and V. Terzija, 'Power system restoration: a literature review from 2006 to 2016', *J. Mod. Power Syst. Clean Energy*, vol. 4, no. 3, pp. 332–341, Jul. 2016.

[4] J. A. P. Lopes, A. G. Madureira, and C. C. L. M. Moreira, 'A view of microgrids', *Wiley Interdiscip. Rev. Energy Environ.*, vol. 2, no. 1, pp. 86–103, Jan. 2013.

[5] S. Liu, Y. Hou, C. C. Liu, and R. Podmore, 'The Healing Touch: Tools and Challenges for Smart Grid Restoration', *IEEE Power Energy Mag.*, vol. 12, no. 1, pp. 54–63, Jan. 2014.

[6] Liang Che, M. Khodayar, and M. Shahidehpour, 'Only Connect: Microgrids for Distribution System Restoration', *IEEE Power Energy Mag.*, vol. 12, no. 1, pp. 70–81, Jan. 2014.

[7] E. Rokrok, M. Shafie-khah, P. Siano, and J. P. S. Catalão, 'A Decentralized Multi-Agent-Based Approach for Low Voltage Microgrid Restoration', *Energies*, vol. 10, no. 10, p. 1491, Sep. 2017.

[8] S. Dimitrijevic and N. Rajakovic, 'Service Restoration of Distribution Networks Considering Switching Operation Costs and Actual Status of the Switching Equipment', *IEEE Trans. Smart Grid*, vol. 6, no. 3, pp. 1227–1232, May 2015.

[9] J. Li, X. Y. Ma, C. C. Liu, and K. P. Schneider, 'Distribution System Restoration With Microgrids Using Spanning Tree Search', *IEEE Trans. Power Syst.*, vol. 29, no. 6, pp. 3021–3029, Nov. 2014.

[10] J. J. Ancona, 'A framework for power system restoration following a major power failure', *IEEE Trans. Power Syst.*, vol. 10, no. 3, pp. 1480–1485, Aug. 1995.

[11] M. M. Adibi and R. J. Kafka, 'Power system restoration issues', *IEEE Comput. Appl. Power*, vol. 4, no. 2, pp. 19–24, Apr. 1991.

[12] C. L. Moreira, F. O. Resende, and J. A. P. Lopes, 'Using Low Voltage MicroGrids for Service Restoration', *IEEE Trans. Power Syst.*, vol. 22, no. 1, pp. 395–403, Feb. 2007.

[13] C. Wang, V. Vittal, V. S. Kolluri, and S. Mandal, 'PTDF-Based Automatic Restoration Path Selection', *IEEE Trans. Power Syst.*, vol. 25, no. 3, pp. 1686–1695, Aug. 2010.

[14] S. Nourizadeh, S. A. Nezam Sarmadi, M. J. Karimi, and A. M. Ranjbar, 'Power system restoration planning based on Wide Area Measurement System', *Int. J. Electr. Power Energy Syst.*, vol. 43, no. 1, pp. 526–530, Dec. 2012.

[15] J. W. Feltes and C. Grande-Moran, 'Black start studies for system restoration', in *2008 IEEE Power and Energy Society General Meeting - Conversion and Delivery of Electrical Energy in the 21st Century*, 2008, pp. 1–8.

[16] J. Quirós-Tortós, P. Wall, L. Ding, and V. Terzija, 'Determination of sectionalising strategies for parallel power system restoration: A spectral clustering-based methodology', *Electr. Power Syst. Res.*, vol. 116, pp. 381–390, Nov. 2014.

[17] C. Wang, V. Vittal, and K. Sun, 'OBDD-Based Sectionalizing Strategies for Parallel Power System Restoration', *IEEE Trans. Power Syst.*, vol. 26, no. 3, pp. 1426–1433, Aug. 2011.
[18] Z. Qin, Y. Hou, S. Liu, J. Yan, and D. Li, 'A branch-and-cut method for computing load restoration plan considering transmission network and discrete load increment', in *2014 Power Systems Computation Conference*, 2014, pp. 1–7.
[19] J. N. Jiang *et al.*, 'Power system restoration planning and some key issues', in *2012 IEEE Power and Energy Society General Meeting*, 2012, pp. 1–8.
[20] M. M. Adibi and L. H. Fink, 'Overcoming restoration challenges associated with major power system disturbances - Restoration from cascading failures', *IEEE Power Energy Mag.*, vol. 4, no. 5, pp. 68–77, Sep. 2006.
[21] J. Feltes and C. Grande-Moran, 'Down, but Not Out: A Brief Overview of Restoration Issues', *IEEE Power Energy Mag.*, vol. 12, no. 1, pp. 34–43, Jan. 2014.
[22] M. M. Adibi, N. Martins, and E. H. Watanabe, 'The impacts of FACTS and other new technologies on power system restoration dynamics', in *IEEE PES General Meeting*, 2010, pp. 1–6.
[23] J. W. Feltes *et al.*, 'Some considerations in the development of restoration plans for electric utilities serving large metropolitan areas', *IEEE Trans. Power Syst.*, vol. 21, no. 2, pp. 909–915, May 2006.
[24] D. R. Medina *et al.*, 'Fast assessment of frequency response of cold load pickup in power system restoration', in *2016 IEEE Power and Energy Society General Meeting (PESGM)*, 2016, pp. 1–1.
[25] H. Rastegar and A. Akbari, 'Load shedding scheme based on teaching learning based optimization in radial systems', in *2017 Iranian Conference on Electrical Engineering (ICEE)*, 2017, pp. 1165–1169.
[26] C. Jamroen, B. Piriyanont, and S. Dechanupaprittha, 'Load shedding scheme based on voltage instability index using synchrophasor data', in *2017 International Electrical Engineering Congress (iEECON)*, 2017, pp. 1–4.
[27] L. Wang, H. Ye, Y. Liu, and X. Liu, 'A new method for incorporating load pickup as a control means for standing phase angle reduction in power system restoration', in *Power Engineering Conference (UPEC), 2013 48th International Universities'*, 2013, pp. 1–4.
[28] N. Martins, E. J. de Oliveira, W. C. Moreira, J. L. R. Pereira, and R. M. Fontoura, 'Redispatch to Reduce Rotor Shaft Impacts Upon Transmission Loop Closure', *IEEE Trans. Power Syst.*, vol. 23, no. 2, pp. 592–600, May 2008.
[29] M. M. Adibi and N. Martins, 'Power system restoration dynamics issues', in *2008 IEEE Power and Energy Society General Meeting - Conversion and Delivery of Electrical Energy in the 21st Century*, 2008, pp. 1–8.
[30] D. Abu Talib, H. Mokhlis, M. Sofian ABU TALIP, and K. Naidu, *Parallel power system restoration planning using heuristic initialization and discrete evolutionary programming*, vol. 5. 2017.
[31] F. O. Resende, N. J. Gil, and J. A. P. Lopes, 'Service restoration on distribution systems using Multi-MicroGrids', *Eur. Trans. Electr. Power*, vol. 21, no. 2, pp. 1327–1342, Mar. 2011.
[32] A. M. R. Lede, M. G. Molina, M. Martinez, and P. E. Mercado, 'Microgrid architectures for distributed generation: A brief review', in *2017 IEEE PES Innovative Smart Grid Technologies Conference - Latin America (ISGT Latin America)*, 2017, pp. 1–6.
[33] C. Gouveia, C. L. Moreira, J. A. P. Lopes, D. Varajao, and R. E. Araujo, 'Microgrid Service Restoration: The Role of Plugged-in Electric Vehicles', *IEEE Ind. Electron. Mag.*, vol. 7, no. 4, pp. 26–41, Dec. 2013.
[34] J. A. Lopes, A. Madureira, N. Gil, and F. Resende, *Operation of Multi-Microgrids*. 2014.
[35] J. A. P. Lopes, C. L. Moreira, and A. G. Madureira, 'Defining control strategies for MicroGrids islanded operation', *IEEE Trans. Power Syst.*, vol. 21, no. 2, pp. 916–924, May 2006.
[36] P. C. Loh, D. Li, Y. K. Chai, and F. Blaabjerg, 'Hybrid AC #x2013;DC Microgrids With Energy Storages and Progressive Energy Flow Tuning', *IEEE Trans. Power Electron.*, vol. 28, no. 4, pp. 1533–1543, Apr. 2013.
[37] M. H. Andishgar, E. Gholipour, and R. Hooshmand, 'An overview of control approaches of inverter-based microgrids in islanding mode of operation', *Renew. Sustain. Energy Rev.*, vol. 80, pp. 1043–1060, Dec. 2017.

[38] S. K. Sahoo, A. K. Sinha, and N. K. Kishore, 'Control Techniques in AC, DC, and Hybrid AC-DC Microgrid: A Review', *IEEE J. Emerg. Sel. Top. Power Electron.*, vol. PP, no. 99, pp. 1–1, 2017.
[39] M. Kumar and B. Tyagi, 'A state of art review of microgrid control and integration aspects', in *2016 7th India International Conference on Power Electronics (IICPE)*, 2016, pp. 1–6.
[40] A. Bidram and A. Davoudi, 'Hierarchical Structure of Microgrids Control System', *IEEE Trans. Smart Grid*, vol. 3, no. 4, pp. 1963–1976, Dec. 2012.
[41] Y. Han, P. Shen, X. Zhao, and J. M. Guerrero, 'Control Strategies for Islanded Microgrid Using Enhanced Hierarchical Control Structure With Multiple Current-Loop Damping Schemes', *IEEE Trans. Smart Grid*, vol. 8, no. 3, pp. 1139–1153, May 2017.
[42] D. E. Olivares *et al.*, 'Trends in Microgrid Control', *IEEE Trans. Smart Grid*, vol. 5, no. 4, pp. 1905–1919, Jul. 2014.
[43] D. Doukas, P. Gkaidatzis, A. Bouhouras, K. Sgouras, and D. Labridis, 'On Reverse Power Flow Modelling in Distribution Grids', 2016.
[44] F. Mumtaz and I. S. Bayram, 'Planning, Operation, and Protection of Microgrids: An Overview', *Energy Procedia*, vol. 107, pp. 94–100, Feb. 2017.
[45] A. G. Madureira and J. A. Peças Lopes, 'Ancillary services market framework for voltage control in distribution networks with microgrids', *Electr. Power Syst. Res.*, vol. 86, pp. 1–7, May 2012.
[46] J. T. Saraiva and M. H. Gomes, 'Provision of some ancillary services by microgrid agents', in *2010 7th International Conference on the European Energy Market*, 2010, pp. 1–8.
[47] F. Wang, H. Xu, T. Xu, K. Li, M. Shafie-khah, and J. P. S. Catalão, 'The values of market-based demand response on improving power system reliability under extreme circumstances', *Appl. Energy*, vol. 193, pp. 220–231, May 2017.
[48] F. Shariatzadeh, P. Mandal, and A. K. Srivastava, 'Demand response for sustainable energy systems: A review, application and implementation strategy', *Renew. Sustain. Energy Rev.*, vol. 45, pp. 343–350, May 2015.
[49] J. Shen, C. Jiang, Y. Liu, and J. Qian, 'A Microgrid Energy Management System with Demand Response for Providing Grid Peak Shaving', *Electr. Power Compon. Syst.*, vol. 44, no. 8, pp. 843–852, May 2016.
[50] Q. Zhang and J. Li, 'Demand response in electricity markets: A review', in *2012 9th International Conference on the European Energy Market*, 2012, pp. 1–8.
[51] J. Aghaei, M.-I. Alizadeh, P. Siano, and A. Heidari, 'Contribution of emergency demand response programs in power system reliability', *Energy*, vol. 103, pp. 688–696, May 2016.
[52] J. S. Vardakas, N. Zorba, and C. V. Verikoukis, 'A Survey on Demand Response Programs in Smart Grids: Pricing Methods and Optimization Algorithms', *IEEE Commun. Surv. Tutor.*, vol. 17, no. 1, pp. 152–178, Firstquarter 2015.
[53] D. Q. Oliveira, A. C. Zambroni de Souza, M. V. Santos, A. B. Almeida, B. I. L. Lopes, and O. R. Saavedra, 'A fuzzy-based approach for microgrids islanded operation', *Electr. Power Syst. Res.*, vol. 149, pp. 178–189, Aug. 2017.
[54] G. Strbac, N. Hatziargyriou, J. P. Lopes, C. Moreira, A. Dimeas, and D. Papadaskalopoulos, 'Microgrids: Enhancing the Resilience of the European Megagrid', *IEEE Power Energy Mag.*, vol. 13, no. 3, pp. 35–43, May 2015.
[55] Y. J. Wang, X. Z. Dong, B. Wang, J. Liu, and A. X. Guo, 'Black start studies for micro-grids with distributed generators', in *12th IET International Conference on Developments in Power System Protection (DPSP 2014)*, 2014, pp. 1–6.
[56] J. Liu, A. Chen, C. Du, and C. Zhang, 'An improved method for black start of hybrid microgrids', in *2017 36th Chinese Control Conference (CCC)*, 2017, pp. 9187–9192.
[57] S. Jayasinghe and K. T. M. U. Hemapala, *Multi Agent Based Power Distribution System Restoration—A Literature Survey*, vol. 07. 2015.
[58] R. Belkacemi and A. Bababola, 'Experimental implementation of Multi-Agent System algorithm for distributed restoration of a Smart Grid System', in *IEEE SOUTHEASTCON 2014*, 2014, pp. 1–4.
[59] T. Nagata and K. Okamoto, 'A decentralized distribution power system restoration by using multi-agent Approach', in *2014 International Electrical Engineering Congress (iEECON)*, 2014, pp. 1–4.

[60] Q. Ren, L. Bai, S. Biswas, F. Ferrese, and Q. Dong, 'A BDI multi-agent approach for power restoration', in *2014 7th International Symposium on Resilient Control Systems (ISRCS)*, 2014, pp. 1–6.
[61] L. Sun *et al.*, 'Optimisation model for power system restoration with support from electric vehicles employing battery swapping', *Transm. Distrib. IET Gener.*, vol. 10, no. 3, pp. 771–779, 2016.
[62] B. Zhao, X. Dong, and J. Bornemann, 'Service Restoration for a Renewable-Powered Microgrid in Unscheduled Island Mode', *IEEE Trans. Smart Grid*, vol. 6, no. 3, pp. 1128–1136, May 2015.
[63] A. Arab, A. Khodaei, S. K. Khator, K. Ding, V. A. Emesih, and Z. Han, 'Stochastic Pre-hurricane Restoration Planning for Electric Power Systems Infrastructure', *IEEE Trans. Smart Grid*, vol. 6, no. 2, pp. 1046–1054, Mar. 2015.
[64] A. Castillo, 'Microgrid provision of blackstart in disaster recovery for power system restoration', in *2013 IEEE International Conference on Smart Grid Communications (SmartGridComm)*, 2013, pp. 534–539.
[65] Z. Tan, R. Fan, Y. Liu, and L. Sun, 'Microgrid black-start after natural disaster with load restoration using spanning tree search', in *2016 IEEE Power and Energy Society General Meeting (PESGM)*, 2016, pp. 1–5.
[66] Y. Sun and X. Tang, 'Cascading failure analysis of power flow on wind power based on complex network theory', *J. Mod. Power Syst. Clean Energy*, vol. 2, no. 4, pp. 411–421, Dec. 2014.
[67] Z. Lin, F. Wen, and Y. Xue, 'A Restorative Self-Healing Algorithm for Transmission Systems Based on Complex Network Theory', *IEEE Trans. Smart Grid*, vol. 7, no. 4, pp. 2154–2162, Jul. 2016.
[68] A. E. Zonkoly, 'Integration of wind power for optimal power system black-start restoration', *Turk. J. Electr. Eng. Comput. Sci.*, vol. 23, no. 6, pp. 1853–1866, Nov. 2015.
[69] W. Teng, H. Wang, and Y. Jia, 'Construction and control strategy research of black start unit containing wind farm', in *TENCON 2015 - 2015 IEEE Region 10 Conference*, 2015, pp. 1–5.
[70] A. Arif and Z. Wang, 'Service restoration in resilient power distribution systems with networked microgrid', in *2016 IEEE Power and Energy Society General Meeting (PESGM)*, 2016, pp. 1–5.
[71] S. Papathanassiou, N. Hatziargyriou, and K. Strunz, 'A Benchmark Low Voltage Microgrid Network', *CIGRE Symp.*, Jan. 2005.
[72] 'Robust maximum power point tracker using sliding mode controller for the three-phase grid-connected photovoltaic system - ScienceDirect'. [Online]. Available: https://www.sciencedirect.com/science/article/pii/S0038092X06001113. [Accessed: 12-Feb-2018].
[73] H. J. El-Khozondar, R. J. El-Khozondar, K. Matter, and T. Suntio, 'A review study of photovoltaic array maximum power tracking algorithms', *Renew. Wind Water Sol.*, vol. 3, no. 1, p. 3, Feb. 2016.
[74] Y. Zhu and K. Tomsovic, 'Development of models for analyzing the load-following performance of microturbines and fuel cells', *Electr. Power Syst. Res.*, vol. 62, no. 1, pp. 1–11, May 2002.
[75] S. K. Nayak and D. N. Gaonkar, 'Modeling and performance analysis of microturbine generation system in grid connected/islanding mode', in *2012 IEEE International Conference on Power Electronics, Drives and Energy Systems (PEDES)*, 2012, pp. 1–6.
[76] S. R. Guda, C. Wang, and M. H. Nehrir, 'Modeling of Microturbine Power Generation Systems', *Electr. Power Compon. Syst.*, vol. 34, no. 9, pp. 1027–1041, Sep. 2006.
[77] C. L. Moreira and J. A. P. Lopes, 'MicroGrids Operation and Control under Emergency Conditions', in *Smart Power Grids 2011*, A. Keyhani and M. Marwali, Eds. Berlin, Heidelberg: Springer Berlin Heidelberg, 2012, pp. 351–399.
[78] F. Mohamed, 'MicroGrid Modelling and Online Management', *978-951-22-9234-9*, Jan. 2008.
[79] R. K. Shah, 'Introduction to Fuel Cells', 2007, pp. 1–9.
[80] R. Bove, 'Solid Oxide Fuel Cells: Principles, Designs and State-of-the-Art in Industries', in *Recent Trends in Fuel Cell Science and Technology*, Springer, New York, NY, 2007, pp. 267–285.

[81] J. Rocabert, A. Luna, F. Blaabjerg, and P. Rodríguez, 'Control of Power Converters in AC Microgrids', *IEEE Trans. Power Electron.*, vol. 27, no. 11, pp. 4734–4749, Nov. 2012.
[82] Z. Xu, P. Yang, Q. Zheng, and Z. Zeng, 'Study on black start strategy of microgrid with PV and multiple energy storage systems', in *2015 18th International Conference on Electrical Machines and Systems (ICEMS)*, 2015, pp. 402–408.
[83] J. L. Afonso, M. J. S. Freitas, and J. S. Martins, 'p-q Theory power components calculations', in *2003 IEEE International Symposium on Industrial Electronics (Cat. No.03TH8692)*, 2003, vol. 1, pp. 385–390 vol. 1.
[84] J. L. Dominguez-Garcia, O. Bellmunt, F. Bianchi, and A. Sudria-Andreu, 'Power control of voltage source converter for distributed generation', 2011.
[85] S. D. J. McArthur *et al.*, 'Multi-Agent Systems for Power Engineering Applications #x2014;Part I: Concepts, Approaches, and Technical Challenges', *IEEE Trans. Power Syst.*, vol. 22, no. 4, pp. 1743–1752, Nov. 2007.
[86] C.-S. Karavas, G. Kyriakarakos, K. G. Arvanitis, and G. Papadakis, 'A multi-agent decentralized energy management system based on distributed intelligence for the design and control of autonomous polygeneration microgrids', *Energy Convers. Manag.*, vol. 103, pp. 166–179, Oct. 2015.
[87] R. Bayindir, E. Hossain, E. Kabalci, and R. Perez, 'A Comprehensive Study on Microgrid Technology', *Int. J. Renew. Energy Res. IJRER*, vol. 4, no. 4, pp. 1094–1107, Dec. 2014.
[88] C.-S. Hwang, E.-S. Kim, and Y.-S. Kim, 'A Decentralized Control Method for Distributed Generations in an Islanded DC Microgrid Considering Voltage Drop Compensation and Durable State of Charge', *Energies*, vol. 9, no. 12, p. 1070, Dec. 2016.
[89] M. Posypkin and S. T. T. Sin, 'Comparative analysis of the efficiency of various dynamic programming algorithms for the knapsack problem', in *2016 IEEE NW Russia Young Researchers in Electrical and Electronic Engineering Conference (EIConRusNW)*, 2016, pp. 313–316.
[90] 'A Study of Performance Analysis on Knapsack Problem', *Int. J. Comput. Appl.*, p. 6.
[91] J. J. Bartholdi, 'The Knapsack Problem', 2008, pp. 19–31.
[92] S. Choi, S. Park, and H.-M. Kim, 'The Application of the 0-1 Knapsack Problem to the Load-Shedding Problem in Microgrid Operation', in *Control and Automation, and Energy System Engineering*, Springer, Berlin, Heidelberg, 2011, pp. 227–234.
[93] E. P. Luila, 'Multicriteria Knapsack Problem', p. 11.
[94] K. Samarakoon, J. Ekanayake, and N. Jenkins, 'Investigation of Domestic Load Control to Provide Primary Frequency Response Using Smart Meters', *IEEE Trans. Smart Grid*, vol. 3, no. 1, pp. 282–292, Mar. 2012.
[95] C. Gouveia, J. Moreira, C. L. Moreira, and J. A. P. Lopes, 'Coordinating Storage and Demand Response for Microgrid Emergency Operation', *IEEE Trans. Smart Grid*, vol. 4, no. 4, pp. 1898–1908, Dec. 2013.

Appendix

This appendix is divided into three sub-sections. Section A.1 has the purpose of providing the pseudocode that is considered for the implementation of the restoration procedure algorithm, based on the multi-agent system. This pseudocode presents de general guidelines followed in the proposed algorithm. In Section A.2 and Section A.3, it is possible to find the first page of the submitted publications for SEST 2018 and HICSS 2019, respectively.

A.1 – Algorithm Pseudocode

```
Inputs:
      load identifier (i.j),
      weights of each load (active power),
      values of each load (priorities),
      W value (available SSMT reserve)

Calculation:

      Create vector weights_2 (corresponds to the vector that
      comprises the sum of the weights;

      Create matrix D, initially composed only by zeros with dimension
      number_of_items_x_size_of_weights_2;

      Initialize first row of matrix D:

      for j equal to 1 to W+1:

            if weight of item 1 is less or equal than weights_2(j)
                  D(1,j) is equal to the value of item 1;
            else
                  D(1,j) is equal to 0;
      end

      Calculate the remaining rows of matrix D:

      for i equal to 2 to number_of_items:
            for j equal to 1 to W+1

            if: weight of item i is greater than weights_2(j)
                  D(i,j) is equal to D(i-1,j);
```

```
            end


            else:
                  value by excluding item i is equal to D(i-1,j);
                  value by including item i is equal to the value of
                  item i added to the element D(i-1,(j-weights(i)));

                  if value by excluding is greater than value by
                  including item i:
                        D(i,j) is equal to value by excluding item i;

                  if value by including is greater than value by
                  excluding item i:
                        D(i,j) is equal to value by including item i;
            end
            end
      end
```

Determine the loads that were chosen:

```
      Best value is equal to D(end,end);

      while i is greater than 1:

            while D(i-1,j) is equal to the best value:

                  i is subtracted by 1;
                  if i is equal to 1, break;
            end

            Place in the solution vector in position i the value 1;

            i is subtracted by 1;
            j is subtracted by the weight of the item in the
            same line;

            if i is equal to zero
                  break;
            end

            best value will be equal to D(i,j);
      end

      if D(i,j) is different from 0:

            Place in the solution vector in the position 1 (position
            of the first item) the value 1;
      end
```

Present result:

```
      Print chosen loads;
      Print the sum of active power of the chosen loads;
```

Finish

A.2 – Publication for SEST 2018

Multi-Agent System for Renewable Based Microgrid Restoration

João P. P. Carvalho
FEUP, Porto,
Portugal
pedrojo.carvalho@gmail.com

Miadreza Shafie-khah, Gerardo Osório, Ebrahim Rokrok
C-MAST/UBI, Covilhã, Portugal
miadreza@ubi.pt
osorio.silva@ubi.pt
ebrahim.rokrok@gmail.com

João P. S. Catalão
INESC TEC and FEUP, Porto,
C-MAST/UBI, Covilha, and
INESC-ID/IST-UL, Lisbon, Portugal
catalao@fe.up.pt

***Abstract*—Power system restoration (PSR) is a very important procedure to ensure the consumer supply. In this paper, a decentralized multi-agent system (MAS) for dealing with the microgrid restoration procedure is proposed. In this proposed method, each agent is associated with a consumer or micro-source (MS) and these will communicate with each other to reach a common decision. The agents solve a 0/1 knapsack problem to determine the best load connection sequence during the microgrid restoration procedure. The proposed MAS is tested in one specific scenario where the microgrid is subjected to a blackout that has occurred, which means that all the resources and loads are disconnected. It is developed in Matlab/Simulink environment and is validated by performing the corresponding dynamic simulations.**

Keywords—black-start; demand response; distributed resources; microgrid; multi-agent system; restoration

I. Introduction

One of the most critical problems to be addressed is the power system restoration (PSR) issue. In a conventional way, restoration process begins in the transmission system by starting the power plants that provide the black start capability in the shortest possible time, such as hydroelectric generating units, gas and fuel turbine units and also incoming power from the interconnected systems in the vicinities [1]. This way, it is possible to energize transmission system and from there supply the consumers near the power plants first, thus the consumers at the distribution system will wait a long time to be supplied. In recent developments a new concept has emerged, the microgrid (MG). This changes the paradigm completely because the power flow becomes bi-directional and this type of grid can also work in islanded mode if necessary [2]. This new characteristic, when properly used, can be very beneficial in terms of PSR [3]. Besides, it will allow distribution system consumers to be supplied faster than using the conventional way.

There have been several studies and simulations in terms of taking advantage of the microgrid capabilities in terms of PSR [1]. In [4] the restoration of a smart grid system based on a distributed multi-agent system is performed on a six bus system using Tennessee Technological University Smart Grid Laboratory. Ref. [5] addresses a stochastic model that can provide support to the decision making process of the power system restoration procedure in a pre-hurricane situation. It provides two strategies regarding a complete restoration and a partial restoration of the system. A stochastic mixed integer linear program is proposed in order to verify the potential of the microgrids black-start capabilities in [6]. Regarding spanning tree search methods, a graph-theoretic strategy for the power system restoration based on the incorporation of microgrids in the distribution system is presented in [7]. Here, the objective is to maximize the restoration of load by minimizing the number of actuation of the switching devices. The proposed algorithm is capable of determining an optimal solution in terms of network topologies. In [8] the microgrid black-start capabilities are analyzed, supported by sectionalizing the existing microgrids in the power system. The unserved critical loads are then supplied by the microgrids with enough generation margins, through the application of a spanning tree search algorithm. In [3], the feasibility of microgrid restoration is examined using dynamic modeling of microgrid components. The microgrid central controller (MGCC) decides a proper sequence of restoration actions including setting-up the generation units with black start capability, energizing feeders, and reconnecting the loads and other generation units. The sequence of actions is determined by MGCC using the information received periodically from the microsource controllers (MCs) and load controllers (LCs), in terms of the level of generation and consumption in the MG. Ref. [9] investigates the restoration of distribution system with multi-microgrid in the presence of multi-MGCC. The sequence of actions is determined by the central autonomous management controller (CAMC).

In this paper a decentralized MAS scheme for microgrid restoration is proposed. Each agent is assigned to a specific distributed energy resource (load or generation unit) and these communicate with each other to obtain the global information of the microgrid, in terms of production and load values. After sharing the information, the agents solve a 0/1 knapsack problem by using the table-based dynamic programming algorithm. This way it is possible to choose the loads that are more suitable to be connected in every step of the restoration process. The model is simulated in one particular case study, considering that a blackout occurred in the MG and therefore, all the loads and generation units are disconnected from the latter.

J.P.S. Catalão acknowledges the support by FEDER funds through COMPETE 2020 and by Portuguese funds through FCT, under Projects SAICT-PAC/0004/2015 - POCI-01-0145-FEDER-016434, POCI-01-0145-FEDER-006961, UID/EEA/50014/2013, UID/CEC/50021/2013, UID/EMS/00151/2013, and 02/SAICT/2017 - POCI-01-0145-FEDER-029803, and also funding from the EU 7th Framework Programme FP7/2007-2013 under GA no. 309048.

A.3 – Publication for HICSS 2019

Decentralized Multi-Agent System Applied to the Decision Making Process of the Microgrid Restoration Procedure towards Sustainability

Abstract

A significant procedure to ensure the consumer supply is Power System Restoration (PSR). Due to the increase of the number of distributed generators in the grid, it is possible to shift from the conventional PSR to a new strategy involving the use of distributed energy resources (DER). In this paper, a decentralized multi-agent system (MAS) is proposed to cope with the restoration procedure in a microgrid (MG). Each agent is assigned to a specific consumer or microsource (MS), communicating with other agents at every stage of the restoration procedure so that a common decision is reached. The 0/1 knapsack problem is the problem that every agent solves to determine the best load connection sequence during the restoration of the MG. Two different case studies are used to test the MAS on a dynamically modeled benchmark MG: a total blackout and a partial blackout. Regarding the partial blackout case, demand response emergency programs are considered to manage the loads in the MG. The MAS is developed in Matlab/Simulink environment and by performing the corresponding dynamic simulations it is possible to validate this system towards sustainability.

1. Introduction

1.1. Aims and Motivation

The limitation of the operational margins of power systems led to an increase on the risk of power outages and blackouts. On this subject, one of the most important problems to be analyzed is the power system restoration (PSR). Considering the conventional procedure, this process begins with the energization of the transmission system by starting the black-start units/power plants. Possible examples of black-start units are hydroelectric units, gas and fuel turbine units. A black-start feature can also be the incoming power from the remaining interconnected systems in the vicinities [1]. Using this procedure, the transmission system will be energized and then the consumers near the power plants will be supplied first, meaning that the distribution system's consumers must wait longer to be supplied.

Over the years, a restructuring of the power systems has been verified, regarding the integration of dispersed generation units (renewable and non-renewable) in the distribution systems, which led to the identification of the relatively new concept called microgrid (MG). As a result, the power flow in a MG is now bi-directional and the islanded operation is also enabled when necessary [2].

The bi-directional power flow feature can be very useful regarding PSR [3]. Furthermore, it is possible to supply the consumers at the distribution system much faster than the conventional way, since the MG can start supplying low voltage consumers at the same time that the transmission system is being restored. Concluding, by combining the distributed energy resources (DER) with the flexibility of the consumptions in the MG, the restoration process can be improved significantly.

1.2. Literature Review

Several studies have been addressed with the purpose of using the advantages of the MG capabilities regarding PSR. Some of these studies regard multi-agent system (MAS), integration of electric vehicles (EV) using stochastic methods, considering spanning tree search and also using complex network theory [1].

In [4] the power restoration of a smart grid was performed based on a MAS. Ref. [5] proposes a multi-agent scheme to tackle the distribution power system restoration, which compares its results with the results obtained by using a mathematical programming strategy. The conclusions show that the quality of the MAS solution is very similar to the other solution and only uses local information, which is an advantage.

The PSR problem is tackled in a renewable-based MG in [6]. Here the MG operates in island mode as a result of an unscheduled disconnection from the medium voltage grid. The uncertainty of the output of renewable sources and the time that the MG is working on island mode are the main challenges. Two stochastic based methods are proposed to address the scheduling problem. In [7], a stochastic model is proposed where the decision making process of the restoration procedure is supported by a stochastic model, according to a pre-hurricane situation. In the same reference it is possible to find two different strategies: one for complete restoration and one for partial restoration.